Integrated Photonic Device Fabrication, Assembly, and Characterization: WPI/QCC LEAP Facility Testing and Customization

A Major Qualifying Project Report:

Submitted to the faculty of

WORCESTER POLYTECHNIC INSTITUTE

in partial fulfillment of the requirements for the

Degree of Bachelor of Science

in Mechanical Engineering

Submitted by:

Cam Tu Le

Project Advisor:

Professor Yuxiang Liu, Advisor

Professor Douglas Petkie, Co-Advisor

Dr. James Eakin, Co-Advisor

Submission Date: 4/3/2021

This report represents the work of one or more WPI undergraduate students submitted to the faculty as evidence of completion of a degree requirement. WPI routinely publishes these reports on the web without editorial or peer review.

Abstract

The objective of the MQP is to test some of LEAP's equipment and develop its protocols. However, due to the scope of the project, we were only able to examine the spin coater, the Profilometer, and the TeraHertz spectroscopy. Among many equipment at the WPI/QCC LEAP, we choose the spin coater and Profilometer for testing because they are essential parts and are frequently used in integrated photonic device fabrication. Furthermore, in this MQP work, we will use the Toptica TeraFlash, a time-domain spectrometer, to extract the Quartz glass slide's refractive index and absorption coefficients and then compare it with available literature.

Contents

Table of Figures iii
List of Tables vii
Chapter 1: Introduction: 9
LEAP@WPI/QCC and its Goals 9
What is Photonics? 9
Applications and the Importance of Photonics 9
Integrated Photonics........ 10
The Objective of Our MQP 10
Chapter 2: LEAP Facility Equipment........ 11
2.1 Spin Coater 11
2.1.1 Equipment Description 11
2.2.2 Spin Coater Working Principle 12
2.2.3 Spin Coater Operation 13
2.2 Profilometer 17
2.2.1 Equipment Description: 18
2.2.2 Basic Operation: 19
2.2.3 Profiling a Sample 20
2.3 TeraHertz Spectroscopy 25
2.3.1 Introduction 25
2.3.2 Toptica TeraFlash Description........ 25
Chapter 3: Spin Coater and Profilometer 28
3.1 Testing the Spin Coater and the KLA Stylus Profiler 28
3.2 Procedure for the testing........ 28
3.3 Measurement Results: 32
3.3.1 Recipe KL5305_1: 32
3.3.2 Recipe KL5305_2: 39
3.3.3 Recipe KL5305_3: 44
3.3.4 Expose and Develop samples with recipe KL5305_3: 50
3.3.5 Recipe KL5305_4: 60

3.3.6 Recipe KL5305_5: 66
3.4 Conclusion: 74
Chapter 4: TeraHertz Spectroscopy 76
4.1 Experimental Method: 76
4.2 Experiment Results 79
4.2.1 Refractive index 79
4.2.2 Absorption Coefficient 91
4.3 Conclusion: 94
Chapter 5: Broader Impacts 95
5.1 Engineering Ethics 95
5.2 Codes and Standards 95
Chapter 6: Conclusion and Outlook 96
6.1 Conclusion: 96
6.1.1 Spin Coater and Profilometer: 96
6.1.2TeraFlash TeraHertz Spectroscopy: 97
6.4 Outlook 97
6.4.1 Spin Coater and Profilometer 97
6.4.2 TeraHertz Spectroscopy 97
Acknowledgments 99
References 100

Table of Figures

Figure 1 The Cee® Apogee™ Spin Coater [6]. 11

Figure 2. Working principle of spin coater.. 12

Figure 3 DataStream™ Process Page. 13

Figure 4. Tool page with control field not selected 14

Figure 5. Tool Page for Manual Operation with control field selected for controlling Plate Temperature [7]. 15

Figure 6. Recipes Controls Page used to Load/Run/New or Edit a recipe [7]. 15

Figure 7. Recipe Selection page after press Load button on Recipes Page on …. 16

Figure 8. The running screen [7]. 17

Figure 9. Basic elements and working principle of a stylus profilometer 18

Figure 10. The Alpha-Step D-600 stylus profiler [8]... 18

Figure 11. The D-600 Stage table with Precision Locator [8]. 19

Figure 12. Video Capture screen with Scan Parameters fields. The three other tab that can be selected at the bottom left of the screen are Real Time Display, Cursor Control and Sequence [8]. 21

Figure 13. Control Panel [8] 22

Figure 14. Sample Data window in the Graph display. R: registering cursor and M: measuring cursor. [8] 23

Figure 15. Data Control tab where we can choose method to level the graph. [8] 24

Figure 16. Schematic shows working principle of terahertz spectroscopy. 26

Figure 17. Schematic representation. Blue lines denote electric connections, red lines the optical signal paths [9] 27

Figure 18. Toptica TeraFlash TeraHertz spectroscopy at LEAP.. 27

Figure 19. KemLab KL 5300 series Spin Curve from manufacturer datasheet [10]...................... 28

Figure 20. The ultrasound cleaner 29

Figure 21. A typical clean wafer after using ultrasound cleaner. 30

Figure 22. Wafer prepared with Kapton tape for making step for thickness measurements. 30

Figure 23. A typical sample after soft bake and Kapton tape removed. 32

Figure 24. The relative position of the cross-sections and the direction for the measurements of the three samples using KL5305_1 recipe. a) Sample 1, b) Sample 2 and c) Sample 3................ 33

Figure 25: A typical profile of photoresist cross-section 1 – Recipe KL5305_1. R: Registering cursor, M: Measuring cursor.. 34

Figure 26: A typical profile of photoresist on sample 2 (section 1) – Recipe KL5305_1 35

Figure 27: A typical profile of photoresist on sample 3 (section 1) – Recipe KL5305_1 35

Figure 28. Schematic explains the general form of the profile in the experiment. (a) shows the dump at the edge due to the restriction of the tape against the photoresist and the flat area of the profile before removing the tape from the wafer and (b) shows the deformed part of the photoresist at the edge after removing the tape from the wafer... 36

Figure 29. The relative position of the cross-sections and the direction for the measurements of the three samples using KL5305_2 recipe. a) Sample 1, b) Sample 2 and c) Sample 3............... 40

Figure 30. A typical profile of photoresist on sample 1 (section 1) – Recipe KL5305_2. 41

Figure 31. A typical profile of photoresist on sample 2 (section 1) – Recipe KL5305_2. 41

Figure 32 A typical profile of photoresist on sample 3 (section 1) – Recipe KL5305_2. 42

Figure 33. The relative position of the cross-sections and the direction for the measurements of the three samples using KL5305_3 recipe. a) Sample 1, b) Sample 2 and c) Sample 3............... 45

Figure 34. A typical profile of photoresist on sample 1 (section 1) – Recipe KL5305_3 46

Figure 35. A typical profile of photoresist on sample 2 (section 1) – Recipe KL5305_3 47

Figure 36. A typical profile of photoresist on sample 3 (section 1)– Recipe KL5305_3 47

Figure 37. Power meter for measuring the power of the UV light source (ThorLabs S302C)...... 51

Figure 38. The UV light source used in the experiment 9 (LightningCure LC8)........................... 51

Figure 39. The schematic shows the working principle of exposing and develop steps of photoresist. 52

Figure 40. Samples after exposing with UV light source and post exposure bake...................... 53

Figure 41. Photomask used to mask the samples. The circle show the region exposed to the UV light source. It helps to explain the area shape that will be developed as in Figure 40. 53

Figure 42. Samples after developing with 0.26 N TMAH developers... 53

Figure 43. Sample after developing with TMAH and typical positions will be measured on samples. 54

Figure 44. The relative position of the cross-sections and the direction for the measurements of the three samples. a) Sample 1, b) Sample 2 and c) Sample 3... 55

Figure 45. Profile of the cross section through the large arc (section 1) of sample 1................. 56

Figure 46. Typical profile of the cross section through the small circle (section 4) of sample 1. 56

Figure 47. Typical profile of the cross section through the small line (section 5) of sample 1. ... 57

Figure 48. The relative position of the cross-sections and the direction for the measurements of the three samples using KL5305_4 recipe. a) Sample 1, b) Sample 2 and c) Sample 3................ 62

Figure 49. A typical profile of photoresist on sample 1 – Recipe KL5305_4. R: The reference cursor, M: measurement cursor. 63

Figure 50. A typical profile of photoresist on sample 2 – Recipe KL5305_4. R: The reference cursor, M: measurement cursor. 63

Figure 51. A typical profile of photoresist on sample 3 – Recipe KL5305_4. R: The reference cursor, M: measurement cursor. 64

Figure 52. The relative position of the cross-sections and the direction for the measurements of the three samples using KL5305_5 recipe. a) Sample 1, b) Sample 2 and c) Sample 3................ 67

Figure 53. A typical profile of photoresist on sample 1 – Recipe KL5305_5 68

Figure 54. A typical profile of photoresist on sample 2 – Recipe KL5305_5 69

Figure 55. A typical profile of photoresist on sample 3 – Recipe KL5305_5 69

Figure 56. The reference cursor (R) and measurement cursor (M) on sample 1 – Recipe KL5305_5... 70

Figure 57. The reference cursor (R) and measurement cursor (M) on sample 2 – Recipe KL5305_5... 70

Figure 58. The reference cursor (R) and measurement cursor (M) on sample 3 – Recipe KL5305_5... 71

Figure 59. The spin curve of KL 5305 from the experiment and from the datasheet 74

Figure 60. Quartz glass sample used in the experiments 76

Figure 61. Typical pulse trace (upper part) and terahertz spectrum (lower part) of quartz slide in transmission mode when acquiring data. 77

Figure 62. Representative time settings of the stationary delay stage. 78

Figure 63. Quartz glass is set up in transmission mode for measuring pulse trace. 79

Figure 64. Typical pulse trace and terahertz spectrum zoom in the range of 0 – 3 THz. The peaks are absorption lines of water vapor. 80

Figure 65. Power spectrum that extract from raw data of point 1 using OriginPro software. The water vapor absorption lines at 1.099, 1.413, and 1.670 THz... 81

Figure 66. Pulse trace in the time domain 82

Figure 67. Unwrapped phase: Reference signal and sample signal on point 1 and 2. 83

Figure 68. Unwrapped phase of reference signal and sample signal on point 3 and 4. 84

Figure 69. Unwrapped phase: From the experiment on literature (Jepsen, 2019)...................... 85

Figure 70. Phase Difference on points 1, and 2. 86

Figure 71. Phase Difference on points 3 and 4. 87
Figure 72. Phase different from literature (Jepsen, 2019) 87
Figure 73. Refractive index of sample on point 1 and point 2 88
Figure 74. Refractive index of sample on point 3 and point 4 89
Figure 75. The average of refractive index of the quartz glass. 90
Figure 76. Refractive index of Quartz glass as in literature (Jepsen, 2007) 90
Figure 77. Absorption Coefficient of quartz sample on point 1 and point 2 91
Figure 78. Absorption Coefficient of quartz sample on point 3 and point 4 92
Figure 79. Average of Absorption Coefficient of the quartz glass slide. 93
Figure 80. Absorption Coefficient of Quartz glass from Jepsen (2007) [12]. 93

List of Tables

Table 1. Spin Coater Parameter for recipe KL5305_1 30
Table 2. Spin Coater Parameter for recipe KL5305_2 31
Table 3. Spin Coater Parameter for recipe KL5305_3 31
Table 4. Spin Coater Parameter for recipe KL5305_4 31
Table 5. Spin Coater Parameter for recipe KL5305_5 31
Table 6. The Delta height measure on sample 1 with a spin coat recipe KL5305_1. 36
Table 7. The Delta height measure on sample 2 with a spin coat recipe KL5305_1. 37
Table 8. The Delta height measure on sample 3 with a spin coat recipe KL5305_1. 38
Table 9. The average height of the three samples with recipe KL5305_1 38
Table 10. The Delta height measure on sample 1 with a spin coat recipe KL5305_2. 42
Table 11. The Delta height measure on sample 2 with a spin coat recipe KL5305_2. 43
Table 12 The Delta height measure on sample 3 with a spin coat recipe KL5305_2. 43
Table 13. The average height of the three samples with recipe KL5305_2 44
Table 14. The Delta height measure on sample 1 with a spin coat recipe KL5305_3. 48
Table 15. The average delta height of sample 2, spin coat with recipe KL5305_3 48
Table 16. The average delta height of sample 3, spin coat with recipe KL5305_3 49
Table 17. The average delta height with recipe KL5305_3 50
Table 18. The Delta height measure on sample 1 57
Table 19. The Delta height measure on sample 2 58
Table 20. The Delta height measure on sample 3 59
Table 21. The average delta height of sample 1, spin coat with recipe KL5305_4 64
Table 22. The average delta height of sample 2, spin coat with recipe KL5305_4 65
Table 23. The average delta height of sample 3, spin coat with recipe KL5305_4 65
Table 24. The average delta height with recipe KL5305_4 66
Table 25. The average delta height of sample 1, spin coat with recipe KL5305_5 71
Table 26. The average delta height of sample 2, spin coat with recipe KL5305_5 72
Table 27. The average delta height of sample 3, spin coat with recipe KL5305_5 73

Table 28. The average delta height with recipe KL5305_5 73
Table 29. A film thickness of photoresist KL 5305 with different recipes. 74

Chapter 1: Introduction:

LEAP@WPI/QCC and its Goals

Quinsigamond Community College (QCC) and Worcester Polytechnic Institute (WPI) have collaborated to establish the Lab for Education & Application Prototypes at WPI's Gateway Park (LEAP). With the initial funding of $4 million from the Massachusetts Manufacturing Innovation Initiative (M2I2) through the American Institute for Manufacturing Integrated Photonics (AIM Photonics), the LEAP @ WPI/QCC will support the integrated photonics manufacturing sector in central Massachusetts. Namely, LEAP @ WPI/QCC houses state-of-the-art equipment and facilities, enables prototyping of these world-changing integrated photonic devices, and trains the workforce needed to manufacture them.

The LEAP@WPI/QCC facility has three primary objectives – prototyping, training and education, and integrated photonics research [1]. All three of LEAP@WPI/QCC's primary goals are implemented to expand the photonics industry and further its technology and capabilities [2]. The LEAP has cutting-edge fabrication, assembly, and characterization facilities, enabling outstanding capabilities that are not readily available in local universities and industry. However, the powers of these facilities have yet to be explored [3] and this project is a small contributor in the exploitation of its equipment.

What is Photonics?

The science and technology of light are called photonics. Its role is to harness light for numerous applications; its focus is on the technologies to generate, transmit, amplify, modulate, detect, analyze, and utilize light for various practical purposes. Photonics technology is primarily built on optical technology, including optoelectronics, laser systems, optical amplifiers, and novel materials. The scientific background of photonics is in physics, mainly in optical physics and related fields [4].

Today, photonics is a technology that allows us to tackle several challenges of the 21st century, especially in the fields of energy, mobility, health, communications, environment, and security. No other technology has as much impact on our daily lives as photonics. Indeed, photonic and optoelectronic devices are now so widely used that they not only dominate long-distance communication through optical fibers but also open up new fields of application, such as sensors, and they are also beginning penetrate to the data processing areas [5].

Applications and the Importance of Photonics

The typical photonics applications include information technology, health care and life sciences (biophotonics), optical metrology, sensing, manufacturing, illumination and lighting, solar power, and defense and space technology. Optics and photonics technology is poised for even more significant societal impact in the next few decades.

Photonics is a critical 21st-century technology. It supplements electronics in optoelectronics and exhibits strong market growth expected to continue for the near future. So far, photonics

has achieved mass-market penetration and large sales volumes in only a few areas, for example, laser diodes in CDs and DVDs and optical data storage technologies. The use of photonics in today's world provides us with more opportunities and a higher standard of living. It assures our health, security, and safety, it drives our economic growth, and it results in jobs and global effectiveness.

Integrated Photonics

The term *integrated photonics* describes the fabrication and integration of several photonic components onto a common substrate. These components include beam splitters, gratings, couplers, polarizers, interferometers, sources, and detectors. Therefore, these can be used as components of more complex planar devices capable of performing various functions, such as optical communication and CATV systems, instrumentation, and sensors.

Integrated photonics is a synthesis of waveguide technology (guided optics) and other disciplines, such as electro-optics, acoustics, nonlinear optics, and optoelectronics. Integrated photonics uses photons instead of electrons to create integrated optical circuits similar to conventional electronics.

The Objective of Our MQP

The objective of the MQP is to test some of LEAP's equipment and develop its protocols. However, due to the scope of the project, we were only able to examine the spin coater, the profilometer, and TeraHertz spectroscopy.

Among many equipment at the WPI/QCC LEAP, we choose the spin coater and profilometer for testing because they are essential parts and are frequently used in integrated photonic device fabrication. The purpose of the MQP is to ensure that the device in consideration matches the manufacturer's specifications. It also provides the documentation necessary to identify whether the device is working correctly, its control parameters, and adapter ranges correctly. Furthermore, in this MQP work, we will use the Toptica TeraFlash, a time-domain spectrometer, to extract the Quartz glass slide's refractive index and absorption coefficients.

In the next chapter, we will describe and demonstrate how to operate these above devices that used in this project and use chapter 3 to present the experiment results using spin coater and profilometer in measuring the thickness of the positive photoresist. In contrast, we will use chapter 4 to present results using the TeraHertz spectroscope to extract the refractive index and absorption coefficient of a quartz glass slide.

Chapter 2: LEAP Facility Equipment

In this chapter, we will generally discuss a few pieces of equipment at WPI/QCC LEAP that we used in this MQP work: The Cee Apogee spin coater, the Alpha-Step profilometer, and the Toptica TeraFlash terahertz spectroscopy.

2.1 Spin Coater

A spin coater is a machine that is used for spin coating. The spin coating process involves depositing thin films onto flat substrates with a small amount of coating material on the center of the substrate, and the substrate is then rotated up to 10,000 revolutions per minute. The spin coating is heavily used in photolithography to deposit layers of Photoresist about 1 micrometer thick, and it can be used to make nanoscale thin films with uniform thicknesses.

The spin coater in the LEAP facility is the Cee® Apogee™ Spin Coater. Its capacity is up to 200 mm round or 7” x 7” square wafer. Figure 1 shows the spin coater appearance and some notable locations [6].

2.1.1 Equipment Description

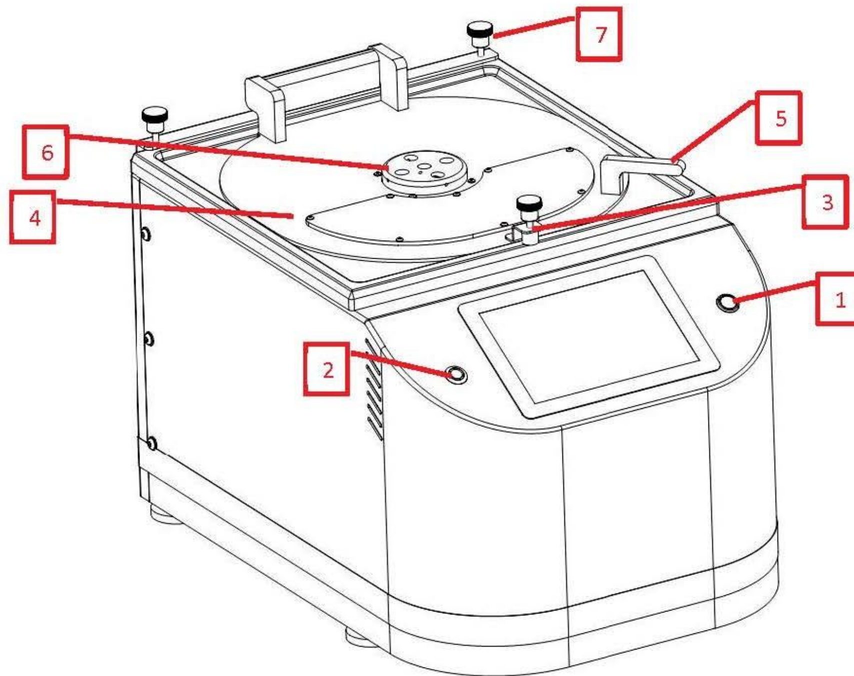

Figure 1 The Cee® Apogee™ Spin Coater [6].

Annotation notes:

1. **Power Button** – Used to turn on and off the tool

2. **User Presence Button** – Used for remote access (see DataStream™ Manual)
3. **Lid Sensor** – Detects when the lid is closed
4. **Spin Coater Lid** – Cover for the spin bowl
5. **Lid Handle** – Used to open and close the lid
6. **Hole Dispense Hub** – Used to dispense material through
7. **Lid Height Adjustment (3X)** – Used to adjust airflow and solvent vapor in the spin bowl

2.2.2 Spin Coater Working Principle

A schematic below shows the working mechanism of the spin coater. The first step in this process is to prepare the substrate (wafer). In substrate preparation, the purpose is to improve the photoresist material's adhesiveness and remove from the wafer any contamination such as small particles, organic films, or water vapor. Next, the wafer is placed on a chuck, and a vacuum is applied to hold the wafer in place. Finally, a thin layer of photoresist is applied by dispensing liquid photoresist and spinning the chuck spindle according to an appropriate recipe.

The figure below illustrates the vacuum chuck that keeps the wafer in place during spindle acceleration while applying centrifugal force to spread the photoresist.

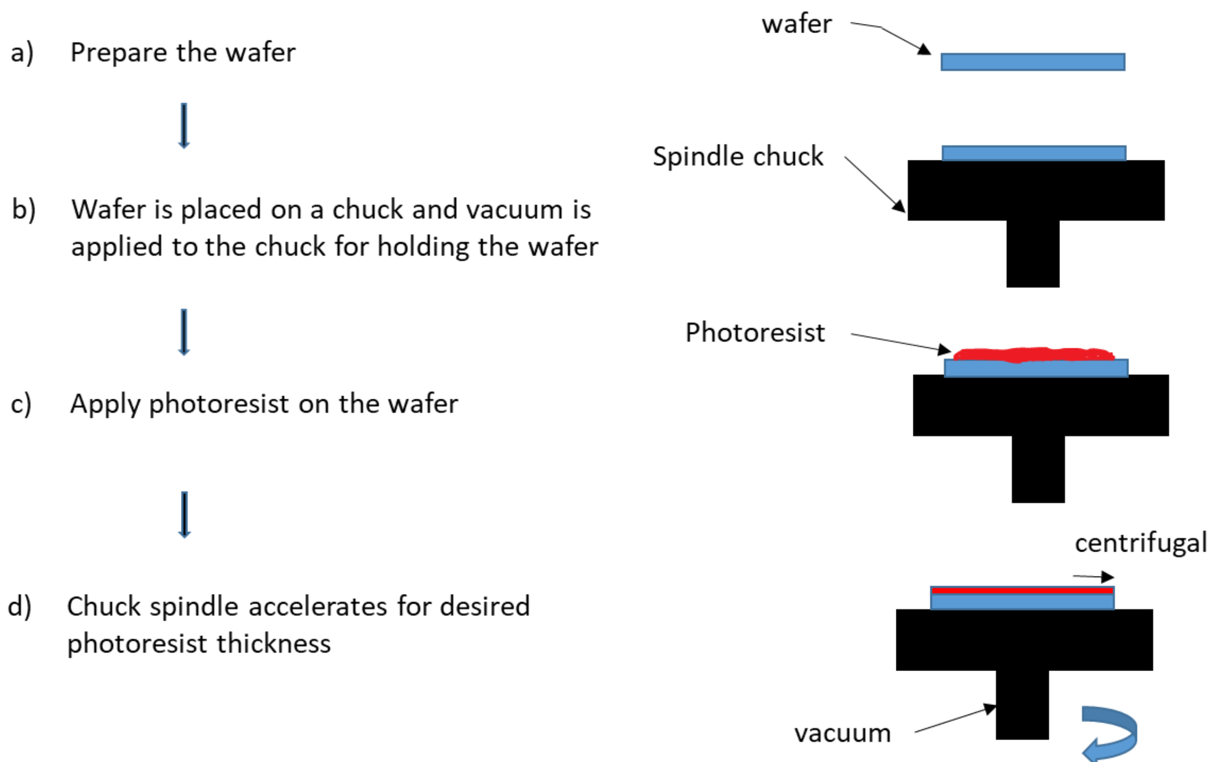

Figure 2. Working principle of spin coater

2.2.3 Spin Coater Operation

The Apogee Spin Coater using DataStream software to operate the equipment. Using the software interface, the user can manually operate the spin coater or run a recipe automatically [7]. The main steps to operate are described in the following sections.

2.2.3.1 Start-Up

1. Turn on the tool power by pressing the lighted power switch. The display should momentarily show the boot screen and then show the main screen.
2. Enter the username and password.
3. The tool will log in and display the Process page as depicted in Figure 3.

   Figure 3 below shows DataStream™ Process Page with annotations: (1) Current user, (2) Active recipe name, (3) Rotate carousel to the graph view, (4) Rotate carousel to the recipe progress view, (5) Process view window, (6) How much of the process has been completed, (7) State of the system parameters, (8) Omni-button that changes depending on the state of the tool
4. Install the spin chuck.
5. Turn on the vacuum pump and checking device before operation (*see* section 2.2.3.2).

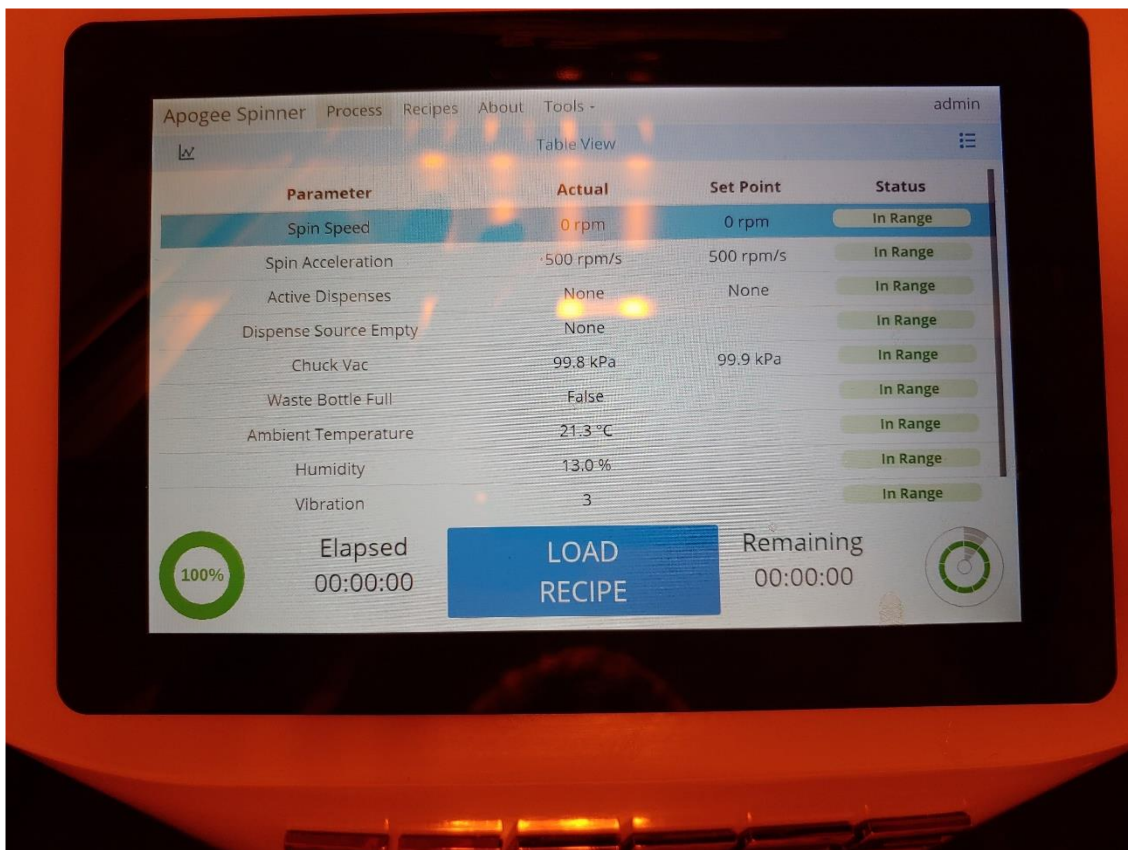

Figure 3 DataStream™ Process Page.

2.2.3.2 Device checking before operation

1. Install the spin chucks. The spin chucks have a slot that matches the pin on the spin-shaft.
2. Test the vacuum of the spin chuck with a substrate using Manual Control. Set the vacuum threshold to 64 kPa. If the vacuum displayed on the monitor screen is less than 64 kPa, the spin chuck passes inspection.
3. Use the Manual Control tool on the Tools page (see section 2.2.3.3) to run system checks on the tool.

2.2.3.3 Tools Page: Manual Tool Operation

The Manual Control page allows users to run many tools independently of a recipe. This mode is useful for prototyping, testing and recovering from failed processes. The Control field lists all the possible options a user has when performing a manual operation. Figure 4 shows Tool page with control field not selected whereas Figure 5 shows an example of Tool page with control field selected for controlling Plate Temperature.

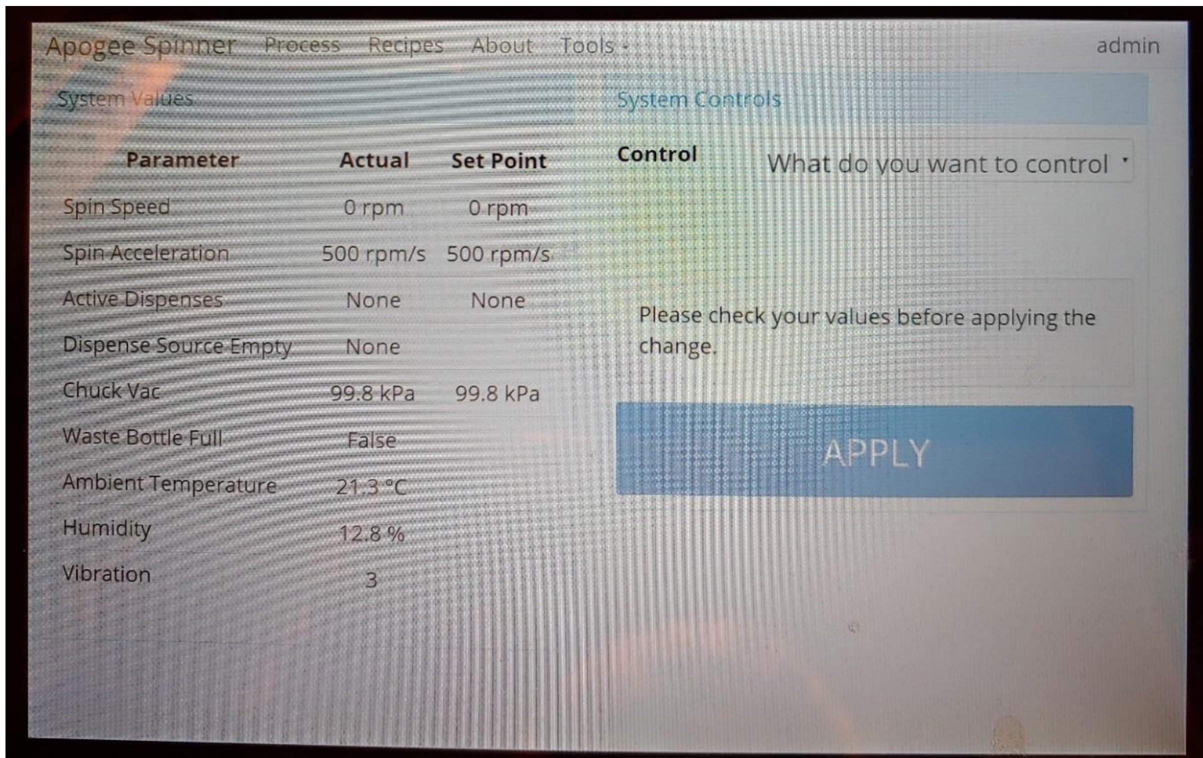

Figure 4. Tool page with control field not selected

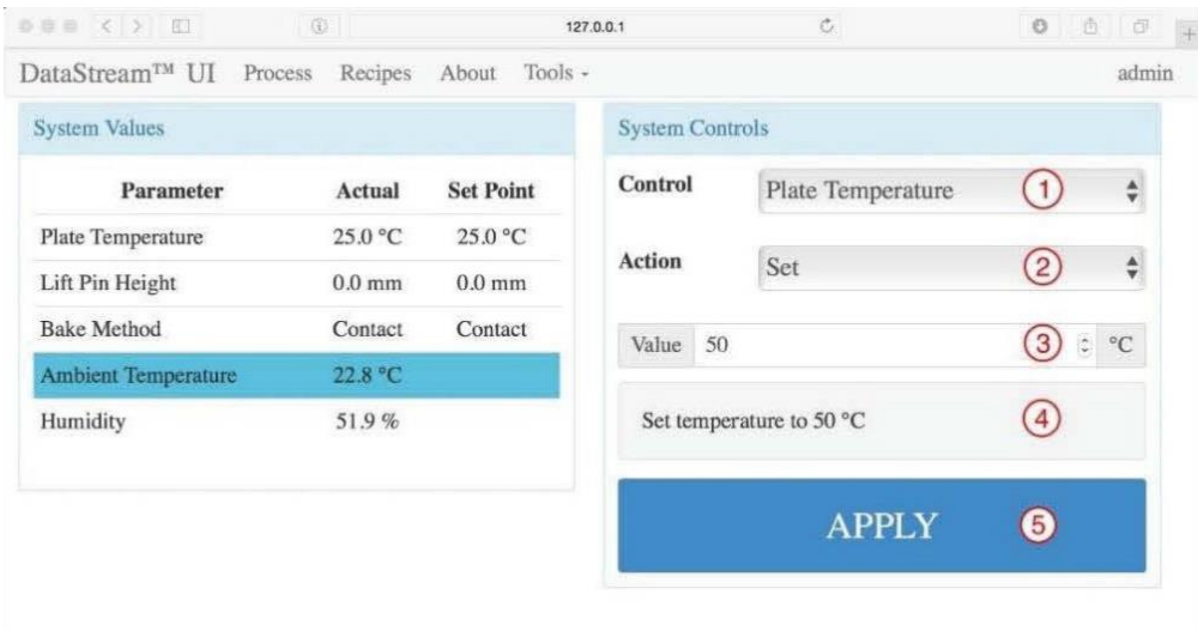

Figure 5. Tool Page for Manual Operation with control field selected for controlling Plate Temperature [7].

2.2.3.4 Running Recipes

After the start-up step, we are ready to run/edit an existed recipe or make a new one by selecting the Recipes page.

1. Select Recipes Page: with this page, we can make a new recipe, edit or load to run an available recipe.

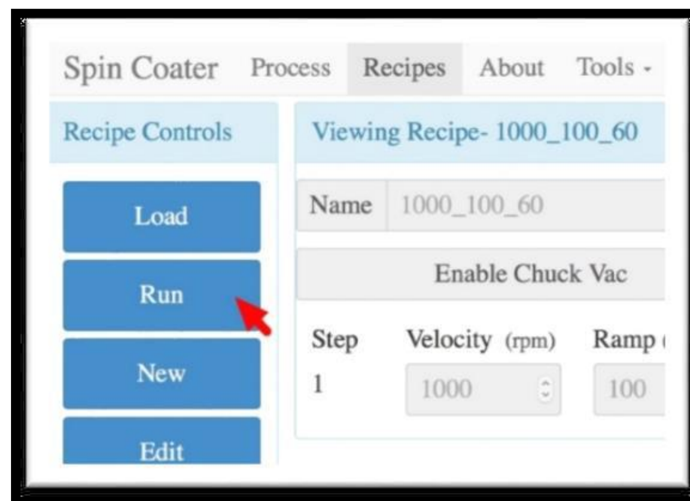

Figure 6. Recipes Controls Page used to Load/Run/New or Edit a recipe [7].

2. Press the Load button to select the recipe to run, the Recipe Selection page appear as in Figure 7. After choosing the appropriate recipe, the screen go back to recipes controls page (Figure 6) where we can run or edit this recipe.

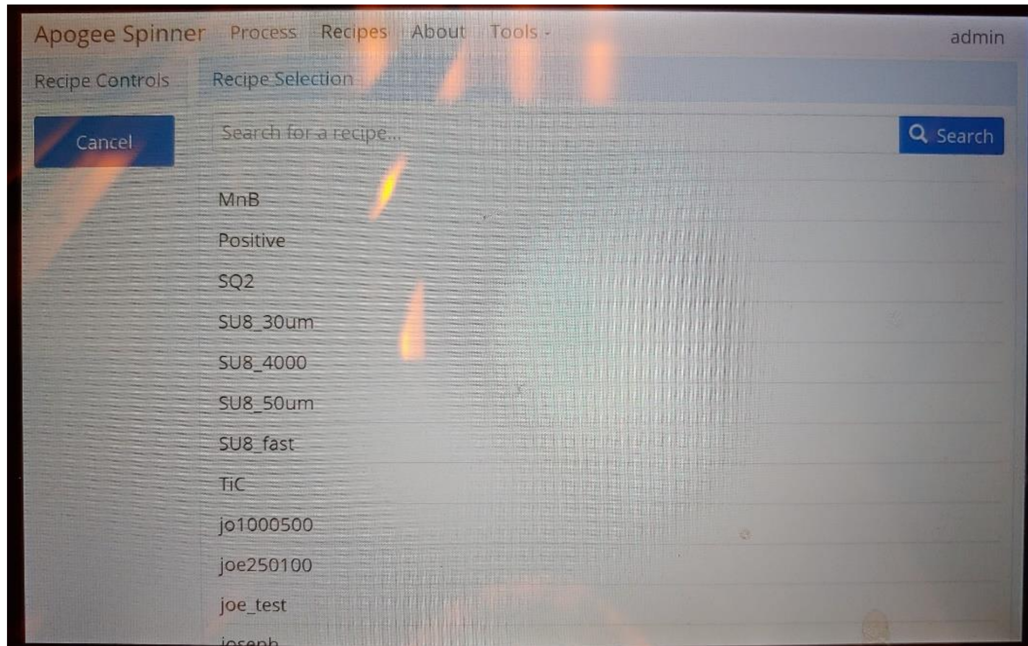

Figure 7. Recipe Selection page after press Load button on Recipes Page on ….

3. We can press the New or Edit button on Recipes Control page to make a new recipe or edit an existing recipe.
4. Click Run button on the Recipes Controls Page for running a recipe. Users may be required to follow prompts on-screen during recipe execution, such as asking the user to confirm if the vacuum is on and the wafer is centered correctly or not. Figure 8 below shows the running screen in process.

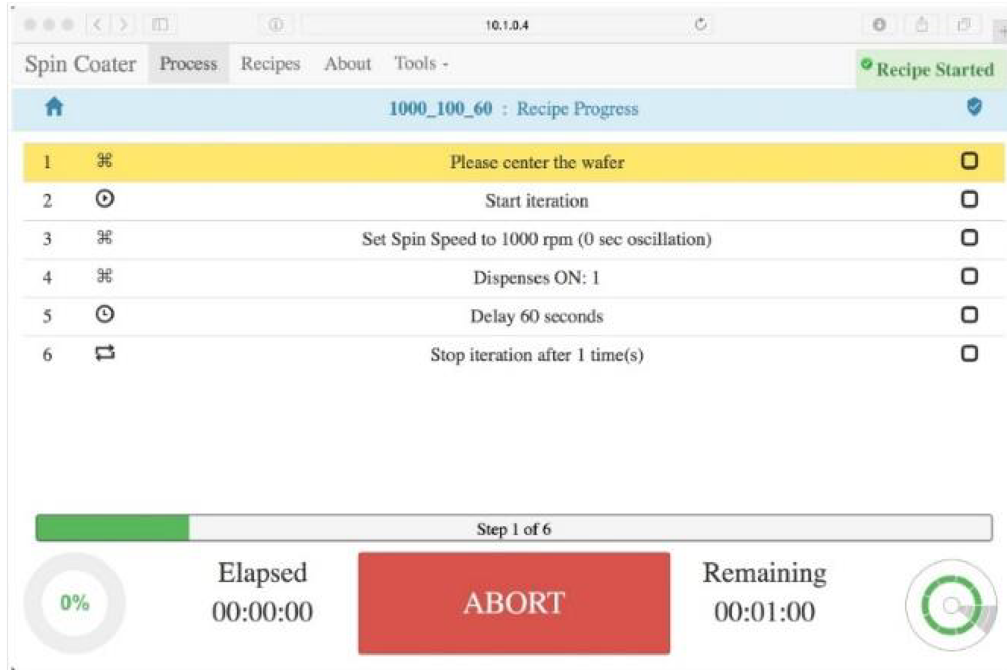

Figure 8. The running screen [7].

2.2 Profilometer

Profilometer are used to measure a surface's topography, such as step, curvature, and flatness, from which their critical dimensions are determined. A mechanical (contact) profilometer is used for the LEAP segment of WPI/QCC, and it can measure very small changes in surface height as a function of position. The diamond stylus generates an analog signal that can be converted into a digital signal, stored, analyzed, and displayed. The tracking force of the diamond stylus can range from 1 to 50 milligrams. The profilometer used in the LEAP core facility is the Alpha-Step Development Series Stylus Profiler made by KLA Tencor.

The working principle of the stylus profilometer shows as in Figure 9. The translation stage can be manually moved on X-Y direction for positioning the location to be measured. When scanning, a translation stage drags the sample under the stylus tip, and the tip remains in contact with the surface. As the stylus shaft rotates about the pivot, laser light reflecting off a mirror above the pivot tracks the motion across a position-sensitive detector. By using an amplified photodetector signal, a computer processes the data and displays a graphical surface profile. At the opposite side of the pivot, the stylus shaft has a static force control system that stabilizes the stylus's force applied to the sample.

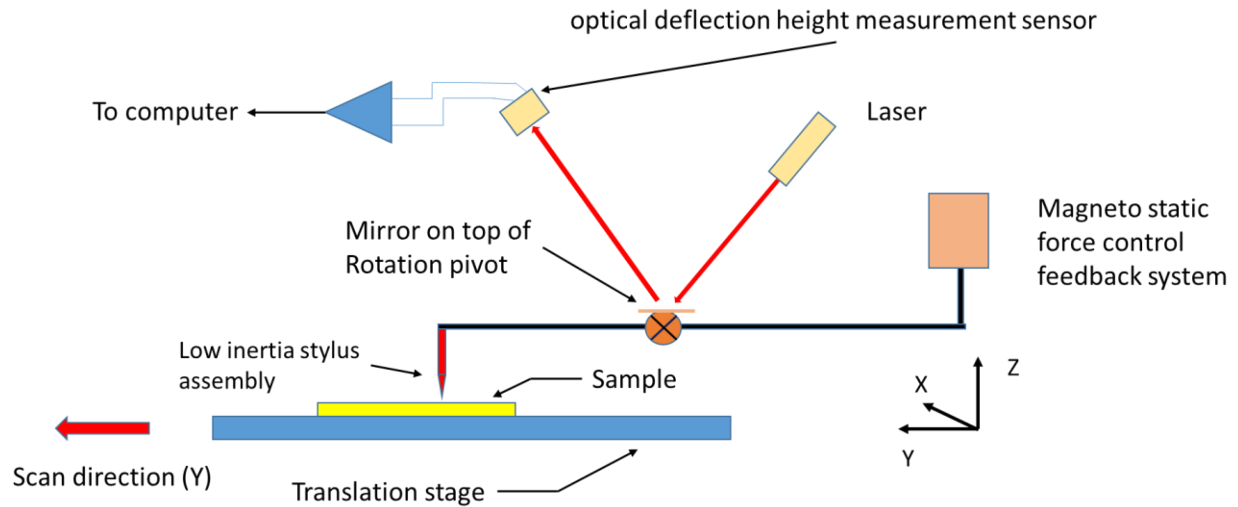

Figure 9. Basic elements and working principle of a stylus profilometer

2.2.1 Equipment Description:

The Alpha-Step D-600 stylus profiler can measure step heights from a few nanometers up to 1200 meters. The D-600 also measures roughness, plus bow and stress in R&D and production environments. The D-600 profiler system includes a motorized stage with a 200mm sample chuck and advanced optics with enhanced video controls [8].

Figure 10. The Alpha-Step D-600 stylus profiler [8].

2.2.2 Basic Operation:

1. Powering up the Instrument
   a) Power on the computer. When the Windows Operating System is fully loaded, the desktop should appear before proceeding to the next step.
   b) After enabling the power to the profiler on the back panel, wait at least 10 seconds before running the profiler software on the PC side, so the Stage and computer can fully establish an USB connection.
   c) Double-click the icon of the control software on the Windows desktop. The system raises the measuring head and moves the sample stage back into its home position.
   d) The system is now ready to use.
2. Loading the Sample
   a) Open the sample stage cover and place the sample on the staging table.
   b) If the stage is not already in the sample load position (closest to the operator, out from under the stylus), select a preset stage position in the Control Panel tab, or manually move the sample stage to the proper point so it can be loaded safely.

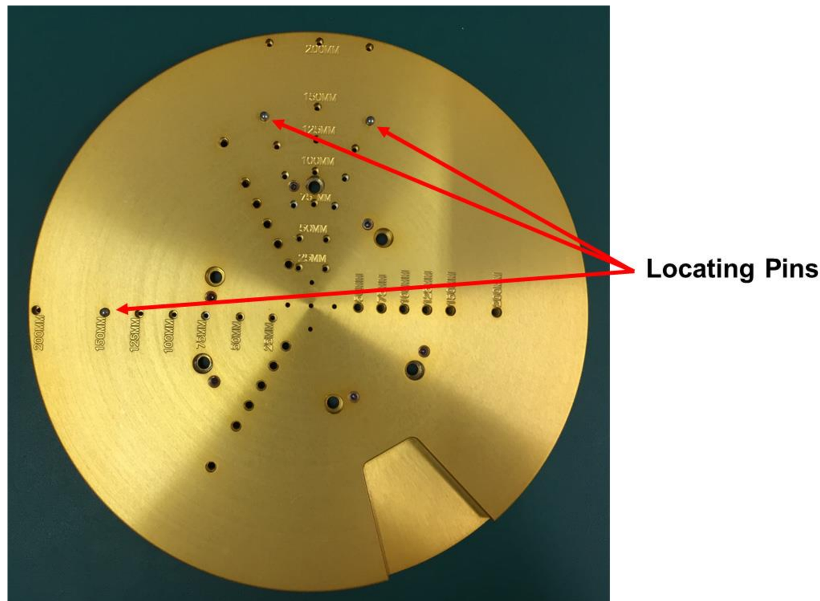

Figure 11. The D-600 Stage table with Precision Locator [8].

   c) Engage the vacuum switch: click Vacuum located on the main software screen in the Z Stage controls panel (see Figure 12).
   d) Move the stage in the Y+ direction using X-Y Stage controls to get the sample to the measurement point. With a naked eye, the user will be able to see whether the

sample is close enough to the measurement point. Use the X-Y controls to position the sample for measurement.

e) Close the sample stage door cover.

2.2.3 Profiling a Sample

1. Load the sample to the stage table.
2. Position the sample stage so that the sample is roughly under the stylus by using X-Y stages control buttons.
3. When the sample has been roughly placed under the stylus, use the Z Stage controls to lower the stylus until the stylus and sample in the Video window can be seen (Figure 11).
4. Click **focus** in the Z stage control panel (Figure 12), the stylus engage the sample and will be lifted from the sample surface after engaging it. The sample will stop in the focus position. If the measurement requires precise positioning then manual move the X-Y stage to the desired position.
5. Set Scan Parameters by selecting the Scan Parameter tab on the bottom left portion of the screen (figure 11) and set the scan parameters appropriate for the measurement. Scan parameters will include scan speed, scan length, scan direction, scan range, stylus force, etc.
6. Press the **Scan** button. The instrument automatically engages the stylus on the sample surface and begins the scan.
7. After the scan is complete, a new Data window displays the profile. The profile appears in the graph display (Figure 13); the Data Control tab is automatically opened along the application window's right side (Figure 14). The Data Control Tab is used to display the cursor information and give options for leveling control.
8. Save the raw data results for 2D scans.

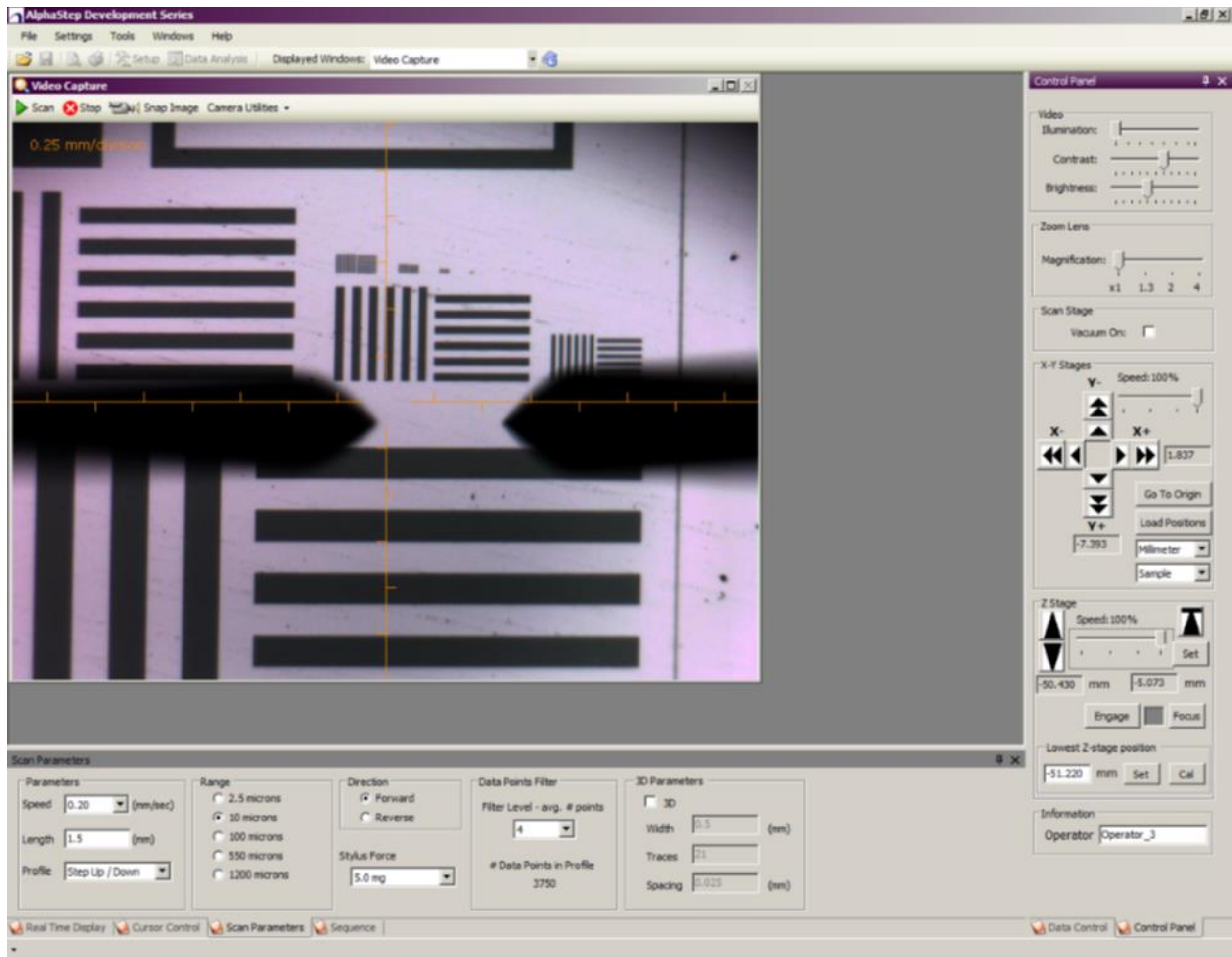

Figure 12. Video Capture screen with Scan Parameters fields. The three other tab that can be selected at the bottom left of the screen are Real Time Display, Cursor Control and Sequence [8].

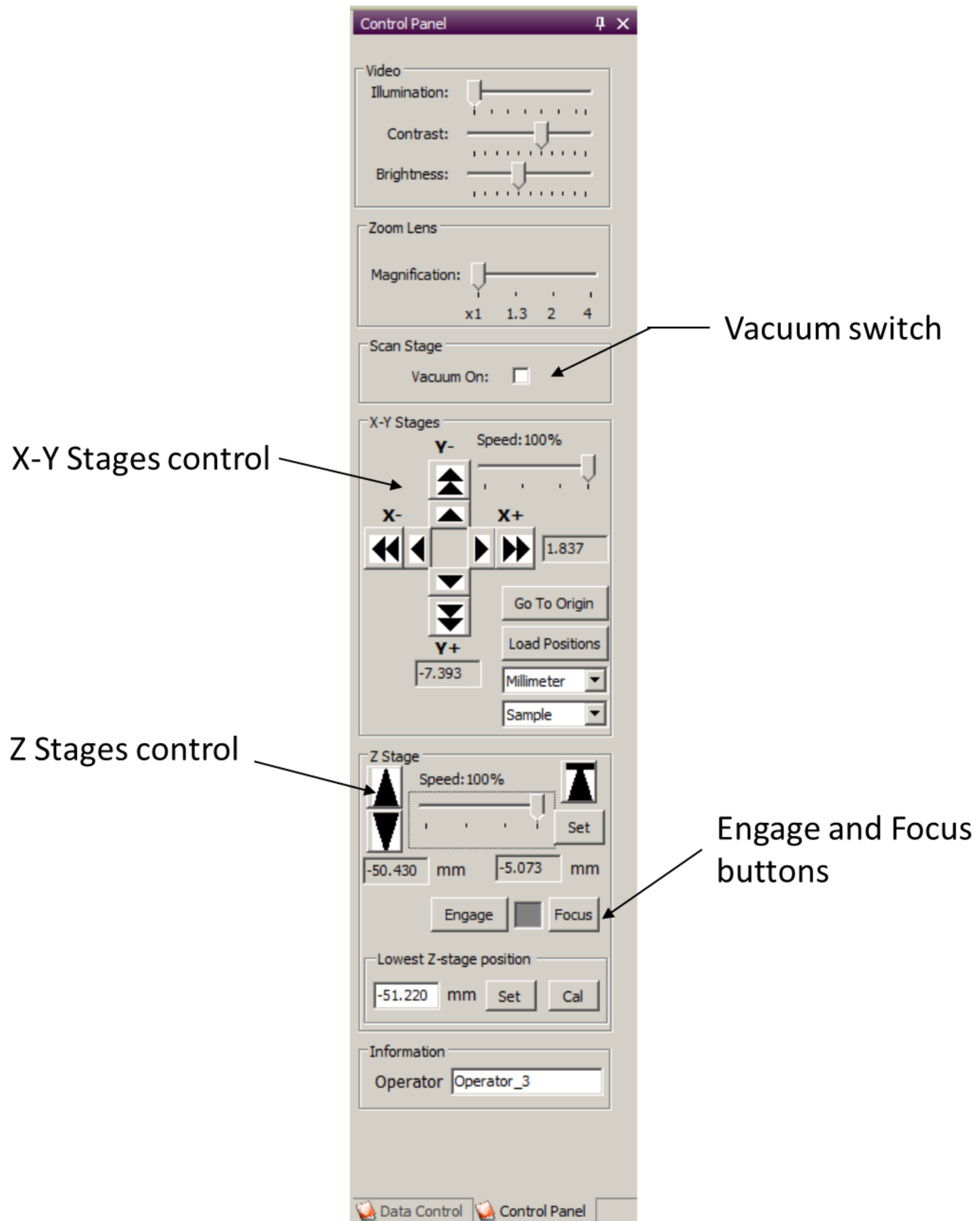

Figure 13. Control Panel [8]

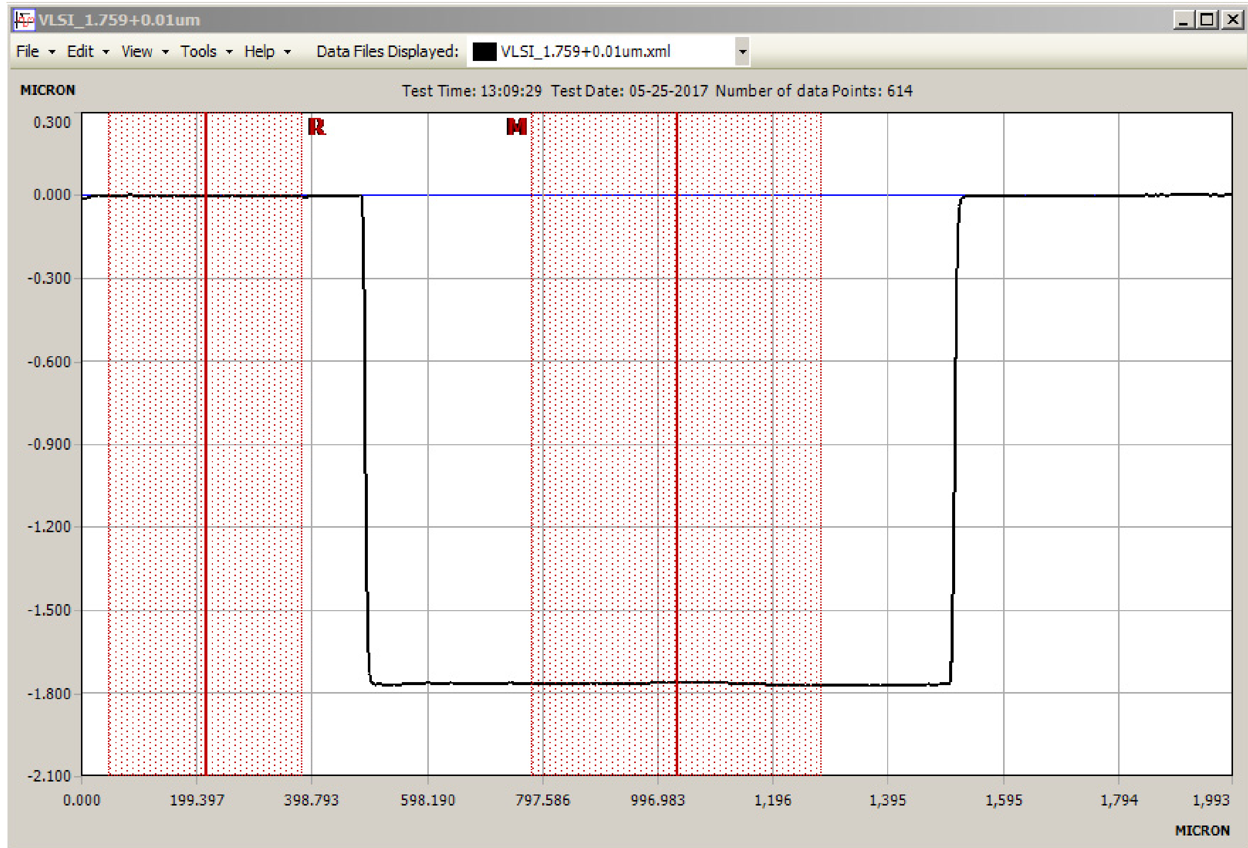

Figure 14. Sample Data window in the Graph display. R: registering cursor and M: measuring cursor. [8]

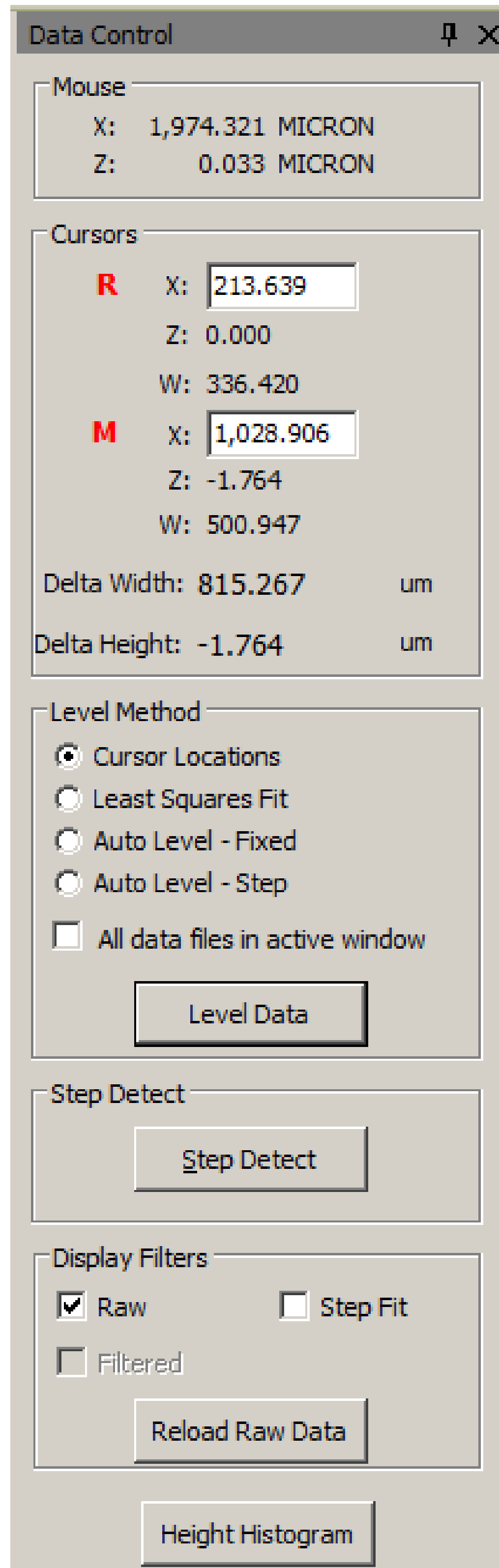

Figure 15. Data Control tab where we can choose method to level the graph. [8]

2.3 TeraHertz Spectroscopy

2.3.1 Introduction

Terahertz Technology refers to electromagnetic waves that propagate in the terahertz range. This term is typically reserved for electromagnetic radiation whose frequencies are between 300 GHz and 3 THz, just above the high-frequency edge of the microwave band. This range corresponds to 0.1 mm (or 100 µm) infrared to 1.0 mm microwave in wavelengths. However, in some literature, THz is included in the spectral region between 0.1 and 30 THz. Terahertz radiation is a non-ionizing submillimeter microwave that can penetrate a wide range of non-conducting materials. It can also penetrate fog and clouds, but cannot penetrate metal or water [11].

In recent years, there has been considerable interest in detecting and characterizing materials using terahertz frequencies using Terahertz spectrometry. In general, spectrometry is a method for measuring a system's properties, e.g., to assess the amount or concentration of a given species. However, terahertz spectrometry goes beyond conventional definitions. In addition to measuring concentration and other analytical properties, it can also identify species via what is known as a *molecular signature spectrum*. This signature spectrum is often unavailable from other spectroscopy methods because some molecular events occur only in the terahertz range, which can only be probed by terahertz spectroscopy.

2.3.2 Toptica TeraFlash Description

In this project, we will use the Toptica TeraFlash, a time-domain spectrometer, to extract the Quartz glass slide's refractive index and absorption coefficients. We use this section to discuss the working principle of a TeraHertz spectroscopy in a typical time-domain setup (THz-TDS) and delay presenting the experiment results to chapter 4.

As depicted in the schema (Figure 15), the pulsed terahertz radiation is generated with femtosecond lasers. The laser pulse is then split in two, with one part traveling to the terahertz emitter and the second part traveling to the detector after interacting with a sample. The ultrashort laser pulses create charge carriers in the emitter, which are then accelerated by an externally applied bias field. The resulting current transient results in an electromagnetic pulse that is radiated into free space.

The detector works in a "pump and probe" fashion: the incident terahertz pulse generates a voltage across the receiver antenna, which accelerates the charge carriers produced simultaneously by the "probe" laser pulse. The photocurrent resulting from the terahertz electric field is directly proportional to it. [9]

The terahertz pulse generated by THz-TDS systems (~1ps) is much longer than the probing laser pulse of 50 - 60 fs. Therefore, each time the laser pulse hits the detector, only a fraction of the terahertz pulse is sampled. To obtain the full pulse shape, a variable delay stage scans the terahertz wave packet with a shorter probe pulse (Figure 16). They are then subjected to a Fast Fourier Transform to produce the terahertz spectrum.

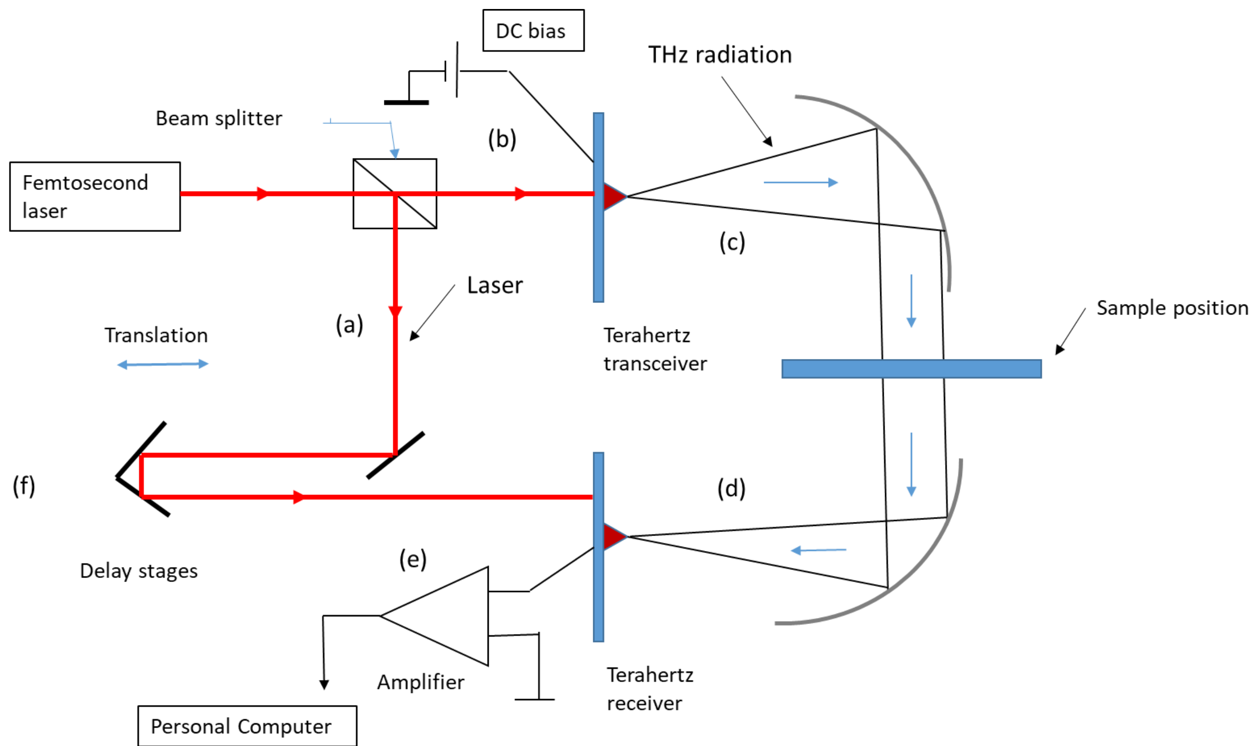

Figure 16. Schematic shows working principle of terahertz spectroscopy.

a) The laser pulse radiation is split in two, with one part traveling to the terahertz emitter and the second part traveling to the detector after interacting with a sample.

b) The ultrashort laser pulses create charge carriers in the emitter, which are then accelerated by an externally applied bias field.

c) The resulting current transient results in an electromagnetic pulse that is radiated into free space.

d) The incident terahertz pulse generates a voltage across the receiver antenna, which accelerates the charge carriers produced simultaneously by the "probe" laser pulse.

e) Each time the laser pulse hits the detector, only a fraction of the terahertz pulse is sampled.

f) To obtain the full pulse shape, a variable delay stage scans the terahertz wave packet with a shorter probe pulse.

The TERAFLASH system (Figure 17) combines femtosecond laser technology and InGaAs photoconductive switches to provide a bandwidth greater than 5 THz and a peak dynamic range greater than 90 dB- thanks to a sophisticated mechanical delay stage. The wavelength is 1560 nm, the repetition rate is 100 MHz, and the pulse width is typically 50 to 60 fs. The laser provides approx.— 80 mW power at the polarization-maintaining fiber output. The dispersion-compensating fibers (DCF) in the fiber-optic beam path help to correct for dispersion effects in the fiber delivery.

The entire system is built on mature 1.5 µm technology, and the antenna modules use single-mode, polarization-maintaining fibers (Figure 17). Optical pulses on both arms are guided to fiber-coupled, In GaAs-based photoconductive switches that work as a terahertz emitter and detector. The fiber-pigtailed design allows either transmission or reflection configuration [9].

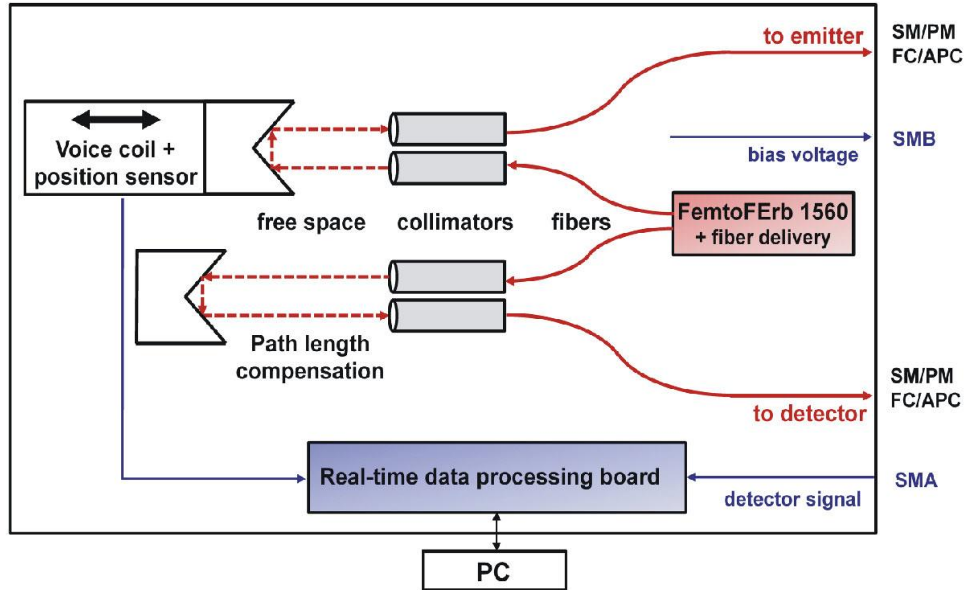

Figure 17. Schematic representation. Blue lines denote electric connections, red lines the optical signal paths [9]

Figure 18. Toptica TeraFlash TeraHertz spectroscopy at LEAP

Chapter 3: Spin Coater and Profilometer

3.1 Testing the Spin Coater and the KLA Stylus Profiler

For testing the spin coater and the profiler, we use a Si wafer coated with KemLab KL 5305 positive photoresist. This photoresist is optimized for i-Line (365 nm wavelength UV radiation for exposure), g-Line (436 nm wavelength UV radiation), and broadband applications. From the manufactured datasheet, the KL5305 photoresist offers high sensitivity, and high throughput suitable for IC fabrication and has a film thickness range of 400 – 900 nm [10]. It is also designed for use with industry-standard 0.26 N TMAH developers.

The objective of this set of experiments is to apply several different recipes on the spin coater, to the samples coated with photoresist, and then using the KLA profiler to measure the corresponding thickness. The results from the measurements will be later compared with the datasheet of the KL 5300 series. Besides, during the preparation and measuring processes, the features and performance of the equipment are also gathered and checked. The data acquired from the testing will be used in the later steps of the MQP such as on the exposure step.

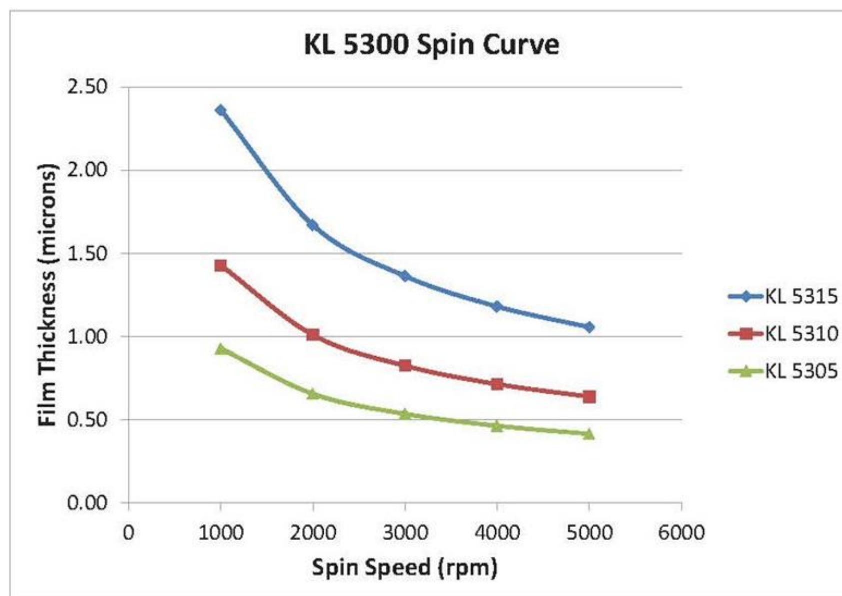

Figure 19. KemLab KL 5300 series Spin Curve from manufacturer datasheet [10].

3.2 Procedure for the testing

Following are the general steps using in the testing process, in each specific measurement we will give more details on the condition of the measurement.

1. Clean the wafer without using Ultrasound Cleaner:
   - Clean the wafer with Acetone in 30 sec and wash it with Isopropyl Alcohol (IPA)
   - Dry it by N_2 blow.

Or,

2. Clean the wafer with Ultrasound Cleaner:

Figure 20. The ultrasound cleaner

- ✓ Fill water into the water bath of the ultrasound cleaner (Figure 20) with the level water high enough so that the baker (which contains acetone) is not touching any solid surface of the bath (bottom and sidewall).
- ✓ Make sure that the beaker floating balance and then put the wafer into the acetone beaker.
- ✓ Apply 3 – 4 minutes of ultrasound.
- ✓ Take out the wafer from acetone and wash it with IPA.
- ✓ Dry it by N_2 blow.

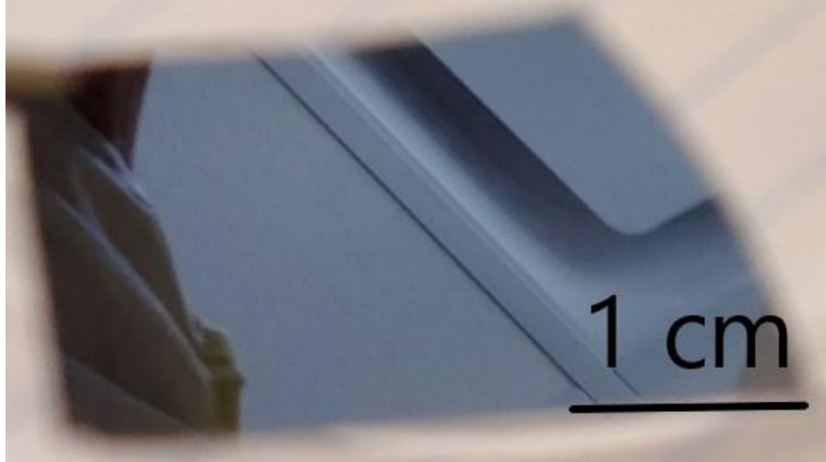

Figure 21. A typical clean wafer after using ultrasound cleaner.

3. Put a piece of Kapton tape on the edge of the clean wafer to make the step for the measurement.

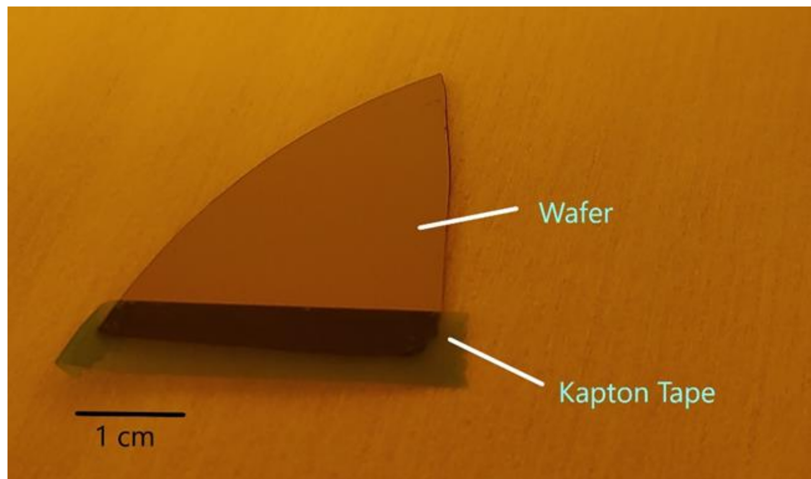

Figure 22. Wafer prepared with Kapton tape for making step for thickness measurements.

4. Take the wafer to the spin coater and apply the corresponding recipe. In this part of the testing, we use five different recipes, named KL5305_1, KL5305_2, KL5305_3, KL5305_4 and KL5305_5 with the parameters shown in the tables below:

Table 1. Spin Coater Parameter for recipe KL5305_1

Recipe	KL5305_1		
	Velocity (rpm)	Ramp (rpm/s)	Time (seconds)
Step 1	500	500	5
Step 2	1000	1000	45

Table 2. Spin Coater Parameter for recipe KL5305_2

Recipe	KL5305_2		
	Velocity (rpm)	Ramp (rpm/s)	Time (seconds)
Step 1	500	500	5
Step 2	2000	1000	45

Table 3. Spin Coater Parameter for recipe KL5305_3

Recipe	KL5305_3		
	Velocity (rpm)	Ramp (rpm/s)	Time (seconds)
Step 1	500	500	5
Step 2	3000	1000	45

Table 4. Spin Coater Parameter for recipe KL5305_4

Recipe	KL5305_3		
	Velocity (rpm)	Ramp (rpm/s)	Time (seconds)
Step 1	500	500	5
Step 2	4000	1000	45

Table 5. Spin Coater Parameter for recipe KL5305_5

Recipe	KL5305_3		
	Velocity (rpm)	Ramp (rpm/s)	Time (seconds)
Step 1	500	500	5
Step 2	5000	1000	45

5. Soft bake of 105 ^{o}C in 3 minutes.

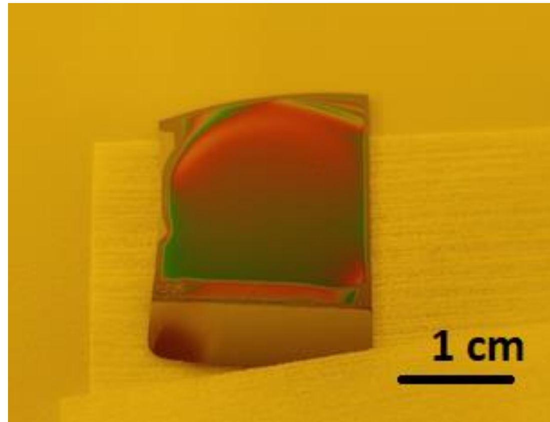

Figure 23. A typical sample after soft bake and Kapton tape removed.

6. Measure the sample on the KLA Stylus profiler.
   - ✓ Take measurements in 3 - 4 sections of each sample where possible. The cross-sections are about 4-5 mm apart.
   - ✓ Set scan length far enough based on the observation of the sample.
   - ✓ Generally, on each cross-section, we measured 3 points, each point is approximately 0.3 mm apart on the graph. Starting at a point about 0.6 - 1 mm from the edge to avoid artifact made by the tape (Figure 28).
7. Save data files for the measurement of each cross-section.
8. Take a screenshot for each measuring point with the measuring cursor so we can collect the Data Height at this location and use it for the thickness calculation later (Figure 25).
9. Make 3 samples for each recipe.

3.3 Measurement Results:

3.3.1 Recipe KL5305_1:

a) <u>Sample description</u>:

The samples prepared by the recipe KL5305_1 have two separate regions, which can be easily seen by naked eyes. It was created by the influence of the tape on the photoresist during the spin process (see Figure 28). The region near the edge has a width of about 2 mm that we will discard when collecting the data. Figure 24 shows the relative position of the cross-sections and the arrows in the figures show the direction for the measurements.

Furthermore, we also noted that the coated film's color on the wafer after the soft-bake step is varied greatly. It is most visible in fringe areas or edges of the sample. This phenomenon proved that the photoresist thickness is not uniform due to the uneven heat distribution during the soft bake step.

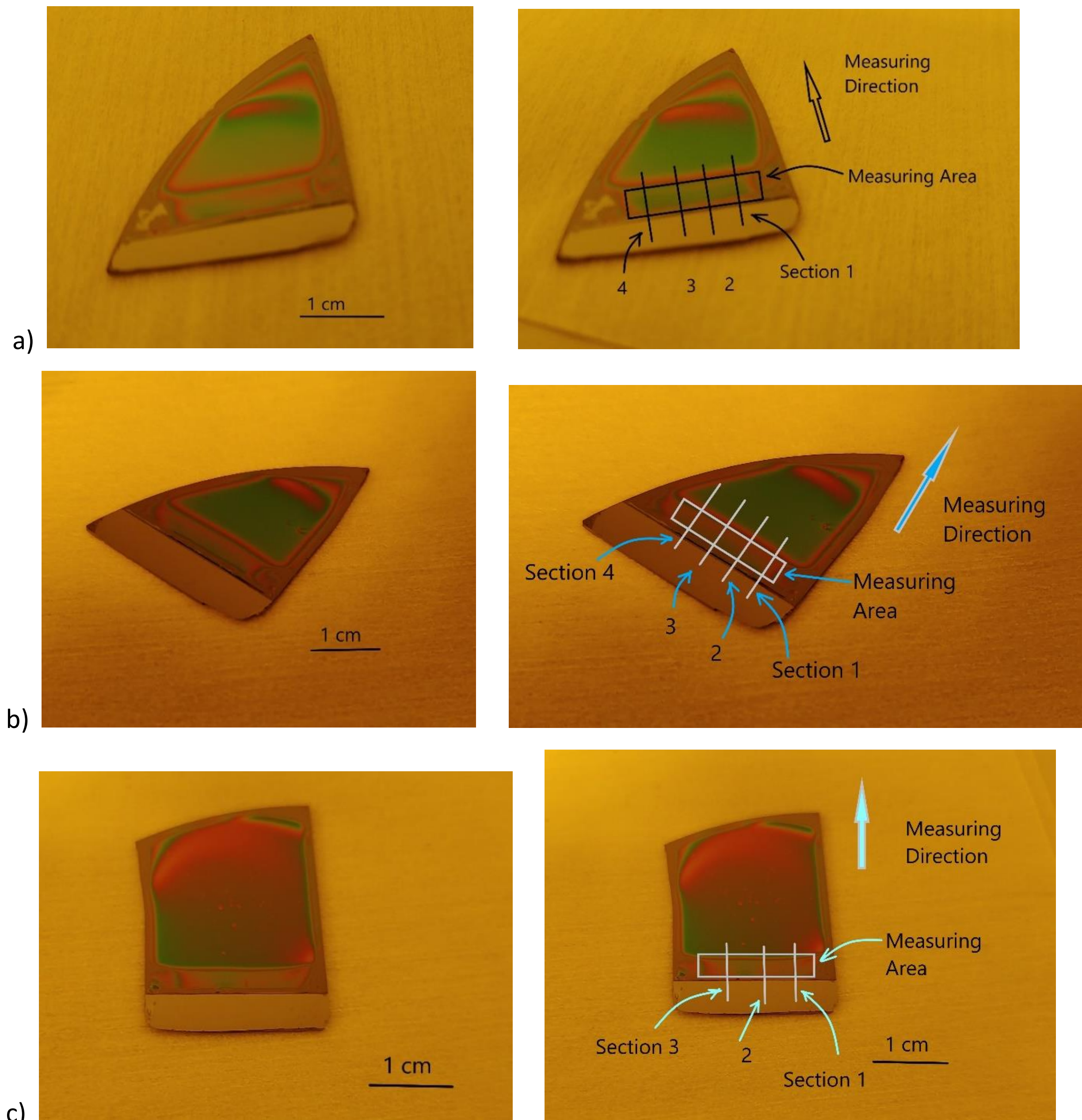

Figure 24. The relative position of the cross-sections and the direction for the measurements of the three samples using KL5305_1 recipe. a) Sample 1, b) Sample 2 and c) Sample 3

b) <u>Scan parameters</u>:

- Speed: 0.05 mm/sec
- Length: 3 mm
- Range: 100 microns
- Stylus force: 5 mg
- Level method: Cursor location

c) Scan results:

The following pictures (Figures 25, 26 and 27) show the typical profile for each sample with the same above scan parameters.

In general, the graphs can be distinguished into three regions: a sharp peak at the beginning of the graph, followed by a short dump and finally a flat area. The below schematic in Figure 28 (not in scale) suggest an explanation for this phenomena.

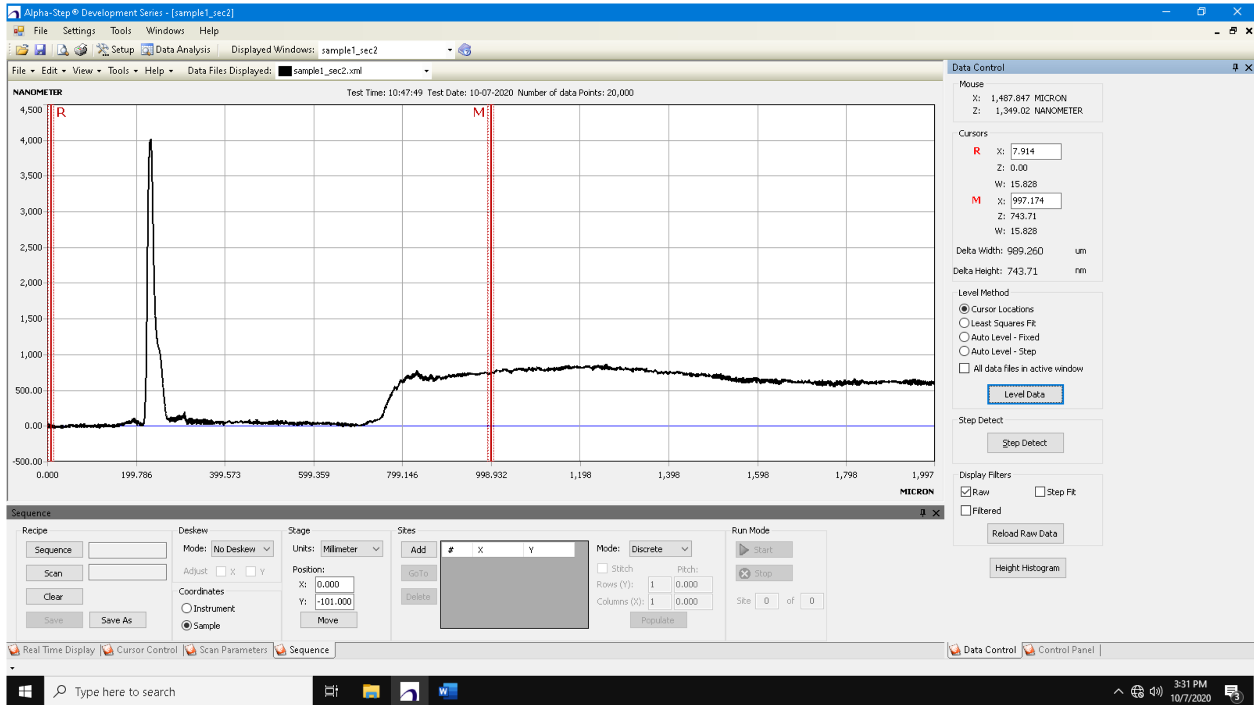

Figure 25: A typical profile of photoresist cross-section 1 – Recipe KL5305_1. R: Registering cursor, M: Measuring cursor

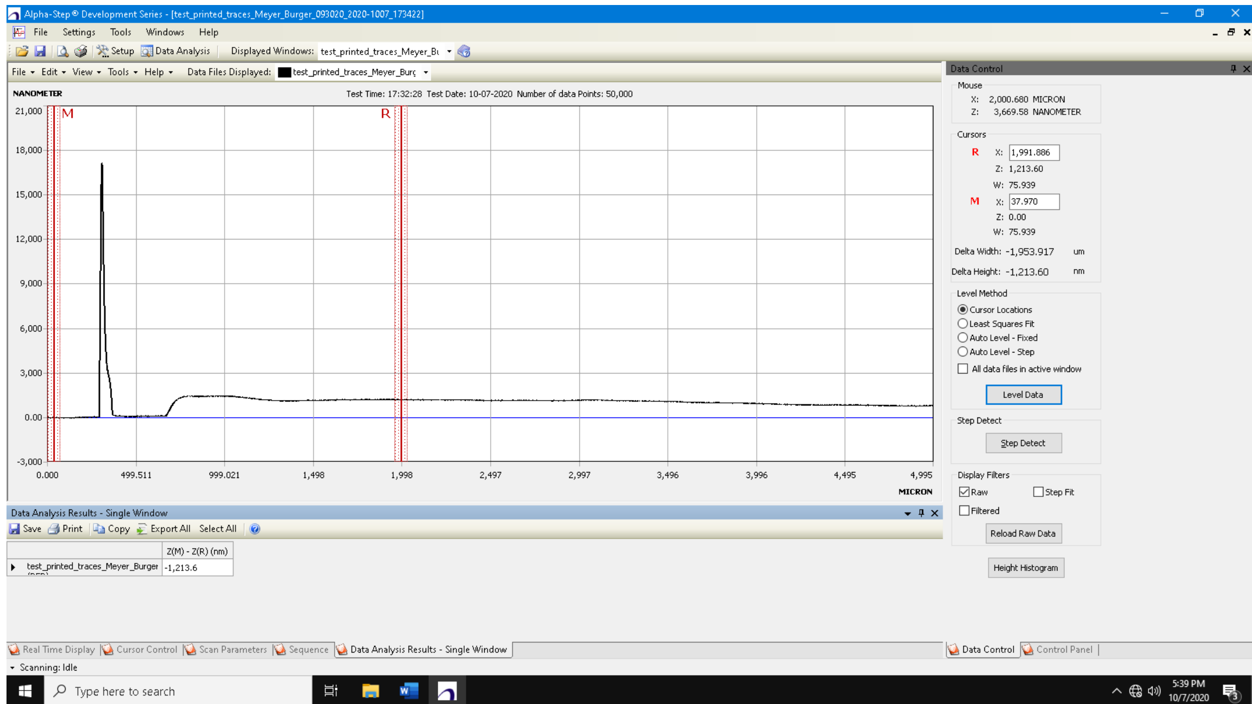

Figure 26: A typical profile of photoresist on sample 2 (section 1) – Recipe KL5305_1

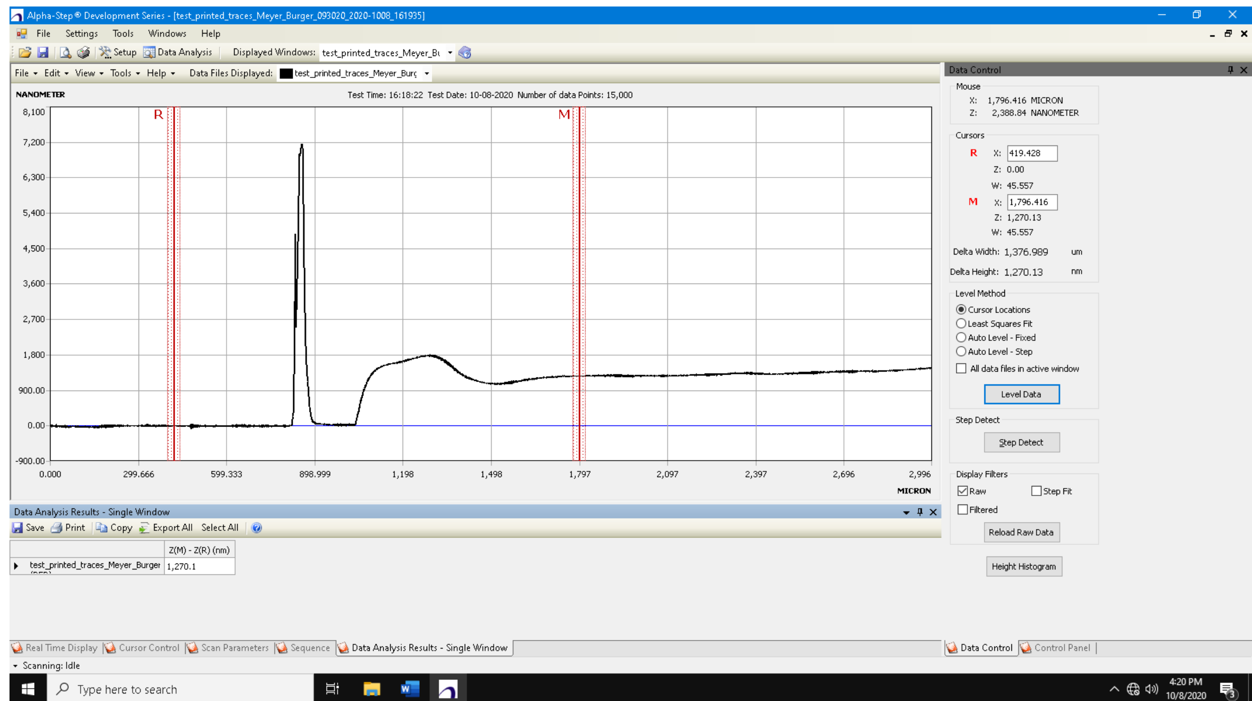

Figure 27: A typical profile of photoresist on sample 3 (section 1) – Recipe KL5305_1

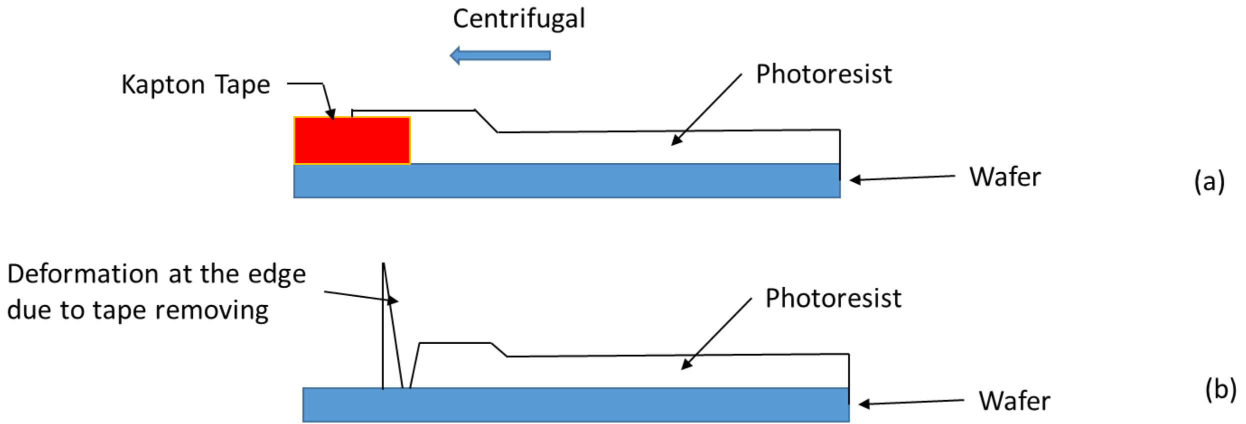

Figure 28. Schematic explains the general form of the profile in the experiment. (a) shows the dump at the edge due to the restriction of the tape against the photoresist and the flat area of the profile before removing the tape from the wafer and (b) shows the deformed part of the photoresist at the edge after removing the tape from the wafer.

d) <u>Measurement results and Analyzing data on the sample with recipe KL5305_1</u>:

After putting the measurement data of the three samples with recipe of 1000 rpm into Excel for analysis, the results of the measurements can be summarized as below:

Table 6. The Delta height measure on sample 1 with a spin coat recipe KL5305_1.

<table>
<tr><th></th><th>Delta Height (nm)</th><th>Average Delta Height (nm)</th><th>Standard Deviation (nm)</th><th>Average height of sample (nm)</th></tr>
<tr><td>Section 1</td><td></td><td rowspan="5">1143.68</td><td rowspan="5">16.62</td><td rowspan="15">997.80 ± 150.02</td></tr>
<tr><td>1</td><td>1146.74</td></tr>
<tr><td>2</td><td>1131.58</td></tr>
<tr><td>3</td><td>1165.98</td></tr>
<tr><td>4</td><td>1130.43</td></tr>
<tr><td colspan="4"></td></tr>
<tr><td>Section 2</td><td></td><td rowspan="5">847.98</td><td rowspan="5">95.88</td></tr>
<tr><td>1</td><td>982.43</td></tr>
<tr><td>2</td><td>849.15</td></tr>
<tr><td>3</td><td>792.46</td></tr>
<tr><td>4</td><td>767.86</td></tr>
<tr><td colspan="4"></td></tr>
<tr><td>Section 3</td><td></td><td rowspan="3">890.73</td><td rowspan="3">38.41</td></tr>
<tr><td>1</td><td>941.46</td></tr>
<tr><td>2</td><td>893.22</td></tr>
</table>

3	878.76			
4	849.46			
Section 4				
1	1129.69	1108.83	37.24	
2	1144.58			
3	1101.09			
4	1059.96			

Table 7. The Delta height measure on sample 2 with a spin coat recipe KL5305_1.

	Delta Height (nm)	Average Delta Height (nm)	Standard Deviation (nm)	Average height of sample (nm)
Section 1				1183.24 ± 67.07
1	1213.60	1179.54	31.65	
2	1151.04			
3	1173.97			
Section 2				
1	1212.02	1218.13	30.30	
2	1191.36			
3	1251.02			
Section 3				
1	1110.12	1090.90	24.27	
2	1063.63			
3	1098.95			
Section 4				
1	1288.14	1244.38	40.69	
2	1207.69			
3	1237.31			

Table 8. The Delta height measure on sample 3 with a spin coat recipe KL5305_1.

	Delta Height (nm)	Average Delta Height (nm)	Standard Deviation (nm)	Average height of sample (nm)
Section 1				
1	1329.98	1390.52	66.89	
2	1379.25			
3	1462.33			
Section 2				
1	1324.85			
2	1388.71			1415.69 ± 46.05
3	1449.56	1387.71	62.36	
	1545.17			
Section 3				
1	1387.94	1468.84	87.49	
2	1418.78			
3	1482.64			
4	1585.99			

e) Data analysis and Conclusion

The average height of each sample is summarized in table 10. From which we can conclude:

Table 9. The average height of the three samples with recipe KL5305_1

	Average Delta Height (nm)	The average height of the three samples (nm)
Sample 1	997.80	1198.91 ± 209.39
Sample 2	1183.24	
Sample 3	1415.69	

- The average height varies significantly from sample to sample.
- On sample 1, the thickness of photoresist vary significantly from section to section.
- It could be due to an artifact induced by the lack of skill on some very first experiment. They may include:
  - ✓ not providing relatively equal amount of photoresist to each sample.

- ✓ not centered the wafer correctly.

- However, we will temporarily accept this result as the thickness of the photoresist with the recipe of 1000 rpm.

3.3.2 Recipe KL5305_2:

a) <u>Sample description</u>:

The samples prepared by the recipe KL5305_2 also have two separate regions, which can be easily seen by naked eyes. The region in the center area of the samples look having the same thickness. The following pictures (Figure 29) show the relative position of the measurement cross-sections. The arrows in the figures show the scan direction.

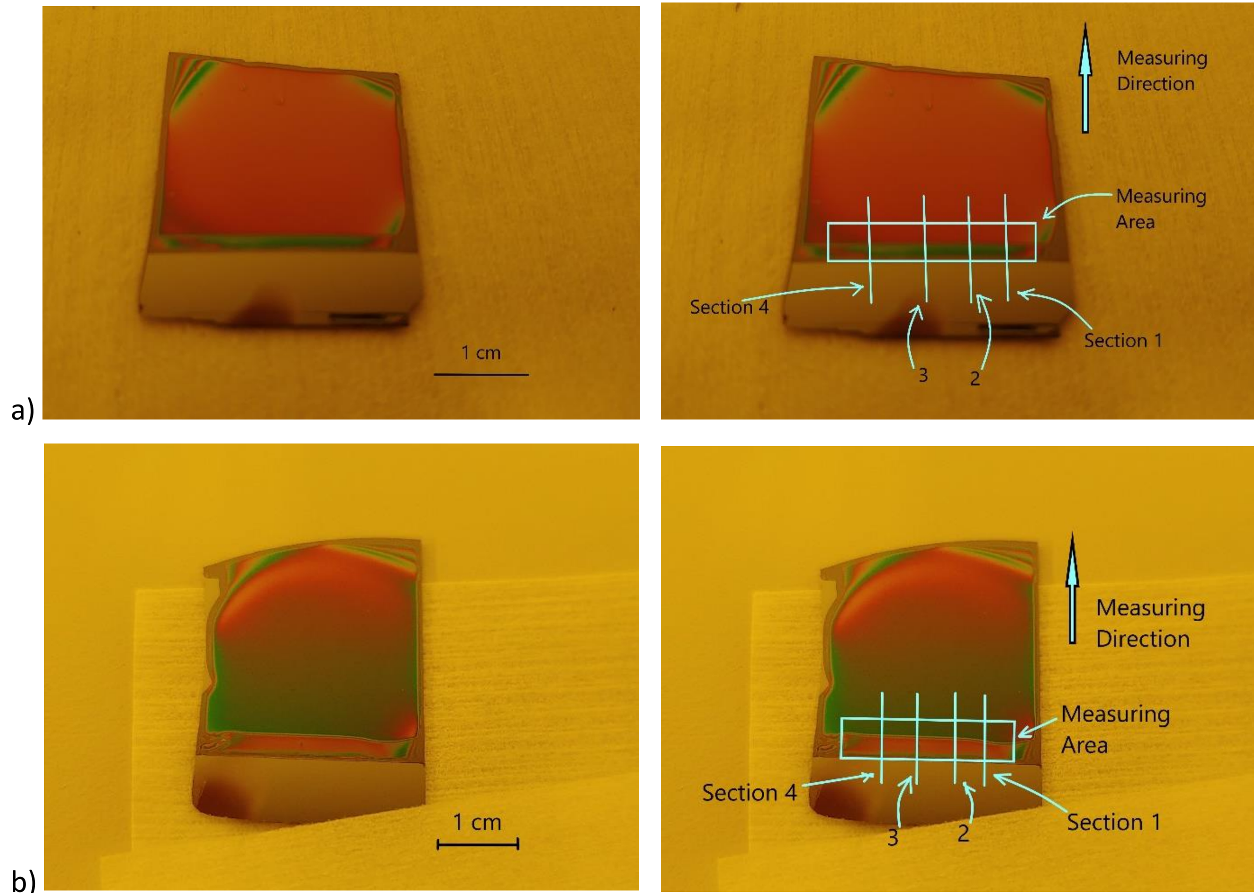

c) 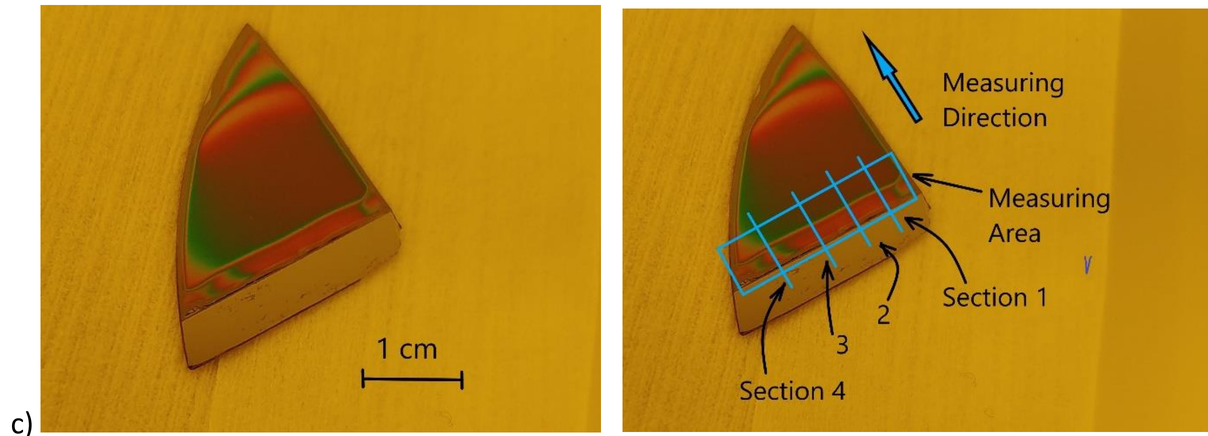

Figure 29. The relative position of the cross-sections and the direction for the measurements of the three samples using KL5305_2 recipe. a) Sample 1, b) Sample 2 and c) Sample 3

b) Scan parameters:

- Length: 4.5 mm
- Range: 100 microns
- Stylus force: 5 mg
- Leveling method: Cursor location

c) Scan results:

The following pictures (Figures 30, 31 and 32) show the typical profile for each sample with the same above scan parameters. In general, there is no special in the shape of the graphs. They look the same as those in the experiment of recipe KL5305_1.

Figure 30. A typical profile of photoresist on sample 1 (section 1) – Recipe KL5305_2.

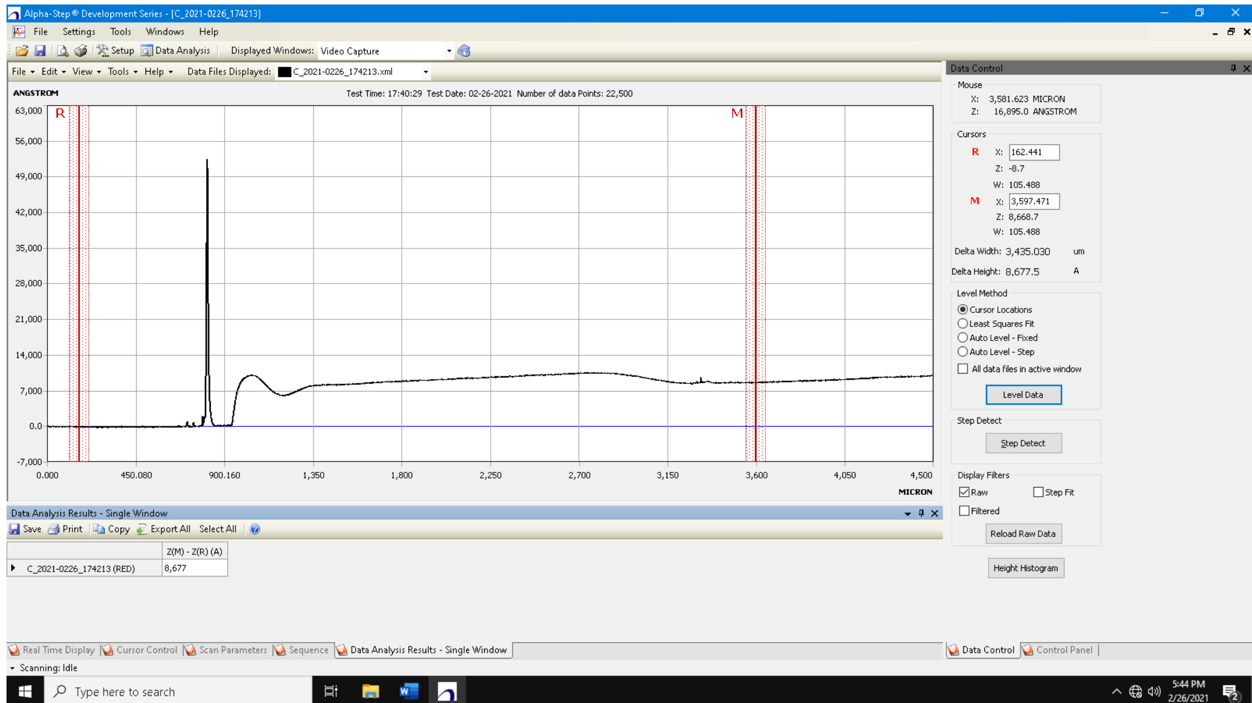

Figure 31. A typical profile of photoresist on sample 2 (section 1) – Recipe KL5305_2.

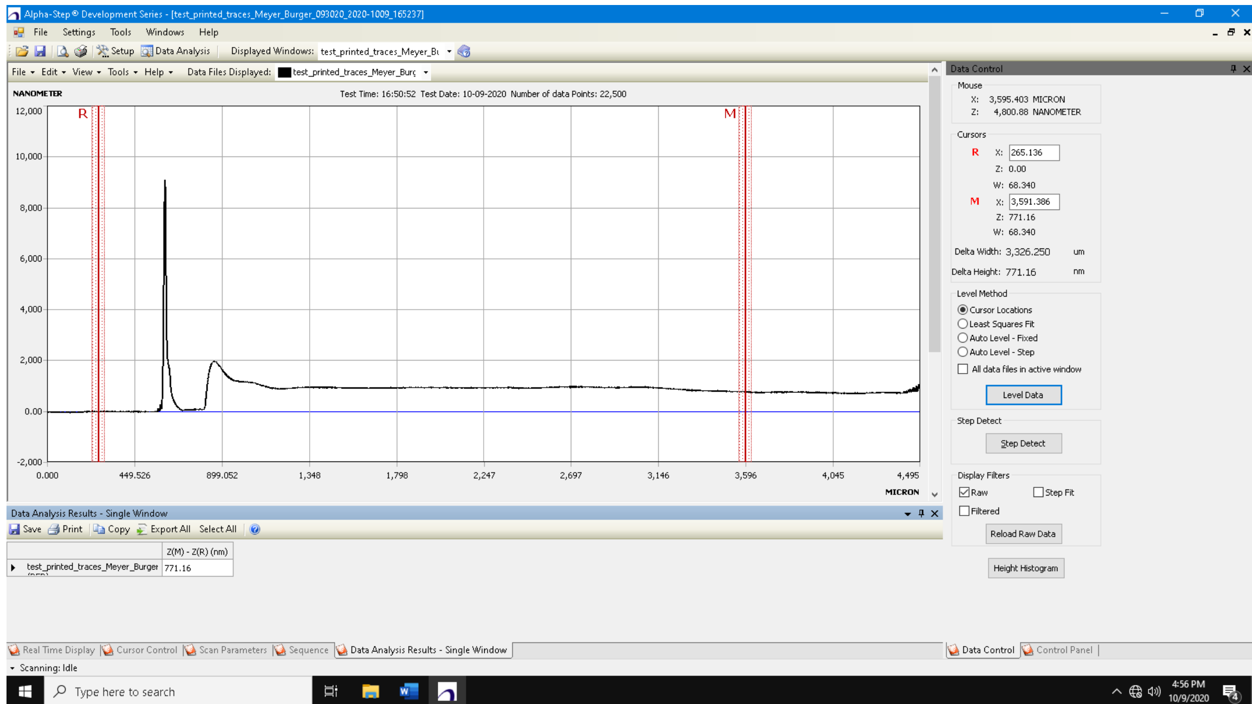

Figure 32 A typical profile of photoresist on sample 3 (section 1) – Recipe KL5305_2.

d) <u>Measurement results and Analyzing data on the sample with recipe KL5305_2</u>:

After putting the measurement data of the sample into Excel for analysis, the results of the measurements can be summarized as in table 10, 11 and 12 as shown below:

Table 10. The Delta height measure on sample 1 with a spin coat recipe KL5305_2.

	Delta Height (nm)	Average Delta Height of section (nm)	Standard Deviation (nm)	Average height of sample (nm)
Section 1		744.26	6.43	
1	750.89			
2	743.83			
3	738.06			
Section 2		741.46	12.44	
1	753.48			794.39 ± 59.58
2	742.26			
3	728.64			
Section 3		849.34	11.79	
1	837.42			
2	849.60			
3	860.99			

Section 4		842.49	32.10	
1	853.16			
2	806.42			
3	867.90			

Table 11. The Delta height measure on sample 2 with a spin coat recipe KL5305_2.

	Delta Height (nm)	Average Delta Height of section (nm)	Standard Deviation (nm)	Average height of sample (nm)
Section 1		893.80	32.18	822.28 ± 87.65
1	883.89			
2	867.75			
3	929.77			
Section 2		901.97	75.45	
1	827.39			
2	900.25			
3	978.27			
Section 3		755.27	28.01	
1	729.76			
2	750.80			
3	785.24			
Section 4		738.06	27.05	
1	767.17			
2	733.32			
3	713.69			

Table 12 The Delta height measure on sample 3 with a spin coat recipe KL5305_2.

	Delta Height (nm)	Average Delta Height (nm)	Standard Deviation (nm)	Average height of sample (nm)
Section 1		842.19	60.15	860.71 ± 18.71
1	881.17			
2	772.92			
3	872.49			
Section 2		880.02	67.36	

1	922.15			
2	802.33			
3	915.58			
Section 3		847.39	29.67	
1	813.58			
2	859.47			
3	869.11			
Section 4		873.24	33.40	
1	842.43			
2	868.55			
3	908.74			

e) Data analysis and Conclusion

The average height of each sample using recipe of KL5302_2 is summarized in Table 17.

Table 13. The average height of the three samples with recipe KL5305_2

	Average Delta Height (nm)	The average height of the three samples (nm)
Sample 1	794.39	825.79 ± 33.30
Sample 2	822.28	
Sample 3	860.71	

From which we can conclude:

- The average height varies from sample to sample, but not exceed 5 % from the average value.
- In general, this data is valid in estimating the thickness of the photoresist layer with this recipe.

3.3.3 Recipe KL5305_3:

a) Sample description:

Like previous samples, the samples prepared by the recipe KL5305_3 also have two separate regions, which naked eyes can easily see. The area near the edge has a width of about 1 mm, which we will skip when taking the measurement. Figure 33 depicts the samples with annotation showing the relative position of the cross-sections to be measured. The arrows on the figures indicate the direction of the scan direction.

Note that on sample 3 we have some particles on the wafer which are contaminated during the spin process but it did not lie in the measuring area.

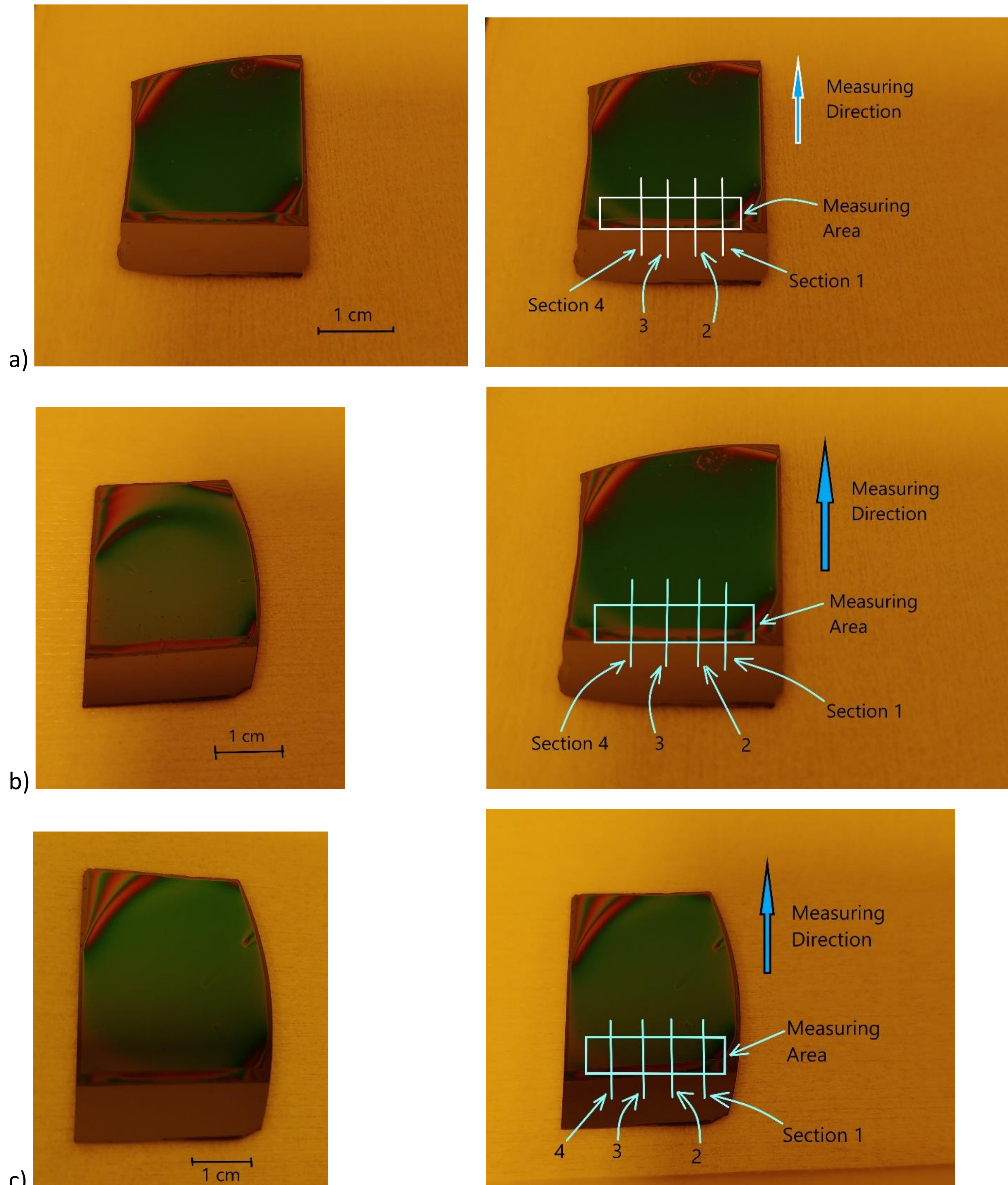

Figure 33. The relative position of the cross-sections and the direction for the measurements of the three samples using KL5305_3 recipe. a) Sample 1, b) Sample 2 and c) Sample 3

b) Scan parameters:

- Speed: 0.05 mm/sec
- Length: 5 mm
- Range: 100 microns
- Stylus force: 10 mg
- Level method: Auto Level – fixed or Cursor location.

c) Scan results:

Figures 34, 35 and 36 show the typical profile for each sample with the same scan parameters. They show how the profiles are leveled. They also show the reference cursor (R) and the measurement cursor (M).

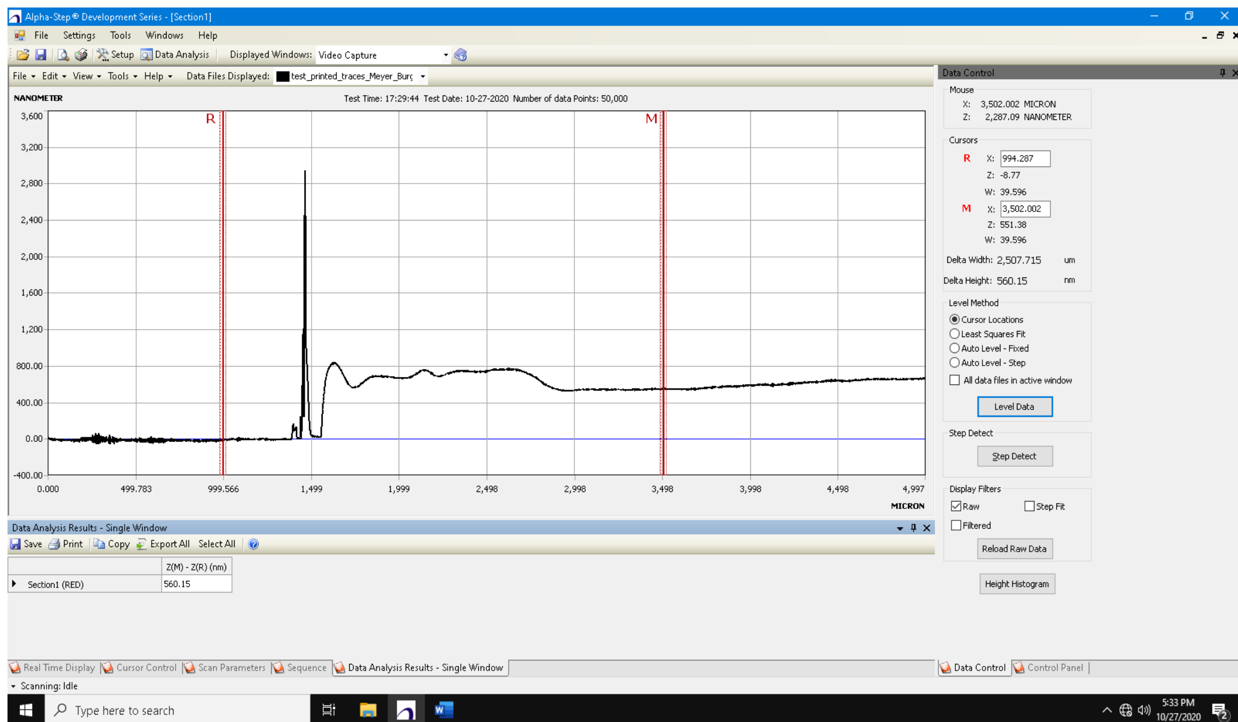

Figure 34. A typical profile of photoresist on sample 1 (section 1) – Recipe KL5305_3

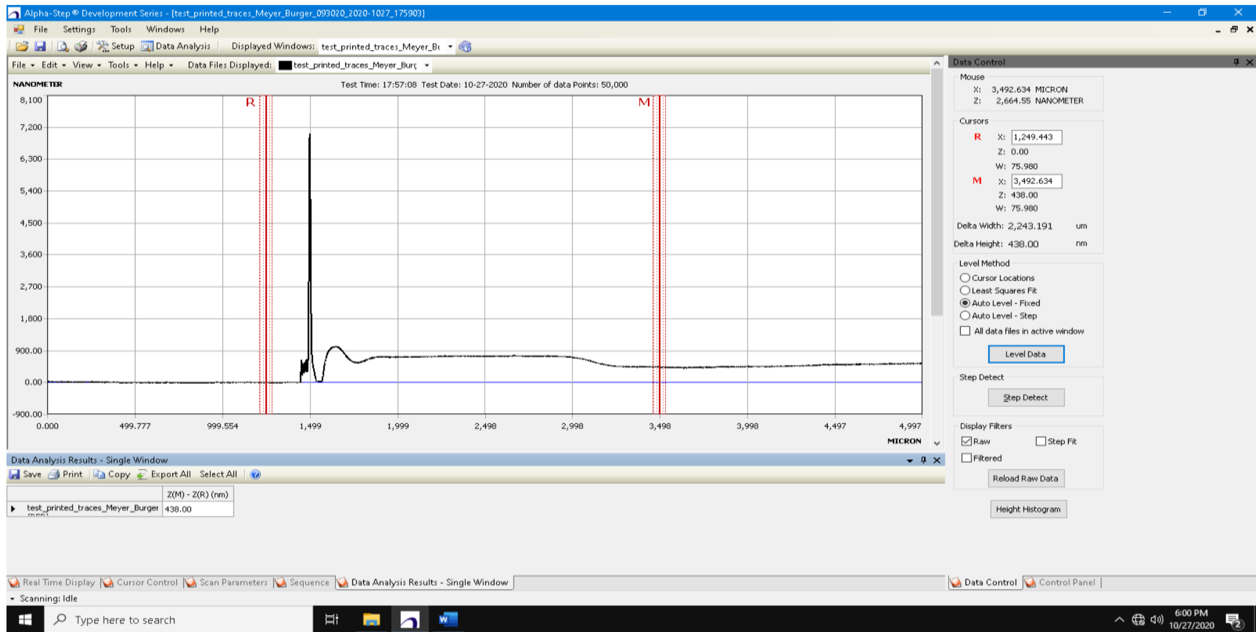

Figure 35. A typical profile of photoresist on sample 2 (section 1) – Recipe KL5305_3

Figure 36. A typical profile of photoresist on sample 3 (section 1)– Recipe KL5305_3

d) Measurement results and Analyzing data on the sample with recipe KL5305_3:

After putting the measurement data of the sample into Excel, the results of the measurements can be summarized in tables 14, 15 and 16 as shown below:

Table 14. The Delta height measure on sample 1 with a spin coat recipe KL5305_3.

	Delta Height (nm)	Average Delta Height (nm)	Standard Deviation	Average height (nm)
Section 1		588.91	47.45	596.65 ± 29.05
1	544.51			
2	560.15			
3	600.20			
4	650.78			
Section 2		618.61	36.82	
1	613.63			
2	577.29			
3	616.63			
4	666.88			
Section 3		620.26	51.33	
1	568.53			
2	621.06			
3	671.19			
Section 4		558.81	31.44	
1	523.24			
2	544.32			
3	572.97			
4	594.71			

Table 15. The average delta height of sample 2, spin coat with recipe KL5305_3

	Delta Height (nm)	Average Delta Height (nm)	Standard Deviation (nm)	Average height (nm)
Section 1		483.12	47.54	551.43 ± 63.36
1	438.00			
2	449.85			
3	505.51			
4	539.11			

Section 2				
1	505.41	514.29	9.88	
2	506.20			
3	521.33			
4	524.23			
Section 3				
1	608.38	589.34	28.18	
2	557.07			
3	574.84			
4	617.06			
Section 4				
1	644.32	618.95	27.18	
2	589.32			
3	602.58			
4	639.59			

Table 16. The average delta height of sample 3, spin coat with recipe KL5305_3

	Delta Height (nm)	Average Delta Height (nm)	Standard Deviation	Average height (nm)
Section 1		387.21	36.18	431.18 ± 35.39
1	440.35			
2	376.61			
3	372.46			
4	359.41			
Section 2		430.91	14.03	
1	445.24			
2	435.64			
3	430.89			
4	411.87			
Section 3		432.76	8.97	
1	442.19			
2	433.22			

3	434.98			
4	420.63			
Section 4				
1	478.31			
2	469.91	473.86	6.00	
3	479.63			
4	467.58			

e) Data analysis and Conclusion

The average height of each sample is summarized in Table 17. From which we can conclude about the experiment on the photoresist thickness on samples using recipe KL5305_3:

Table 17. The average delta height with recipe KL5305_3

	Average Delta Height (nm)	Average height of the three samples (nm)
Sample 1	596.65	526.42 ± 85.52
Sample 2	551.43	
Sample 3	431.18	

:

- The average height varies largely from sample to sample but within a sample the standard deviation is acceptable (except sample 2).
- In sample 1, the height of the photoresist in section 1 and 4 are lower than those of section 2 and 3. But all the standard deviation are rather low (~5%).
- We will use this result in estimating the thickness of the photoresist layer with recipe KL5305_3.

3.3.4 Expose and Develop samples with recipe KL5305_3:

In this section, we still use the recipe KL5305_3 for the spin coater but the samples are prepared differently. In this experiment, the samples are exposed to the UV light source with 365 nm wavelength, and then developed the samples with TMAH developer. The procedure of the experiment is as below.

a/ Procedure:

1. Coat wafer with KL5305 resist with recipe KL5305_3 (3000 rpm).
2. Soft bake: 105 ^oC in 3 minutes (in the datasheet 90 ^oC, 60 sec)
3. Measure the UV light power with the power meter.

4. Based on Sample Process part of the datasheet of the resist [10], that stated that the exposure used 60mJ@365 nm. I started with this exposure dose and then calculate the exposure time needed.

   Power of UV light source: 37.1 mW
   Exposure time: 60/37.1 = 1.6 sec

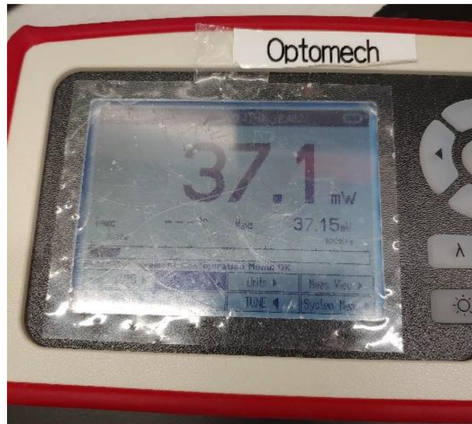

Figure 37. Power meter for measuring the power of the UV light source (ThorLabs S302C)

Figure 38. The UV light source used in the experiment 9 (LightningCure LC8).

5. Put the wafer under the UV light source at the same distance as used to measure the power.
6. Put the photomask in between the glass slide then press it on top of the photoresist.

7. Expose the wafer using the UV light source (Figure 37).
8. Post exposure bake: 115 ^{o}C in 60 seconds.
9. Develop the wafer with 0.26 TMAH developer in 3 min.
10. Hard bake 110 ^{o}C in 3 minutes. Rinse with water, and then IPA.
11. Note that when using the hard bake time 110 ^{o}C, 60 sec as in the datasheet, the resist was mostly washed out when rinsing with IPA.
12. Blow dry with N_2.

The following schematic summarizes the working principle of exposing and develop steps of a photoresist.

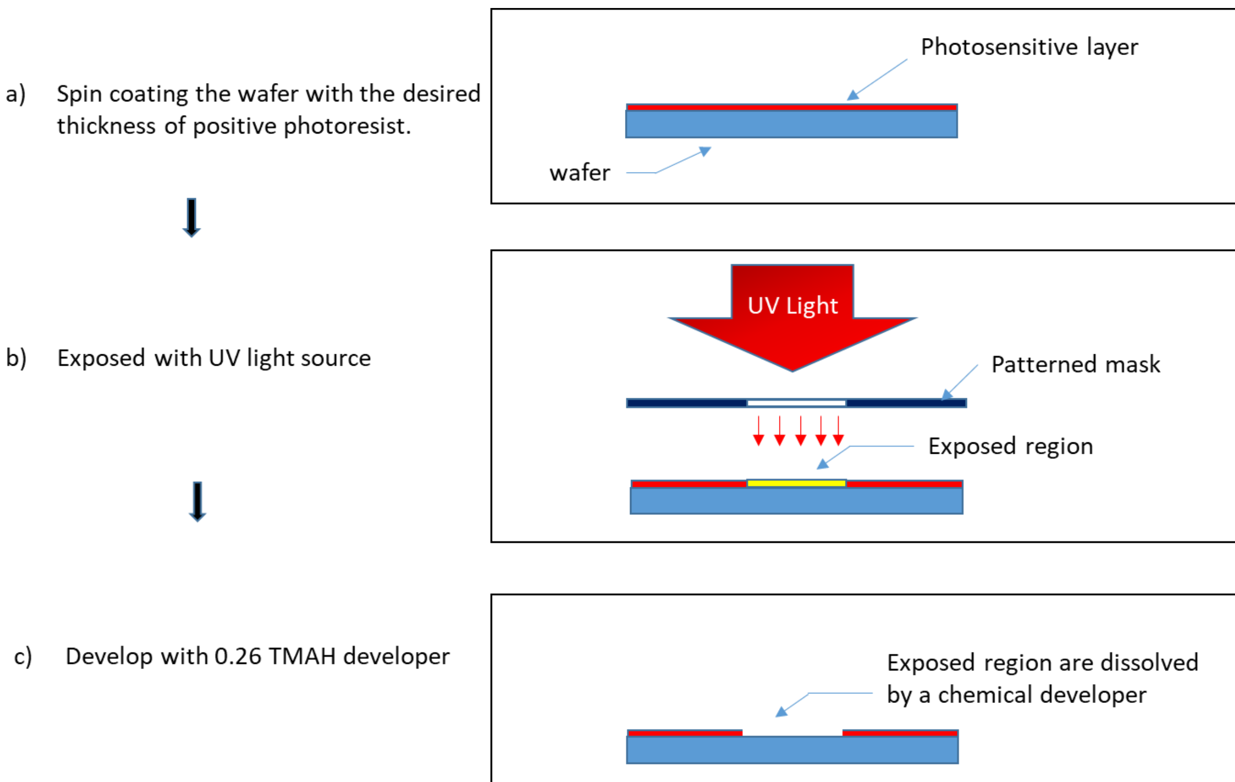

Figure 39. The schematic shows the working principle of exposing and develop steps of photoresist.

b/ <u>Sample description</u>:

Figure 40 shows samples 1, 2, and 3 after exposing with UV light source in using the photomask shown in Figure 41. In Figure 40, we note the sample corners have the color shade difference with the center area and suggested that the film thickness have been changed at those locations. This may be due to the uneven heat distribution during the soft bake and post-exposure bake treatment. Figure 42 shows the sample after developing with the TMAH developer.

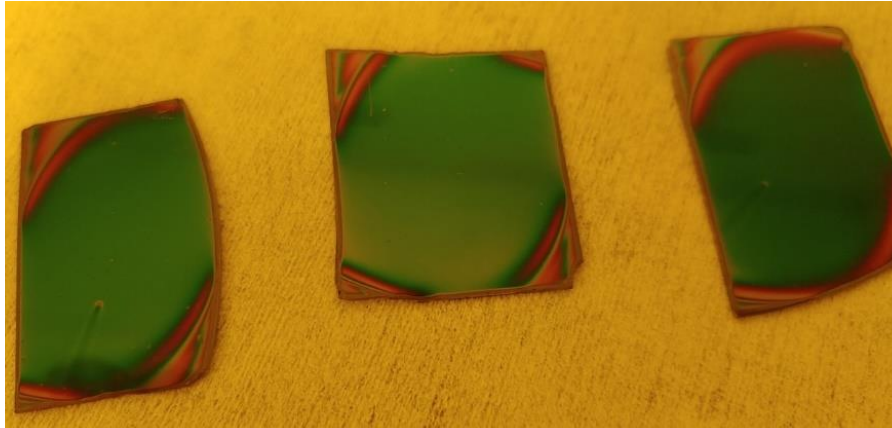

Figure 40. Samples after exposing with UV light source and post exposure bake.

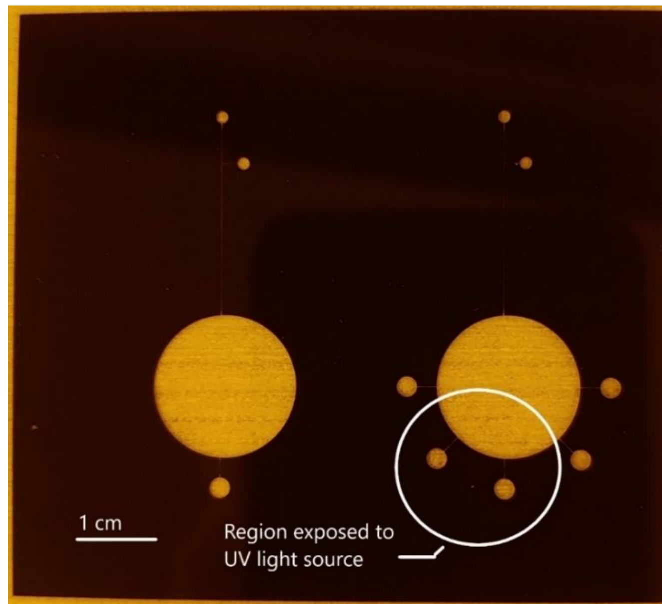

Figure 41. Photomask used to mask the samples. The circle show the region exposed to the UV light source. It helps to explain the area shape that will be developed as in Figure 40.

Figure 42. Samples after developing with 0.26 N TMAH developers.

Figure 43 shows some positions that will be measured for the thickness of the photoresist. In general, we take the measurement in 5 sections on each sample: 3 sections through the large arc, 1 section through the small circle and 1 section through the small line that connect the two circles, as shown in the Figure 44.

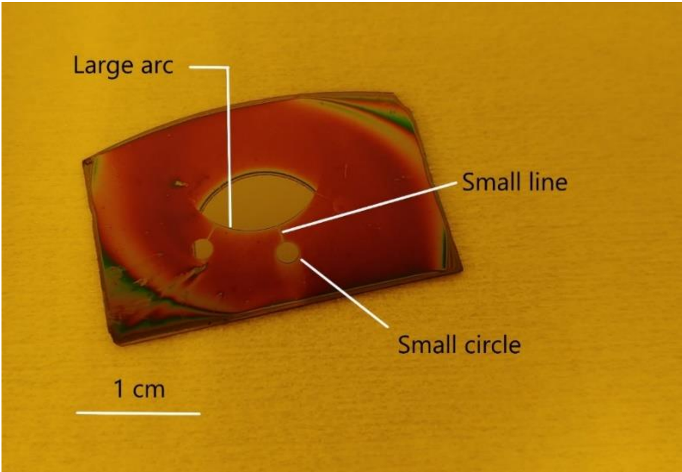

Figure 43. Sample after developing with TMAH and typical positions will be measured on samples.

a) 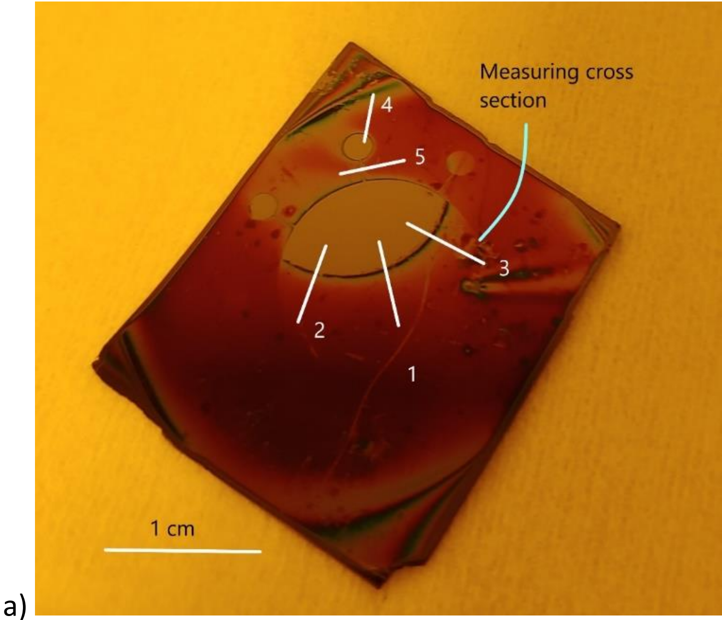

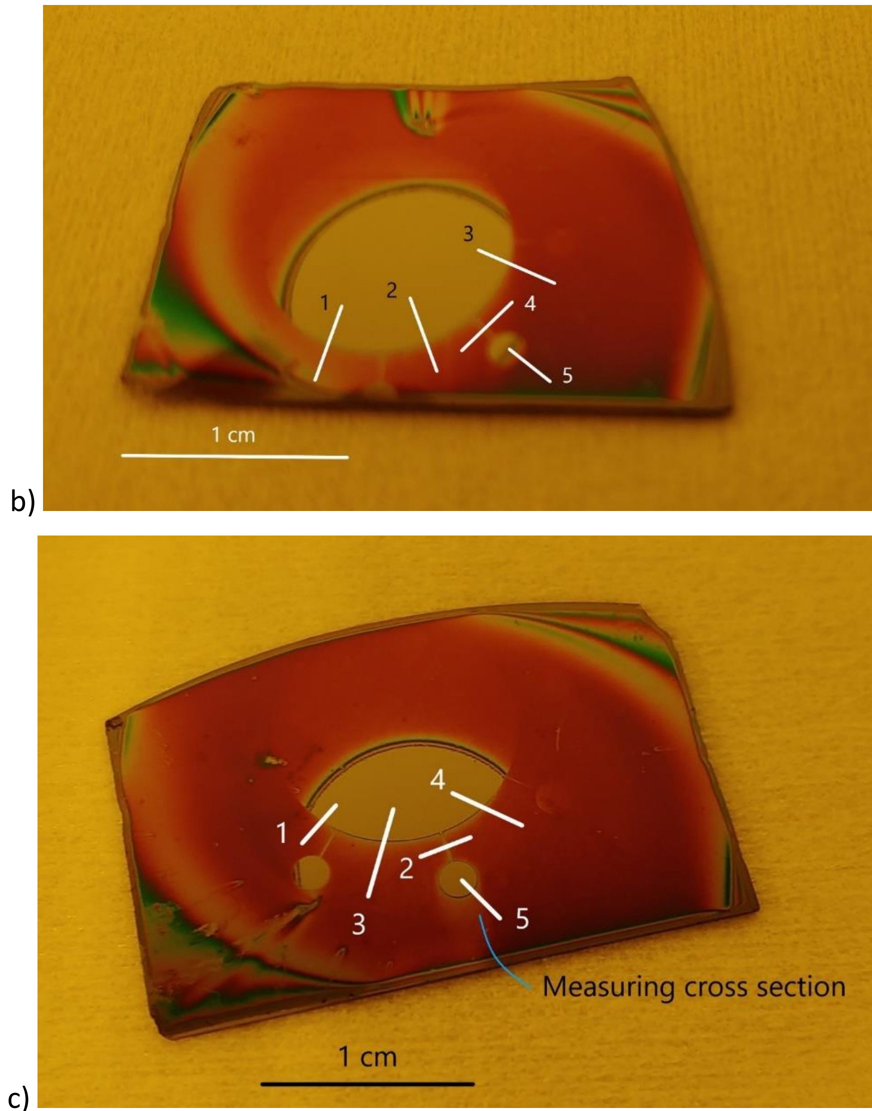

Figure 44. The relative position of the cross-sections and the direction for the measurements of the three samples. a) Sample 1, b) Sample 2 and c) Sample 3

c) <u>Scan results:</u>

Following are the profile graph of the various cross-section of sample 1 that take through the step of the large arc (Figure 45), the small circle (Figure 46), and across the small line (Figure 47). All sections numbers in these figures are referred to Figure 44 – a.

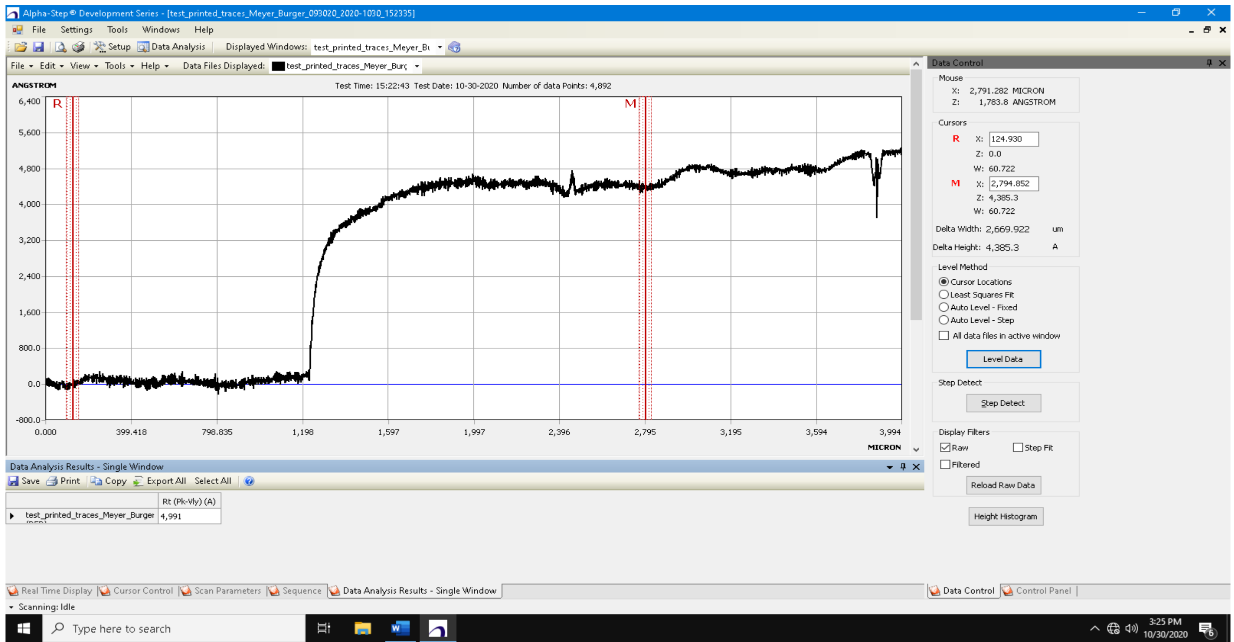

Figure 45. Profile of the cross section through the large arc (section 1) of sample 1.

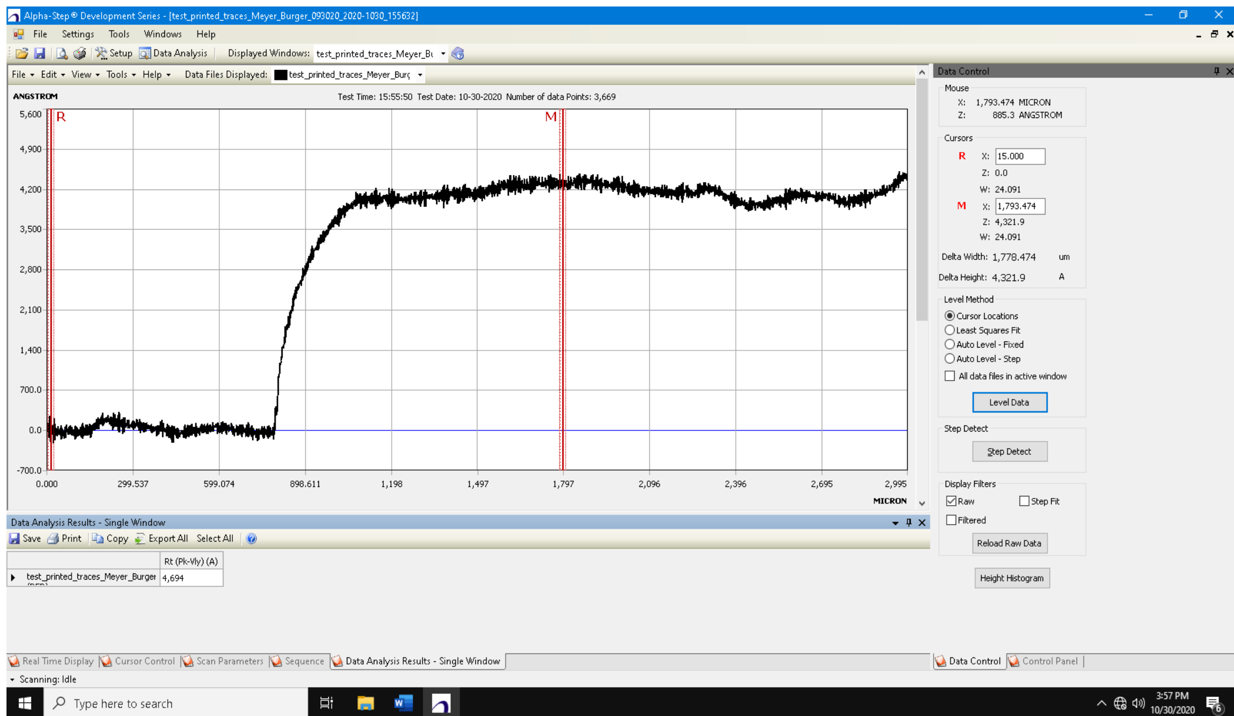

Figure 46. Typical profile of the cross section through the small circle (section 4) of sample 1.

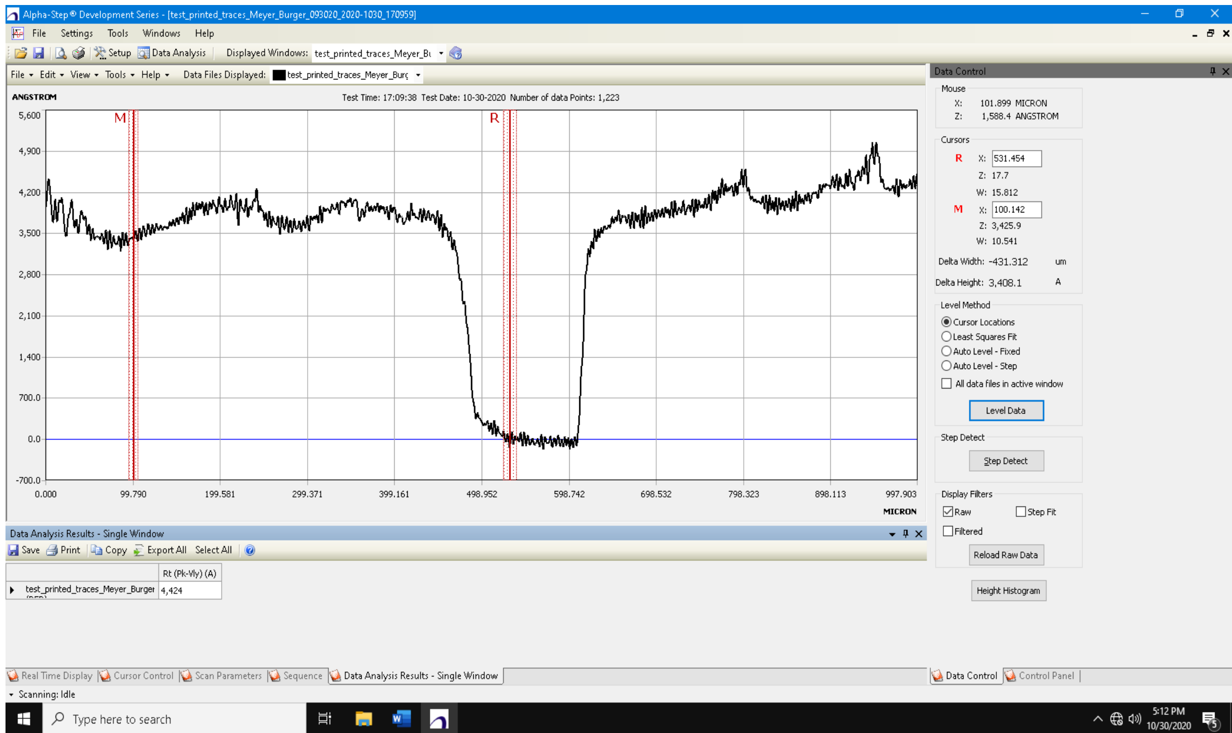

Figure 47. Typical profile of the cross section through the small line (section 5) of sample 1.

d) Measurement results:

After putting the measurement data of the sample into Excel, the results of the measurements can be summarized in table 18, 19 and 20 as shown below:

Table 18. The Delta height measure on sample 1

	Delta Height (nm)	Average Delta Height (nm)	Standard Deviation (nm)	Average Delta Height of sample (nm)
Section 1		455.67	19.16	400.51 ± 46.53
1	452.13			
2	438.53			
3	476.35			
Section 2		377.26	36.15	
1	418.87			
2	359.36			
3	353.55			
Section 3		384.07	32.40	
1	360.52			

2	421.02			
3	370.68			
Section 4				
1	413.27			
2	432.19			
3	417.95	418.91	15.42	
4	400.21			
5	408.20			
6	441.62			
Section 5				
1	357.59			
2	351.91			
3	373.53			
4	362.40	366.66	11.65	
5	358.40			
6	366.14			
7	375.90			
8	387.42			

Table 19. The Delta height measure on sample 2

	Delta Height (nm)	Average Delta Height (nm)	Standard Deviation (nm)	Average Delta Height of sample (nm)
Section 1				
1	472.34			
2	452.63	476.29	25.87	
3	503.91			
Section 2				
1	474.53			
2	478.75	489.25	21.94	435.94 ± 44.18
3	514.46			
Section 3				
1	428.83			
2	399.01	417.81	16.36	
3	425.58			
Section 4		389.31	18.82	

1	381.03			
2	383.19			
3	404.31			
4	377.99			
5	389.23			
6	375.26			
7	408.32			
8	360.07			
9	388.18			
10	425.53			
Section 5				
1	386.63			
2	376.28			
3	369.09			
4	429.62	407.04	27.46	
5	428.36			
6	441.51			
7	423.88			
8	400.91			

Table 20. The Delta height measure on sample 3

	Delta Height (nm)	Average Delta Height (nm)	Standard Deviation (nm)	Average Delta Height of sample (nm)
Section 1				
1	431.70			
2	432.92			
3	460.18	480.11	45.97	
4	501.16			
5	508.70			
6	545.99			
				425.33 ± 44.97
Section 2				
1	393.66			
2	340.81			
3	394.26	399.18	37.84	
4	367.52			
5	384.28			
6	380.82			

7	438.02			
8	432.04			
9	461.18			
Section 3				
1	379.35	412.18	31.31	
2	415.49			
3	441.70			
Section 4				
1	430.14	462.95	28.68	
2	475.45			
3	483.26			
Section 5				
1	389.88	372.25	11.98	
3	365.61			
5	363.99			
7	369.53			

e) Data analysis and Conclusion

The average height of each sample is summarized in Table 21. From which we can conclude:

	Average Delta Height (nm)	Average height of the three samples (nm)
Sample 1	400.51	420.59 ± 18.18
Sample 2	435.94	
Sample 3	425.33	

- The average height (420.59 nm) is much lower than that of samples which used Kapton tapes to make the step (560.79 nm). This value also lower than that in the datasheet (~ 515 nm). However, in this set of samples, the average height doesn't change much from sample to sample.
- The post-exposure bake and hard bake may affect the height of the photoresist. In addition, based on observing the surface of the photoresist is wrinkled, therefore, we can conclude that the sample may be overexposed.

3.3.5 Recipe KL5305_4:

a/ Sample description:

In this section and the next section, we are back to use the sample prepare with Kapton tape. Same as with previous recipes (KL5305_1, KL5305_2, and KL5305_3), we also have two regions

on the wafer but the region near the edge now are much narrower, with a width of about 1 mm. Figure 48 show the relative position of the cross-sections and the direction for the measurements.

Note that on sample 3 we have some particles (which are contaminants introduced during the spin process) on the wafer but they did not lie in the measuring area.

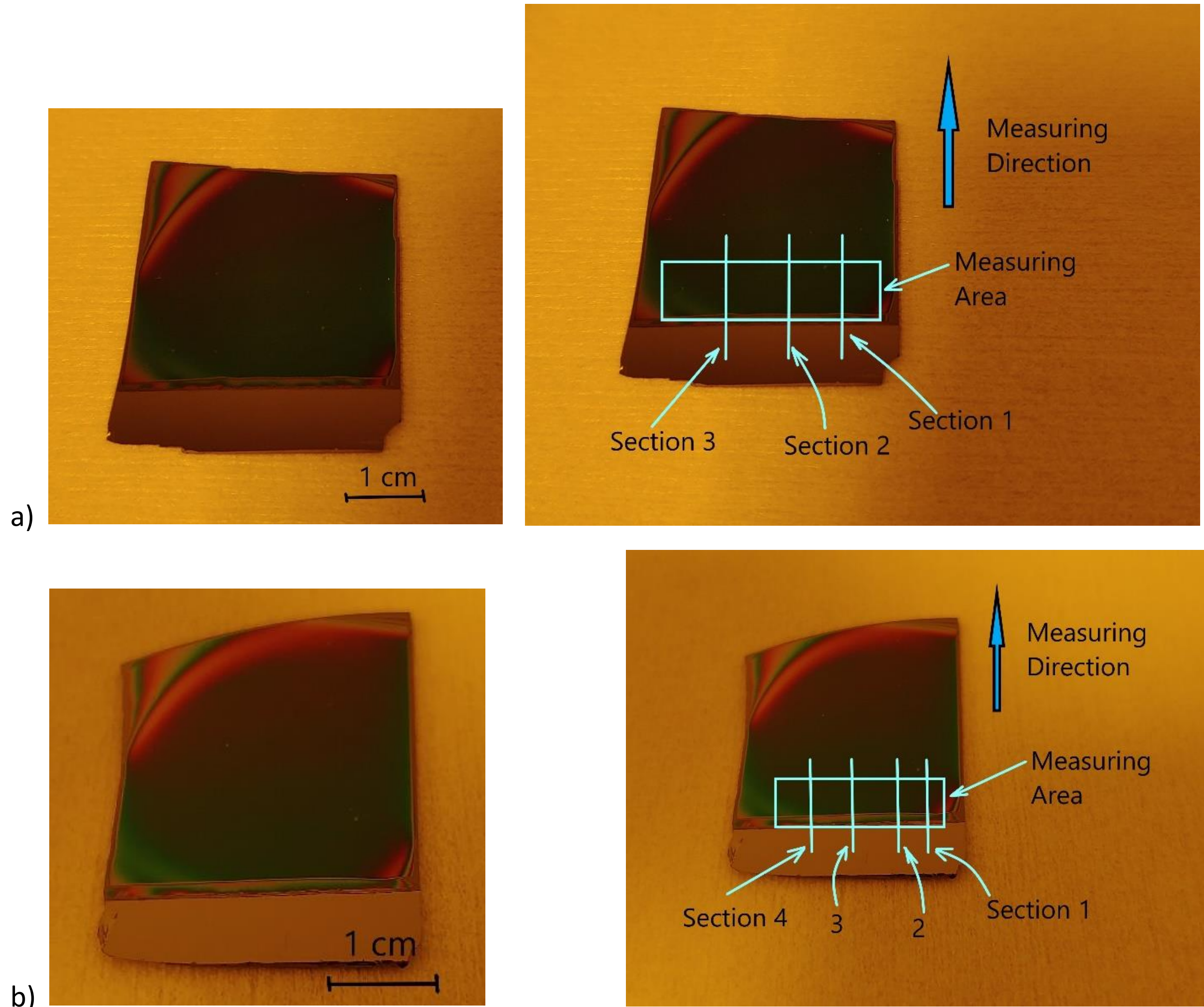

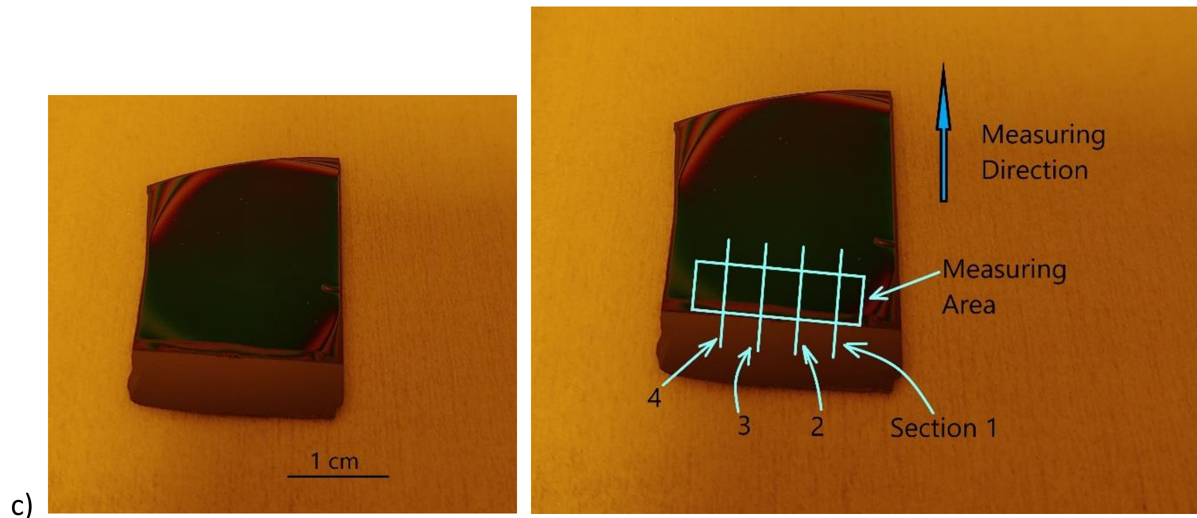

Figure 48. The relative position of the cross-sections and the direction for the measurements of the three samples using KL5305_4 recipe. a) Sample 1, b) Sample 2 and c) Sample 3

<u>b/ Scan parameters</u>:

- Speed: 0.05 mm/sec
- Length: 5 mm
- Range: 100 microns
- Stylus force: 10 mg
- Level method: Auto Level – fixed or Cursor location.

c) <u>Scan results:</u>

Figures 49, 50 and 51 show the typical profile for each sample with the same above scan parameters. They also show how the profiles are leveled.

In general, there is a low height area next to the edge of the wafer. We use this height for the measurements because that was the height the photoresist would have reached if it were not obstructed by the tape.

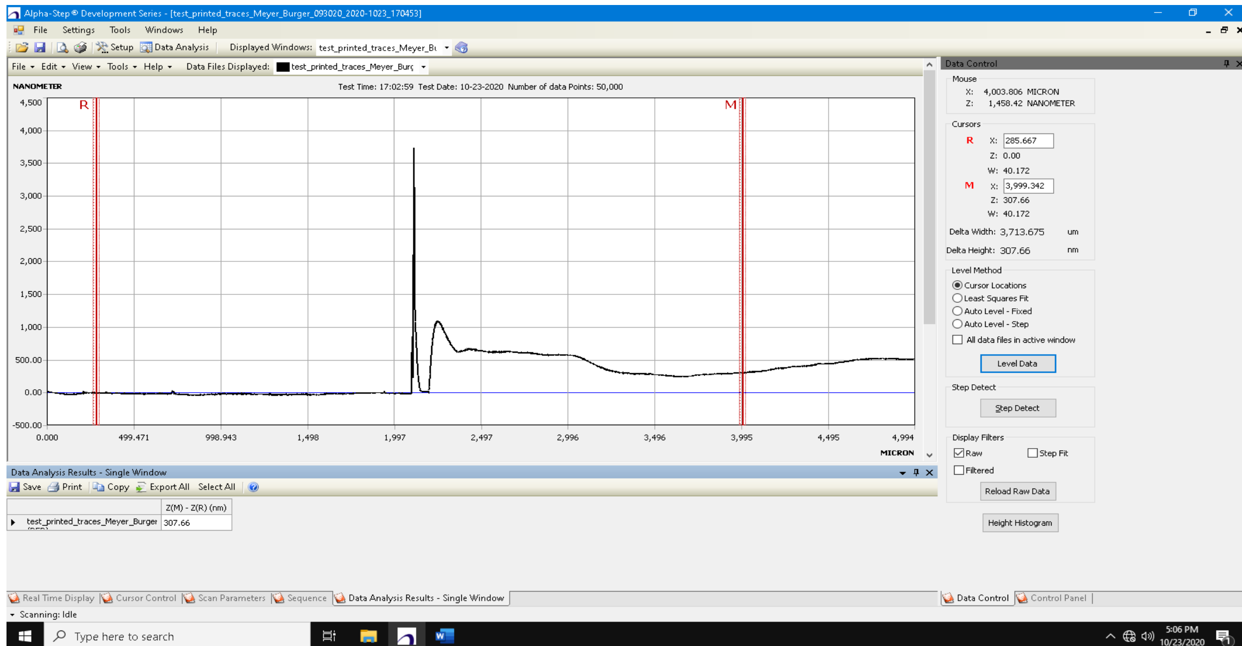

Figure 49. A typical profile of photoresist on sample 1 – Recipe KL5305_4. R: The reference cursor, M: measurement cursor.

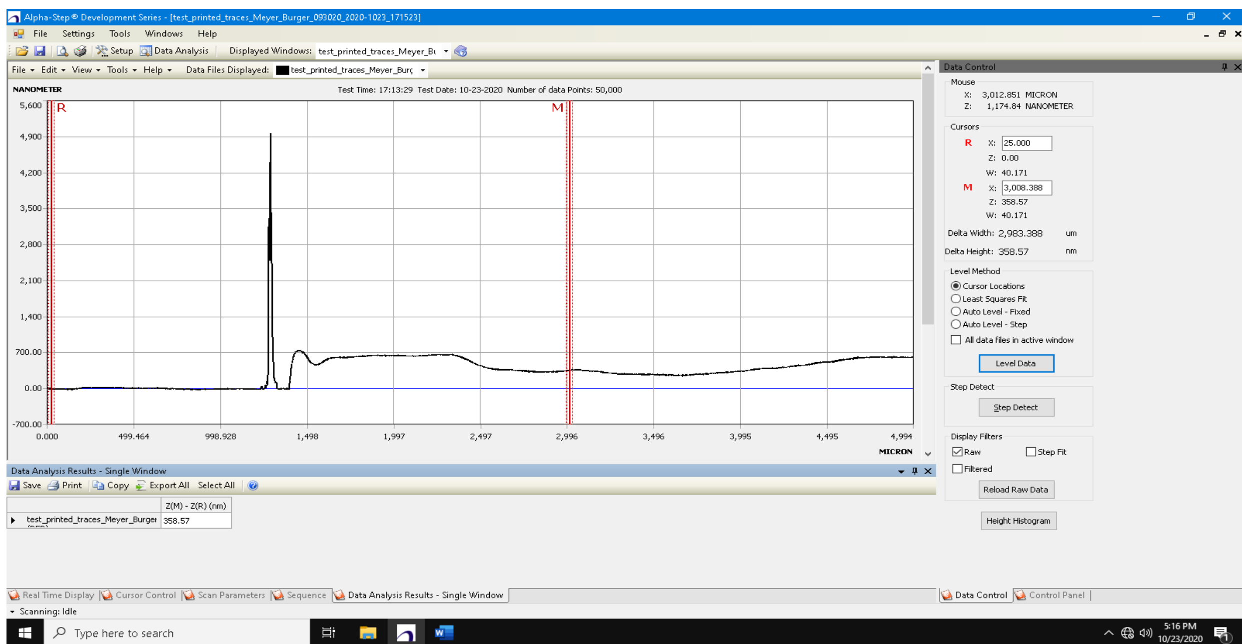

Figure 50. A typical profile of photoresist on sample 2 – Recipe KL5305_4. R: The reference cursor, M: measurement cursor.

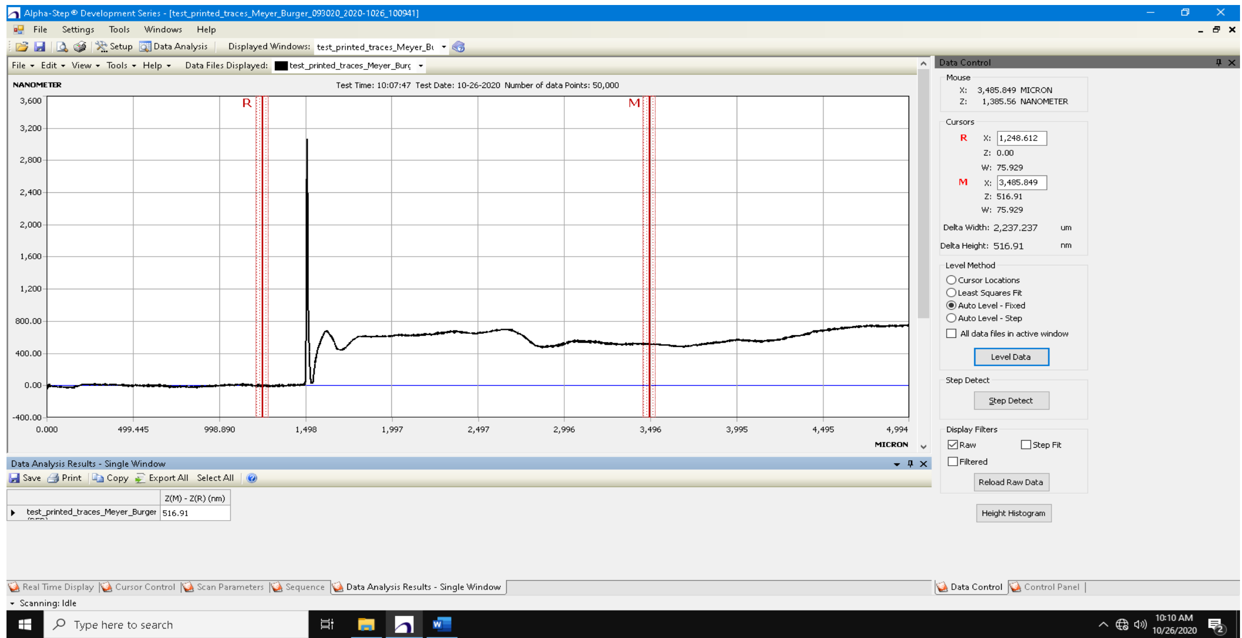

Figure 51. A typical profile of photoresist on sample 3 – Recipe KL5305_4. R: The reference cursor, M: measurement cursor.

d) <u>Measurement results and Analyzing data on the sample with recipe KL5305_4</u>:

Table 21. The average delta height of sample 1, spin coat with recipe KL5305_4

	Delta Height (nm)	Average Delta Height of section (nm)	Standard Deviation (nm)	Average height of sample (nm)
Section 1		438.93	94.19	407.93 ± 79.27
1	401.20			
2	414.36			
3	351.93			
4	427.71			
5	599.44			
Section 2		397.54	71.84	
1	422.87			
2	401.60			
4	344.36			
5	501.30			
6	317.58			
Section 3		387.31	111.48	
1	280.75			
2	307.66			
3	446.89			

4	513.95			

Table 22. The average delta height of sample 2, spin coat with recipe KL5305_4

	Delta Height (nm)	Average Delta Height (nm)	Standard Deviation (nm)	Average height of sample (nm)
Section 1		427.55	125.26	466.66 ± 41.02
1	450.30			
2	358.57			
3	277.33			
4	343.49			
5	521.97			
6	613.63			
Section 2		499.25	162.21	
1	405.65			
2	321.49			
3	433.16			
4	625.65			
5	710.31			
Section 3		504.80	90.25	
1	489.30			
2	418.98			
3	479.00			
4	631.93			
Section 4		435.02	93.58	
1	418.66			
2	347.98			
3	405.84			
4	567.60			

Table 23. The average delta height of sample 3, spin coat with recipe KL5305_4

	Delta Height (nm)	Average Delta Height (nm)	Standard Deviation (nm)	The average height of sample (nm)
Section 1		534.34	27.71	599.78 ± 97.66
1	519.81			
2	516.91			

3	566.29			
Section 2		567.49	33.54	
1	559.63			
2	538.57			
3	604.26			
Section 3		697.51	83.89	
1	621.40			
2	773.61			
3	734.55			

Table 24. The average delta height with recipe KL5305_4

	Average Delta Height (nm)	The average height of the three samples (nm)
Sample 1	407.93	491.46 ± 98.30
Sample 2	466.66	
Sample 3	599.78	

e) <u>Data analysis and Conclusion</u>

- The standard deviation in sample 3 is large.
- Overall, the average delta height also varies widely from sample 3 to the rest. Perhaps this is because we couldn't precisely control the center of the wafer when we put it on the spin coater. The distance between the measured position on the wafer and the rotation center varies from sample to sample, and on top of that, the tape may have the negative effect of obstructing the photoresist when it is free moving.
- However, based on the average height of the set of samples and the KL 5300 Spin Curve from the datasheet, in general, this data is suitable for estimating the thickness of the photoresist layer.

3.3.6 Recipe KL5305_5:

a/ <u>Sample description</u>:

Same as with the previous recipe (KL5305_4), we also have two regions on the wafer, but the region near the edge now is much narrower, with a width of about less than 1 mm. The following pictures (Figure 52) show the relative position of cross-sections and the direction for measurements.

Note that on some samples, some particles remained, but not near the measurement area. On samples 1 and 3, we noted that the photoresist did not adhere well to the wafer surface.

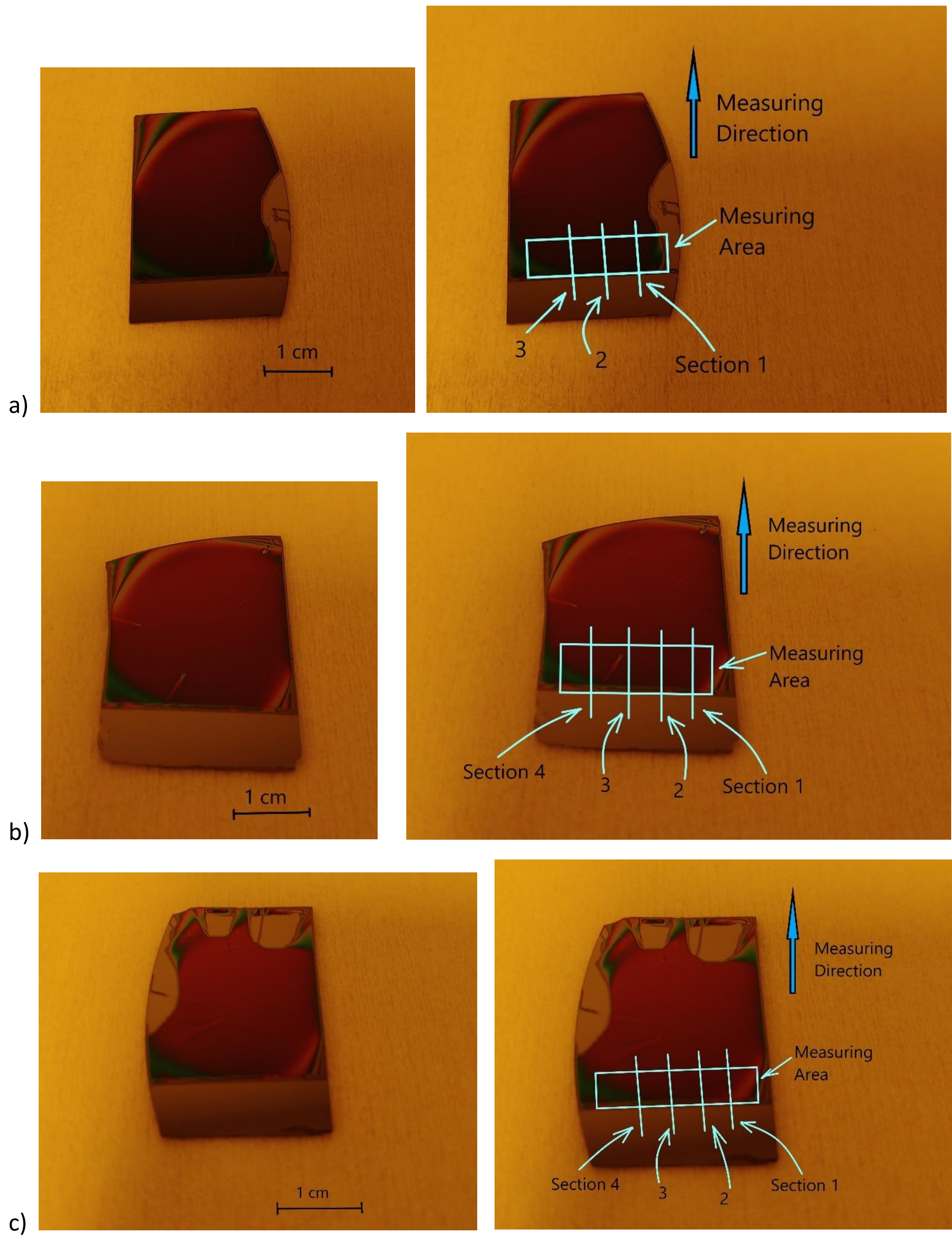

Figure 52. The relative position of the cross-sections and the direction for the measurements of the three samples using KL5305_5 recipe. a) Sample 1, b) Sample 2 and c) Sample 3

b/ Scan parameters:

- Speed: 0.05 mm/sec
- Length: 5 mm
- Range: 100 microns
- Stylus force: 10 mg
- Level method: Auto Level – fixed or Cursor location.

c) Scan results:

Figures 53, 54 and 55 show the typical profile for each sample with the same above scan parameters. They also show how the profiles are leveled.

In general, there is a low height area next to the edge of the wafer. We use this height for measurements because that is the height at which the photoresist would have reached if it were not hindered by the tape.

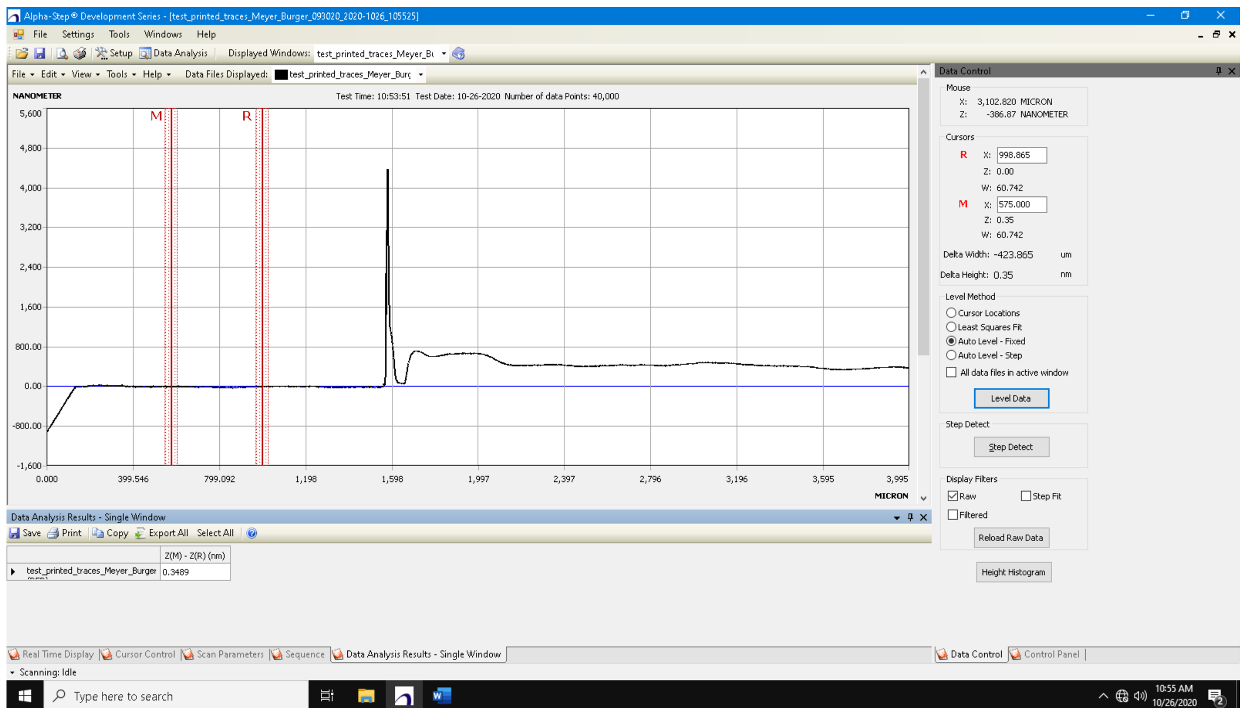

Figure 53. A typical profile of photoresist on sample 1 – Recipe KL5305_5

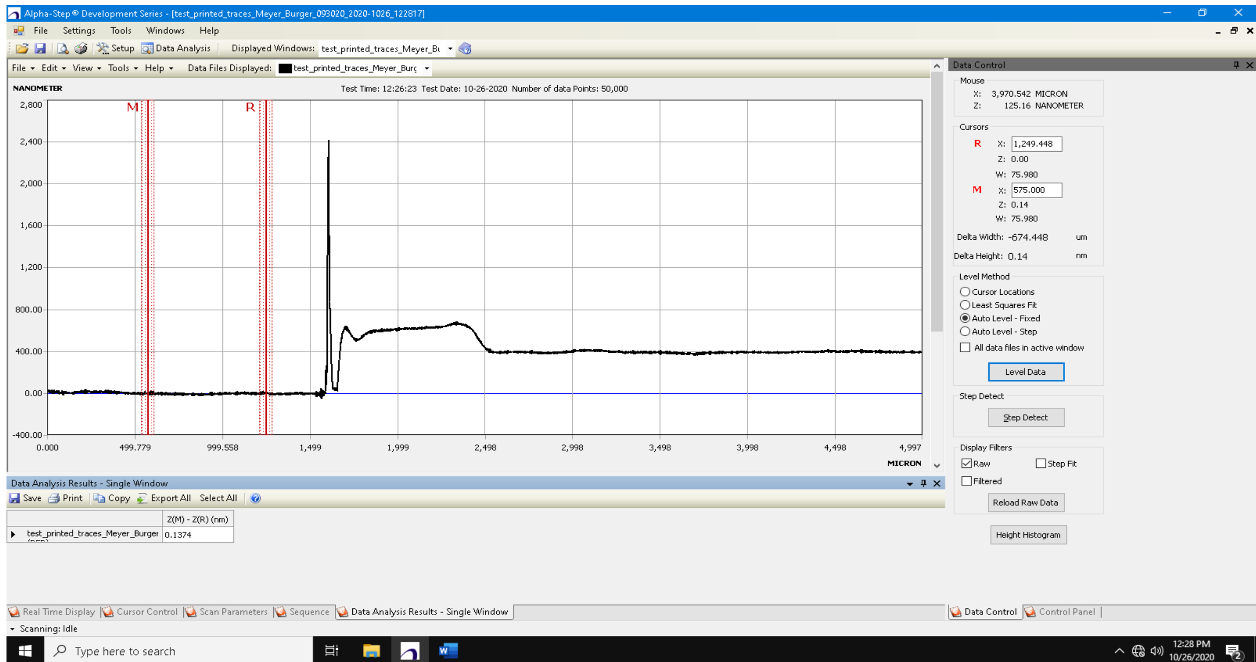

Figure 54. A typical profile of photoresist on sample 2 – Recipe KL5305_5

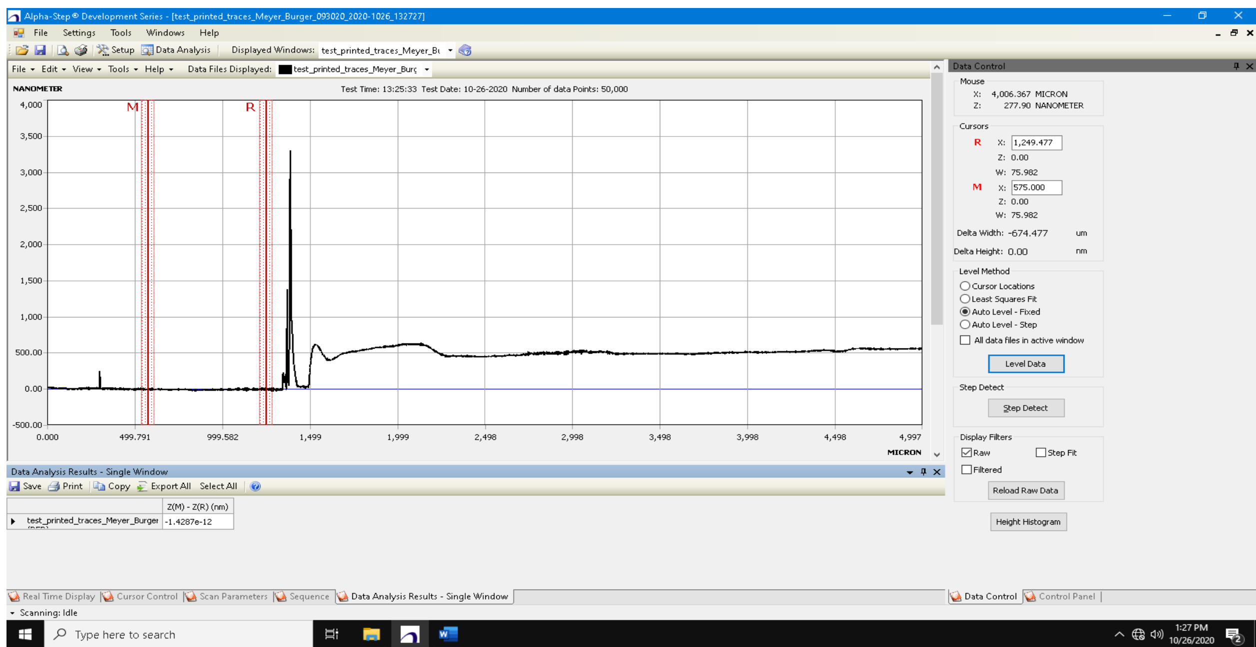

Figure 55. A typical profile of photoresist on sample 3 – Recipe KL5305_5

Figures 56, 57, and 58 show the Reference cursor (R) and Measurement cursor in Data Window.

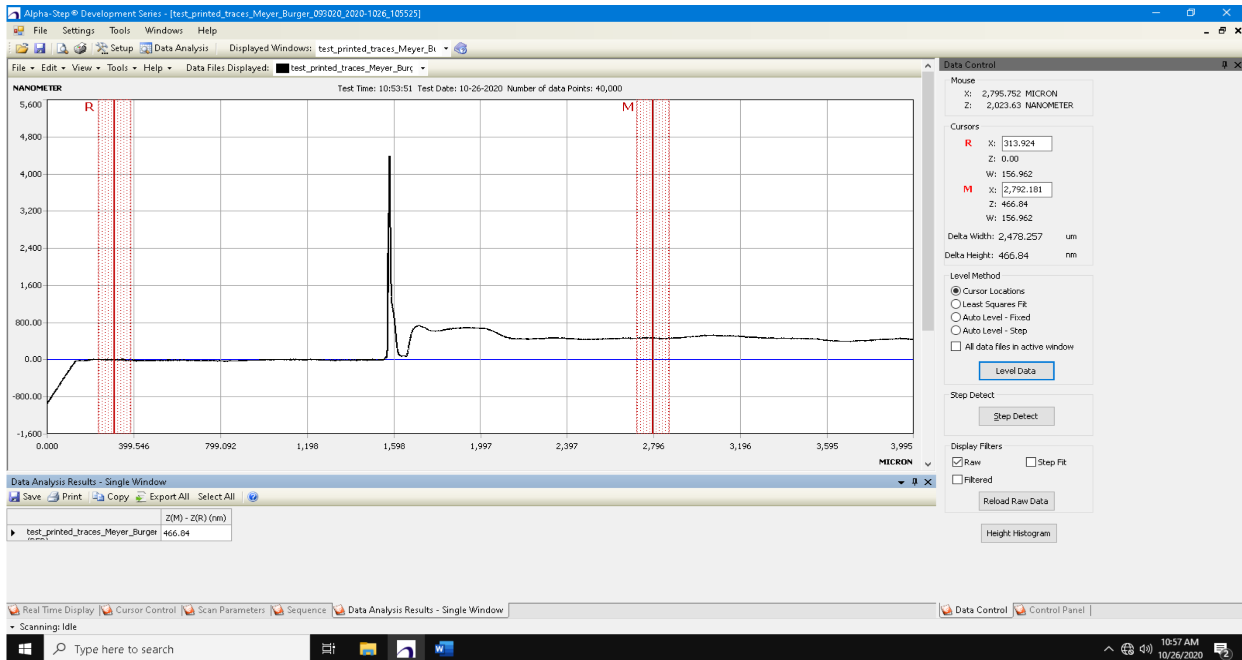

Figure 56. The reference cursor (R) and measurement cursor (M) on sample 1 – Recipe KL5305_5

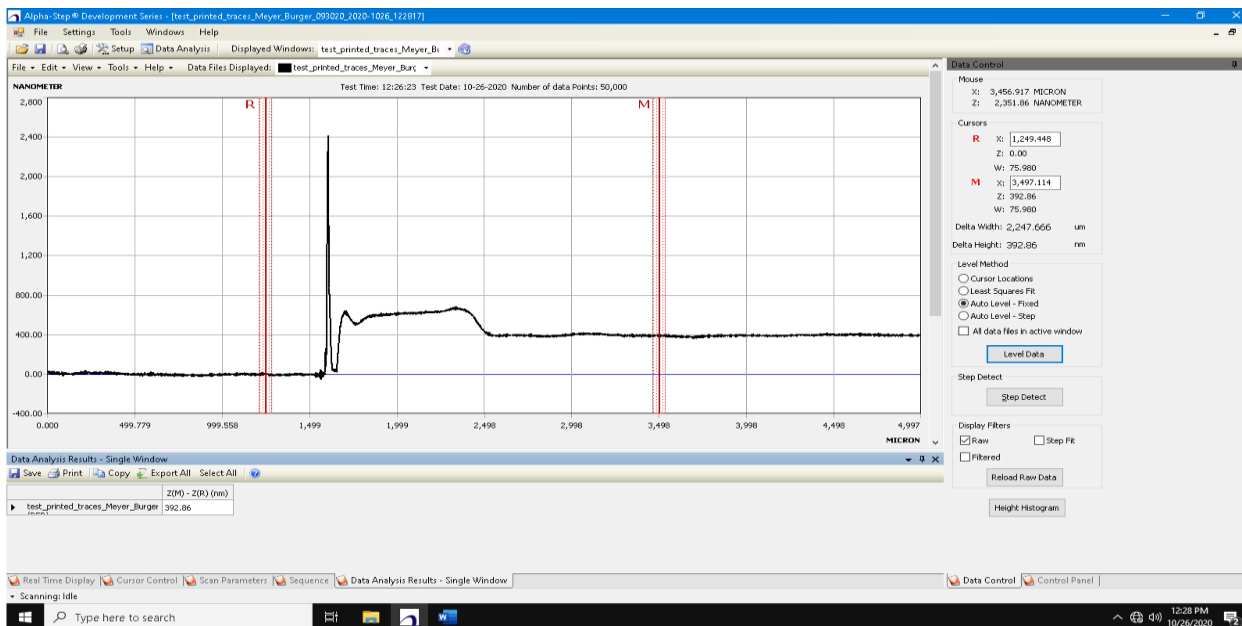

Figure 57. The reference cursor (R) and measurement cursor (M) on sample 2 – Recipe KL5305_5

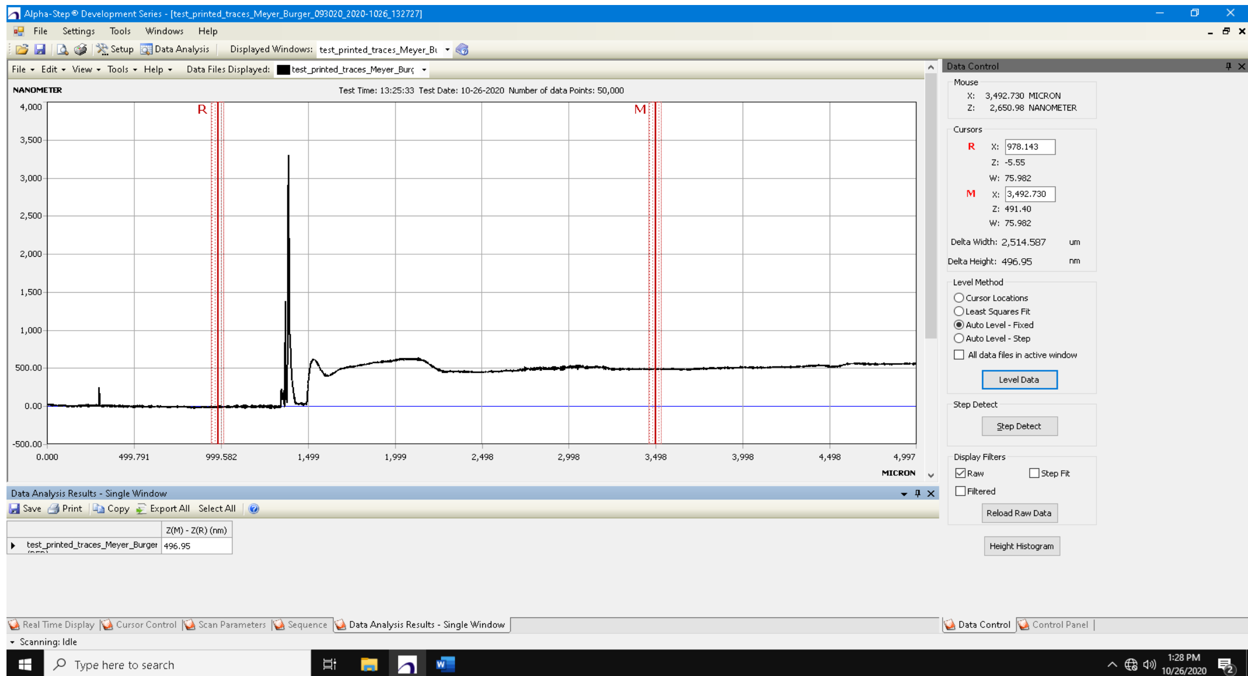

Figure 58. The reference cursor (R) and measurement cursor (M) on sample 3 – Recipe KL5305_5

d) <u>Measurement results and Analyzing data on the sample with recipe KL5305_5</u>:

Table 25. The average delta height of sample 1, spin coat with recipe KL5305_5

	Delta Height (nm)	Average Delta Height of section (nm)	Standard Deviation	Average Height of Sample (nm)
Section 1		460.04	28.93	402.39 ± 51.75
1	459.95			
2	466.84			
3	502.09			
4	422.56			
5	448.74			
Section 2		387.18	54.97	
1	440.08			
2	418.82			
3	421.52			
4	323.02			
5	332.48			
Section 3		359.94	71.79	
1	441.75			

2	394.19			
3	392.55			
4	267.81			
5	303.38			
Section 4		224.22	29.37	
1	256.33			
2	217.61			
3	198.71			

Table 26. The average delta height of sample 2, spin coat with recipe KL5305_5

	Delta Height (nm)	Average Delta Height of section (nm)	Standard Deviation	Average Height of Sample (nm)
Section 1		397.68	5.07	434.38 ± 30.50
1	404.69			
2	392.86			
3	394.83			
4	401.33			
5	394.67			
Section 2		468.18	26.61	
1	460.07			
2	460.63			
3	478.76			
4	506.68			
5	434.78			
Section 3		423.64	10.26	
1	425.51			
2	413.05			
3	413.02			
4	434.98			
5	431.66			
Section 4		448.02	13.65	
1	447.51			
2	433.23			
3	436.35			
4	465.13			
5	457.87			

Table 27. The average delta height of sample 3, spin coat with recipe KL5305_5

	Delta Height (nm)	Average Delta Height (nm)	Standard Deviation	Average Height of Sample (nm)
Section 1		535.72	68.24	521.51 ± 18.19
1	465.64			
2	539.56			
3	601.95			
4	684.83			
Section 2		501.01	51.19	
1	442.56			
2	483.64			
3	513.71			
4	564.12			
Section 3		527.80	26.46	
1	520.57			
2	496.95			
3	517.39			
4	536.01			
5	568.06			

Table 28. The average delta height with recipe KL5305_5

	Average Delta Height (nm)	Average height of the three samples (nm)
Sample 1	357.84	437.91 ± 81.89
Sample 2	434.38	
Sample 3	521.51	

e) <u>Data analysis and Conclusion</u>

Experiment on samples using recipe KL5305_5:

- In sample 1 (Table 25), we do not consider the data of section 4 in calculating the average height of the film. We see it as an outliner, and the low value of this section may be because we do not put sufficient photoresist material to the wafer. Therefore, the photoresist did not fully cover the edge of the sample.

- The standard deviation on each sample is relatively low compared to the sample using KL5305_4.
- Overall, the average delta height also varies greatly from sample to sample. However, based on the average height of the set of samples, in general, this data is valid for estimating the thickness of the photoresist layer.

3.4 Conclusion:

From the photoresist film thickness results with different recipes, we make the graph showing the variation of photoresist film thickness vs. the spin coater's rotational speed. We also compare our experimental results with the spin curve from the manufacturer datasheet (Figure 59).

Table 29. A film thickness of photoresist KL 5305 with different recipes.

Spin speed (rpm)	Film Thickness (nm)	Estimated thickness in datasheet (nm)	Difference
1000	1045.97	930	12.5 %
2000	825.79	681	21.3 %
3000	526.42	515	0.02 %
4000	491.46	433	13.5 %
5000	437.91	407	7.6 %

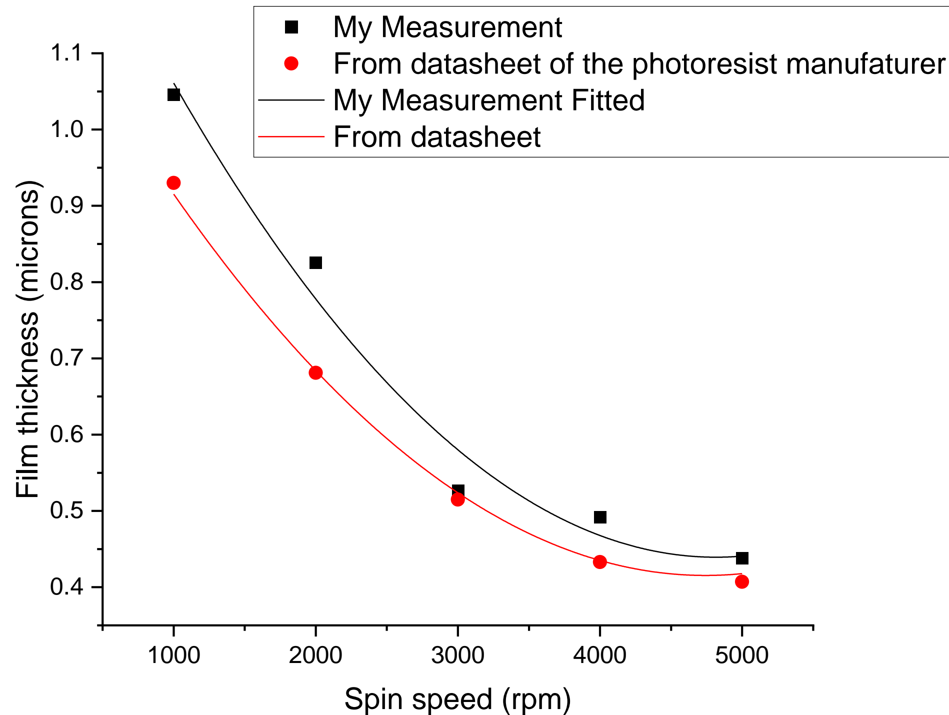

Figure 59. The spin curve of KL 5305 from the experiment and from the datasheet

From Figure 59, we can conclude that, in general, our results are larger than those in the datasheet. As we measured the samples that have gone only to the soft bake step, there are other steps other than the soft bake step in the manufacturer datasheet, including exposure, post-exposure bake, developing, and hard baking. [10] Those steps will affect the final film thickness. Recall that in section 3.3.4, we experiment with the sample going through all the steps as in the datasheet give the result lower than 25% compared to the sample going only to soft bake step. That sample may be overexposed, but it proves that heat dramatically affects the final photoresist film's thickness.

Chapter 4: TeraHertz Spectroscopy

Initially, we planned to combine TeraFlash testing with the photoresist thickness measurement to verify our chapter 3 results. However, after several trials and failed attempts, we realized that due to this equipment's resolution in the time domain is 0.05 ps, we need the sample (assume the refractive index n = 2.5) with a thickness of at least 500 µm to be reliably measured (see formula 1 on next page). Therefore, since the time frame of this project did not permit us to manufacture a sample of that thickness, we used the quartz glass slide with known thickness to test the TeraFlash equipment. But this time, we have the thickness of the glass slide and try to derive the refractive index and then the absorption coefficient.

4.1 Experimental Method:

This chapter describes the result of using TeraFlash terahertz time-domain spectroscopy (THz-TDS) to characterize quartz glass samples. This experiment uses the TeraFlash equipment at LEAP to determine Quartz glass's refractive index via measuring the terahertz pulse trace on the glass. From the refractive index, we also can derive the absorption coefficient of the quartz glass and then compare those results with reported data from the literature.

The measurements were done in transmission mode, and the procedure of the experiment can be summarized as below:

- The sample is a Quartz glass slide with a dimension of 25 x 25 x 1 mm.

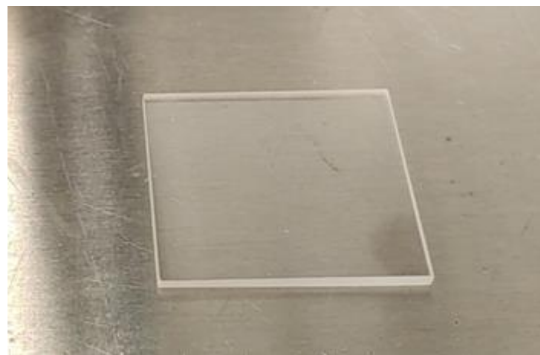

Figure 60. Quartz glass sample used in the experiments

- Set up the TeraFlash in transmission mode and put the glass sample on the stage (Figure 60)
- Switch on the TERAFLASH at the red Power switch at the front panel. Wait until the green System Ready LED lights up continuously (see Figure 17).
- Turn on the PC and Start the TERAFLASH Control Software (TF5-Host).
- Click the **Laser** button at the top right of the screen. The indicator in the button turns green and the Laser Emission warning LEDs at the TERAFLASH Main Unit front panel light up (Figure 60).

- Click the **RUN** button to start a scan.
- We can save the raw data by clicking the **WAIT** button and then the **SAVE** button. Follow the prompt on the screen to give the name and the location to save the file.
- In this experiment we take four different points for the measurement.
- The graph will display on the screen show the pulse trace (time domain) in the upper part and the power spectrum (frequency domain) in the lower part of the screen (Figure 60).

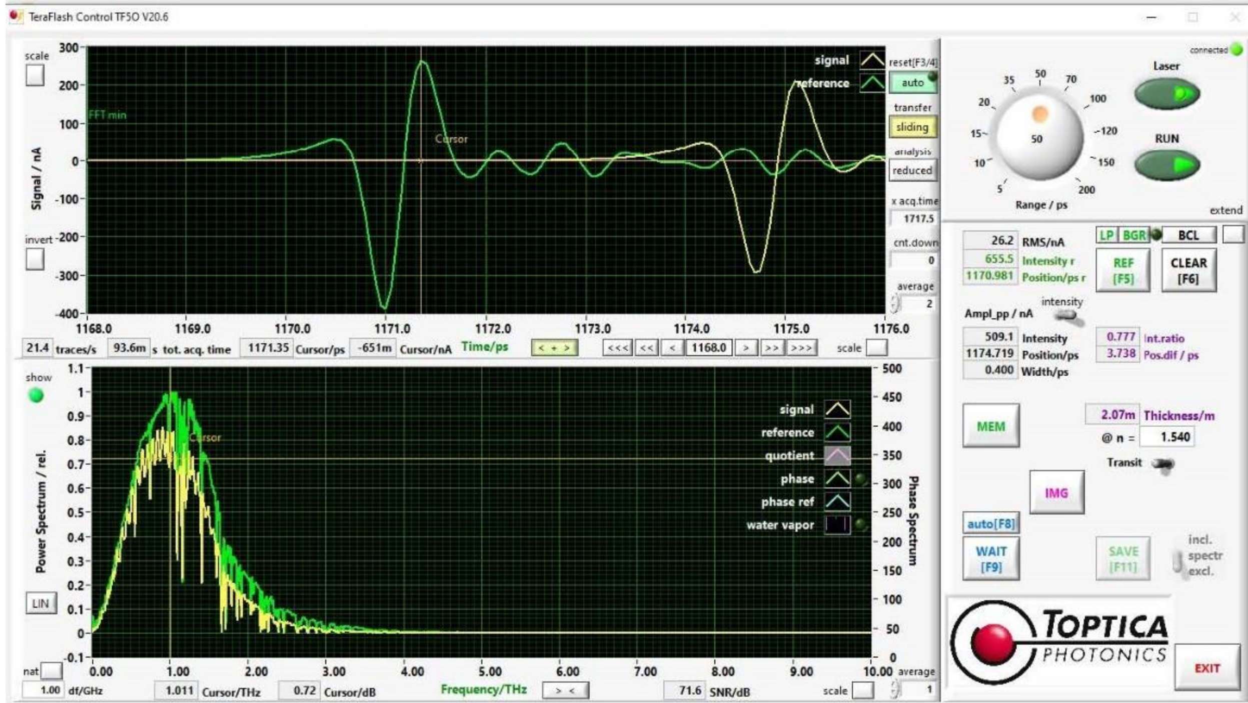

Figure 61. Typical pulse trace (upper part) and terahertz spectrum (lower part) of quartz slide in transmission mode when acquiring data.

- The terahertz pulses are recorded with reference pulse (on room air) and with pulse traces on four separate points on the material to get the data in the time domain. From the time domain raw data, the refractive index of quartz glass can be estimated as

$$n \approx c\Delta t/d + n_{\text{air}} , \qquad (1)$$

where Δt is the time delay between sample and reference signal in the time-domain waveform, d is the sample's thickness, and n_{air} is the refractive index of air, which approximately equal to 1.

- The pulse traces data then are FFT to the frequency domain using OriginPro Software.
- From the phase difference of these spectra, the refractive index $n(f)$ and the absorption coefficient $\alpha(f)$ of the sample material can be extracted from the following formula [12] (Jepsen, 2019):

$$n(f) = 1 + \varphi(f)\, c/(2\pi f d) \quad (2)$$

where:

n(f): the refractive index.

φ(*f*): the phase difference between two signals after Fourier transform.
d: the thickness of samples.
f: the frequency.
and $c = 3 \times 10^8$ m/s is the speed of electromagnetic wave.

$$\alpha(f) = (2/d) \ln \{[A(f)_{ref} / A(f)_{samp}][4n(f)/(n(f) + 1)^2]\} \quad (3)$$

where:
α(*f*): Absorption coefficient.
$A(f)_{ref}$: the amplitude of the reference signal after Fourier transform.
$A(f)_{samp}$: the amplitude of the sample signal after Fourier transform.

Note:

1. To display the terahertz signal in the time-domain trace of the **upper graph**, use the **arrow** buttons below the pulse trace graph. The time position depends on the distance between the two terahertz antennas (stationary delay stage). In the experiment with quartz glass, we usually set it at around the 1168 ps value (Figure 61).
2. The Toptica TeraFlash can be used for measurements in two modes: Transmission and Reflection mode.

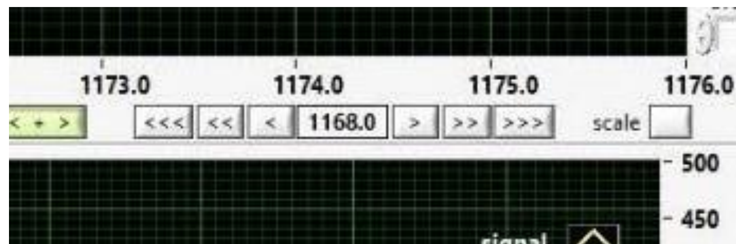

Figure 62. Representative time settings of the stationary delay stage.

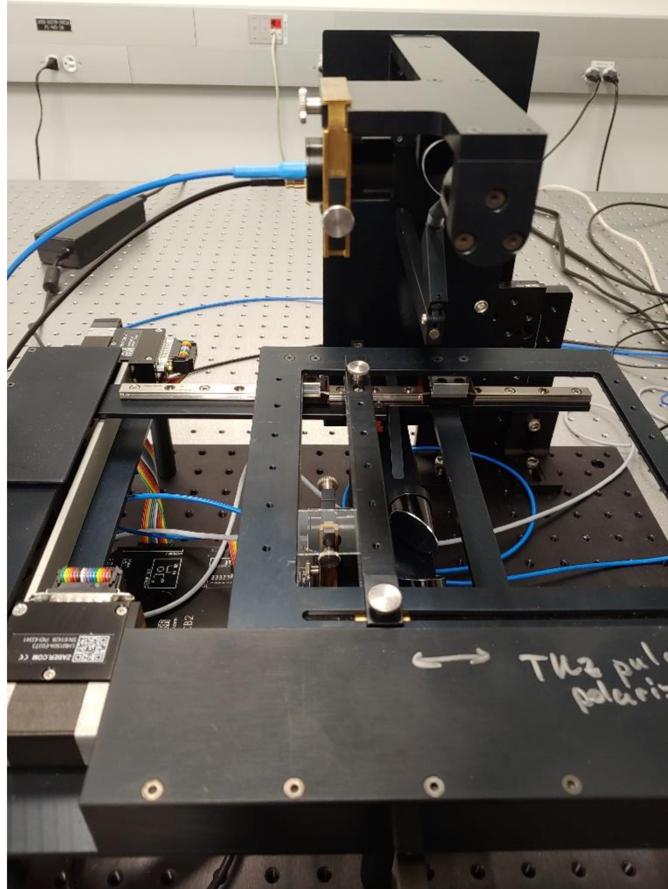

Figure 63. Quartz glass is set up in transmission mode for measuring pulse trace.

4.2 Experiment Results

4.2.1 Refractive index

a/ Collecting raw data

The following figure (Figure 63) shows typical pulse trace and terahertz spectrum zoom in the range of 0 – 3 THz. Please note the upper part is the graph in time domain and the lower part shows the power spectrum in frequency domain. The peaks in the power spectrum (time domain) are absorption lines of water vapor. The frequency-domain spectrum of THz spectroscopy offers a high resolution. Figure 64 shows a typical of the amplitude spectrum in frequency domain by using OriginPro software for FFT signal processing.

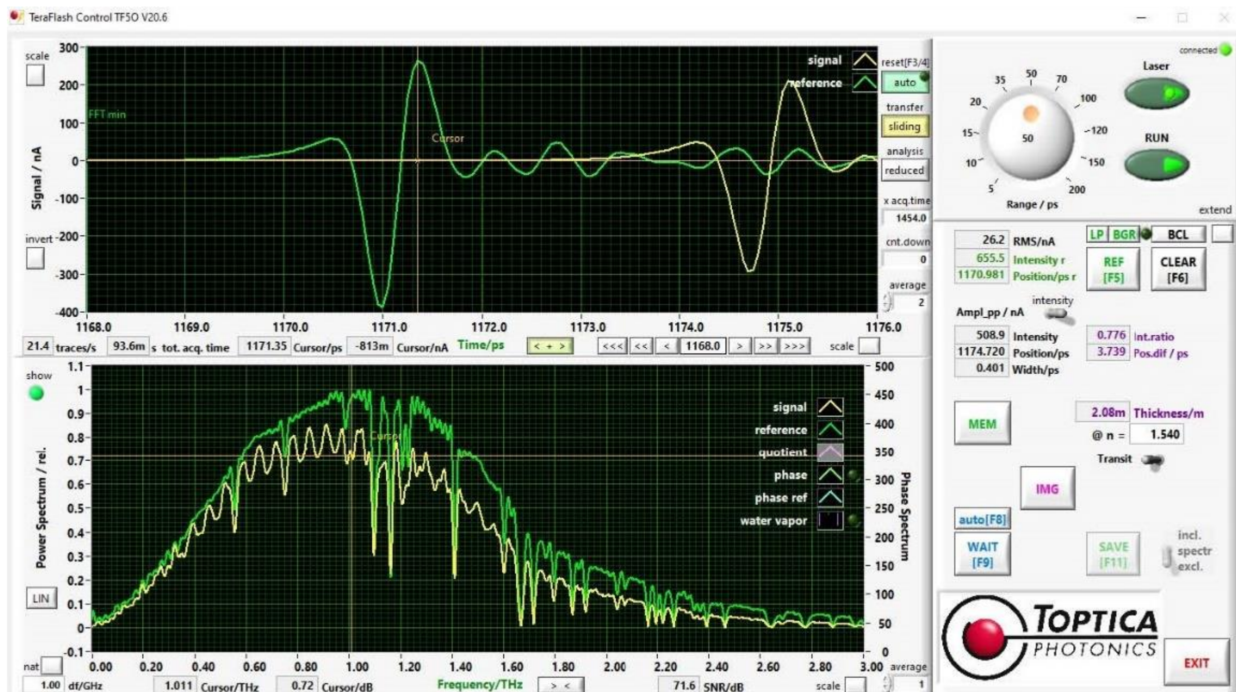

Figure 64. Typical pulse trace and terahertz spectrum zoom in the range of 0 – 3 THz. The peaks are absorption lines of water vapor.

In Figure 65, a THz absorption spectrum of air reference signal is shown and we can see the water vapor absorption lines at 1.099, 1.413, and 1.670 THz.

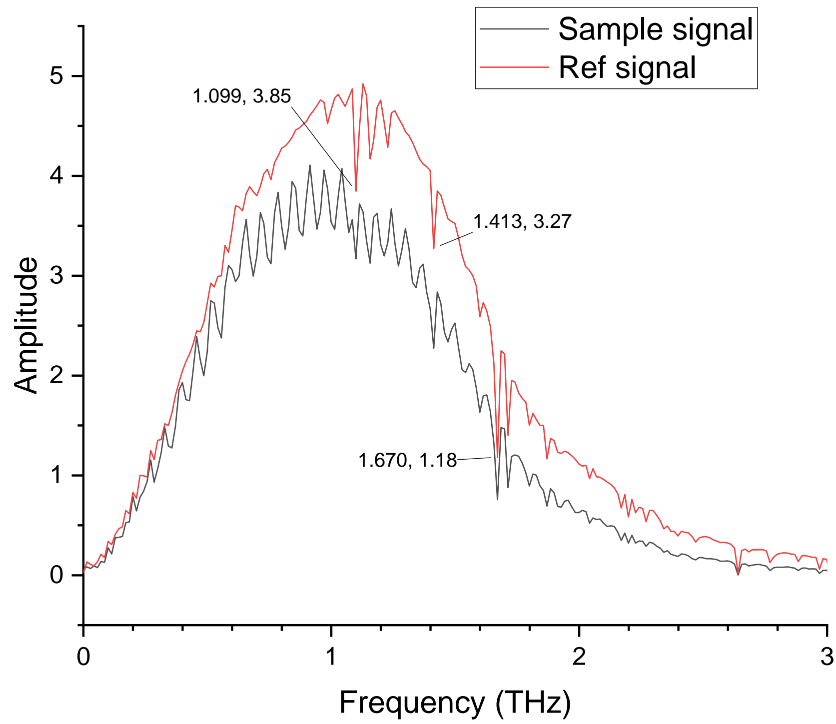

Figure 65. Power spectrum that extract from raw data of point 1 using OriginPro software. The water vapor absorption lines at 1.099, 1.413, and 1.670 THz.

b/ Estimate refractive index:

Figure 65 shows the pulse trace of TeraHertz pulse through sample (black) and room air for reference signal (red). We can directly calculate the refraction index from the time difference between the two absorption peaks and apply directly formula 1.

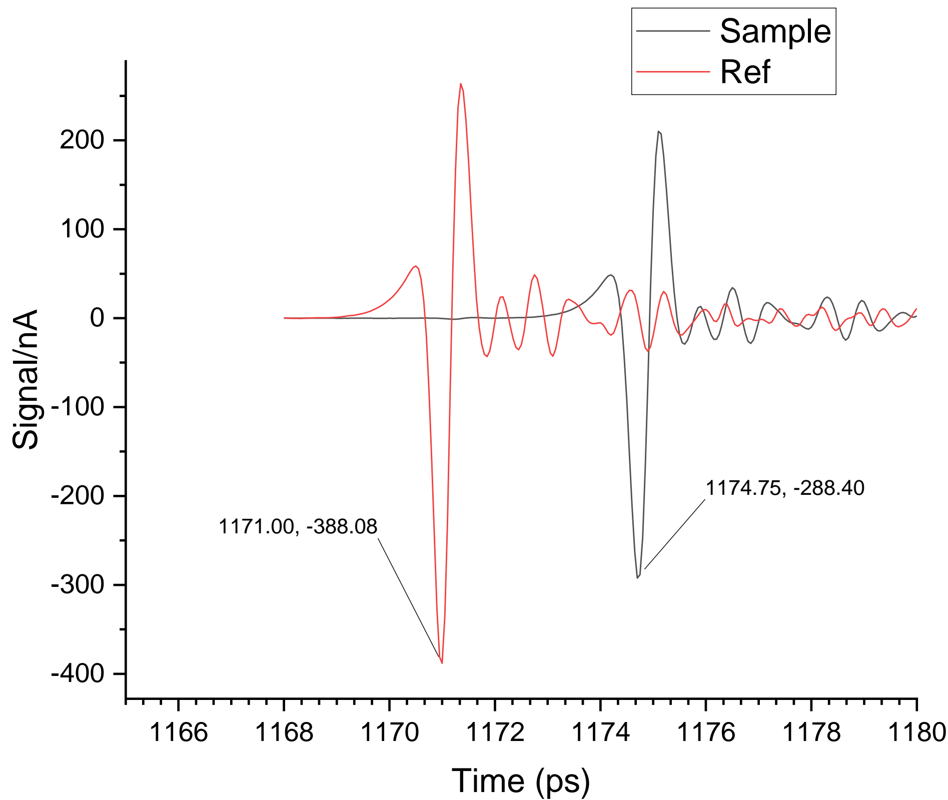

Figure 66. Pulse trace in the time domain

From the measurement raw data, we have the Δt = 1171.00 – 1174.75 = 3.75 ps. Therefore, applying formula (1), the estimated refractive index of the quartz glass can be derived:

$$n = \frac{3\ x\ 10^{8}\ x\ 3.75\ x\ 10^{-12}}{10^{-3}} + 1 = 2.125$$

c/ Extracted refractive index and absorption coefficients from frequency domain:

First, we used the OriginPro software to transfer the raw data from the time domain to frequency domain (Fast Fourier Transform – FFT signal processing). Based on those results in the form of spreadsheet, that have two column of amplitude and unwrapped phase, we can easily calculate the respective phase differences and then extract the refractive index by using formula 2. The results are shown in the following figures. Figures 67 and 68 show the unwrapped phase of reference signal and sample signal from our experiment and Figure 69 shows the result from the experiment on literature.

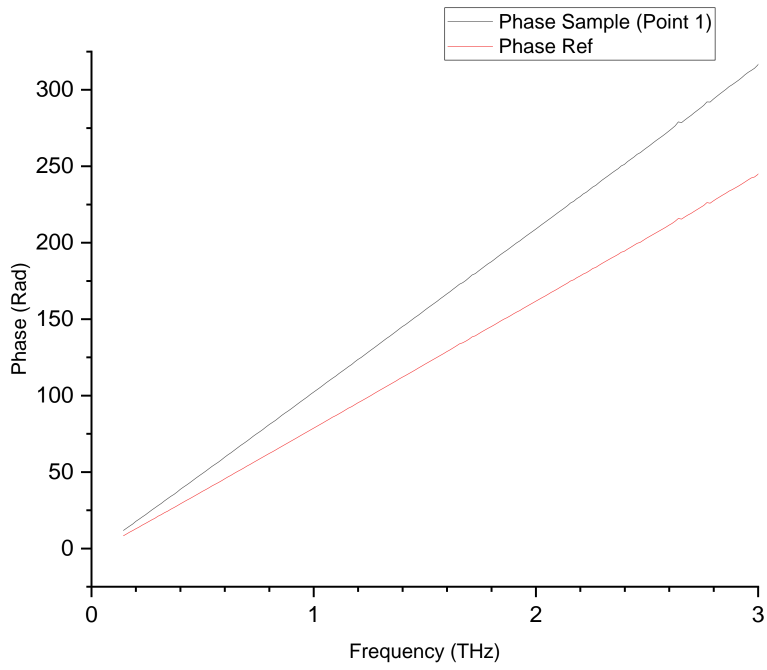

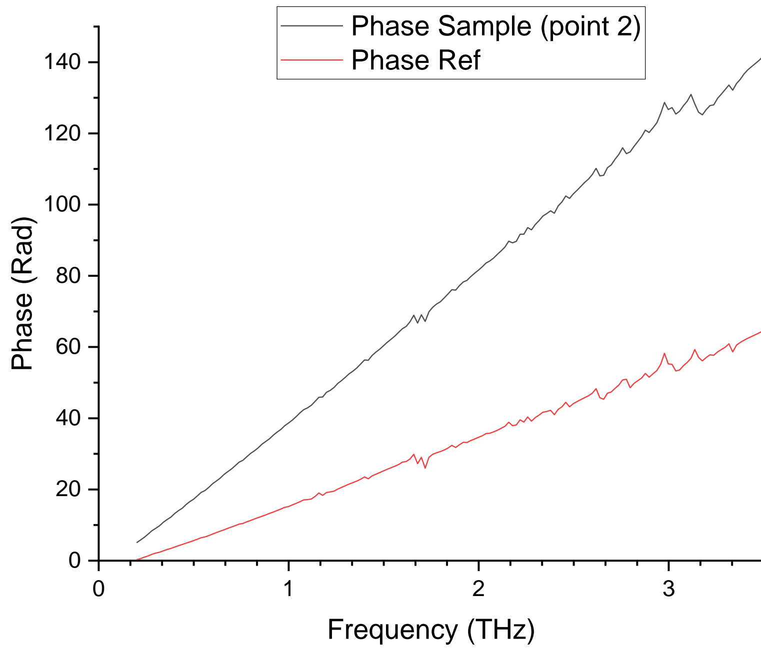

Figure 67. Unwrapped phase: Reference signal and sample signal on point 1 and 2.

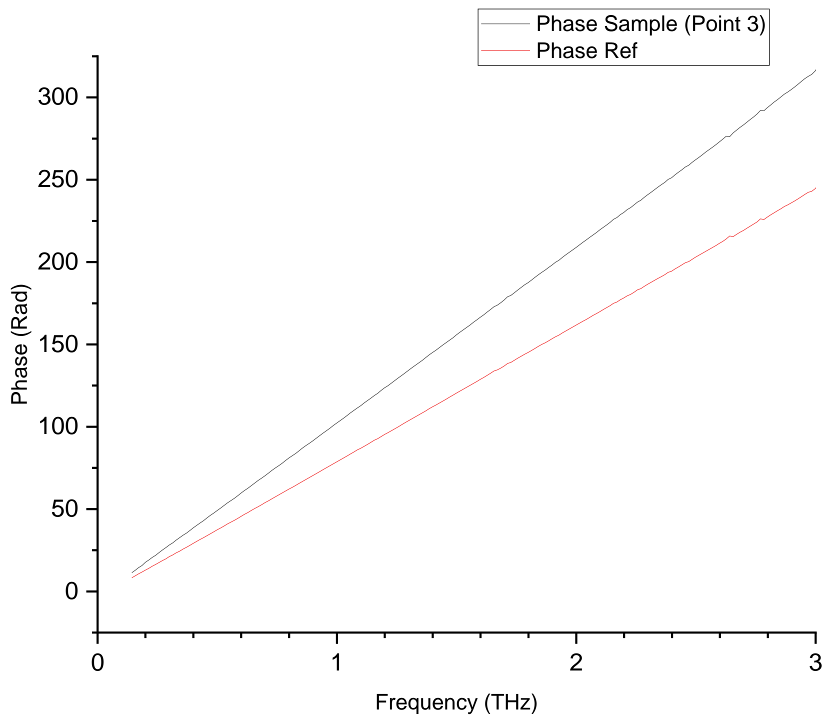

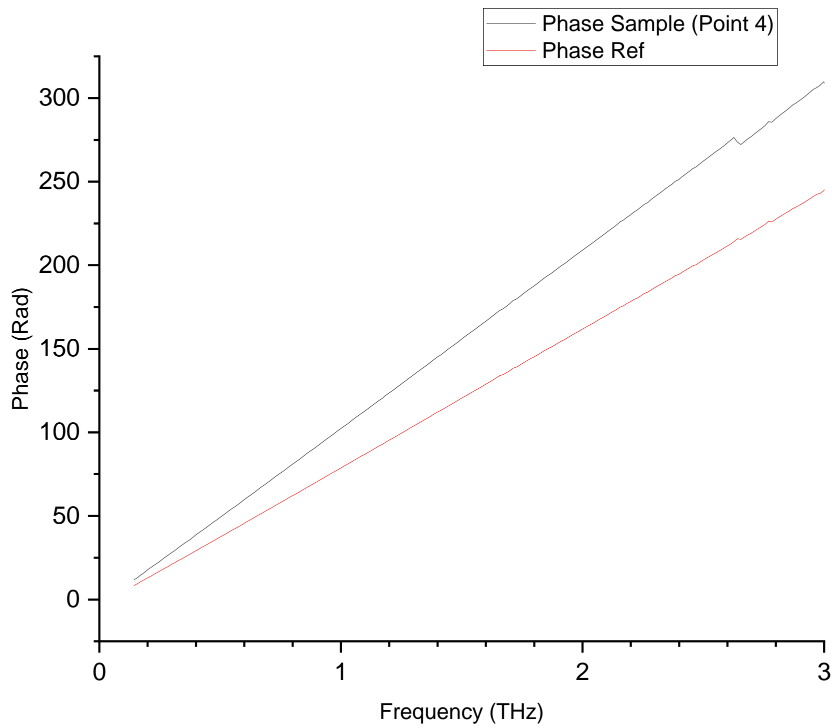

Figure 68. Unwrapped phase of reference signal and sample signal on point 3 and 4.

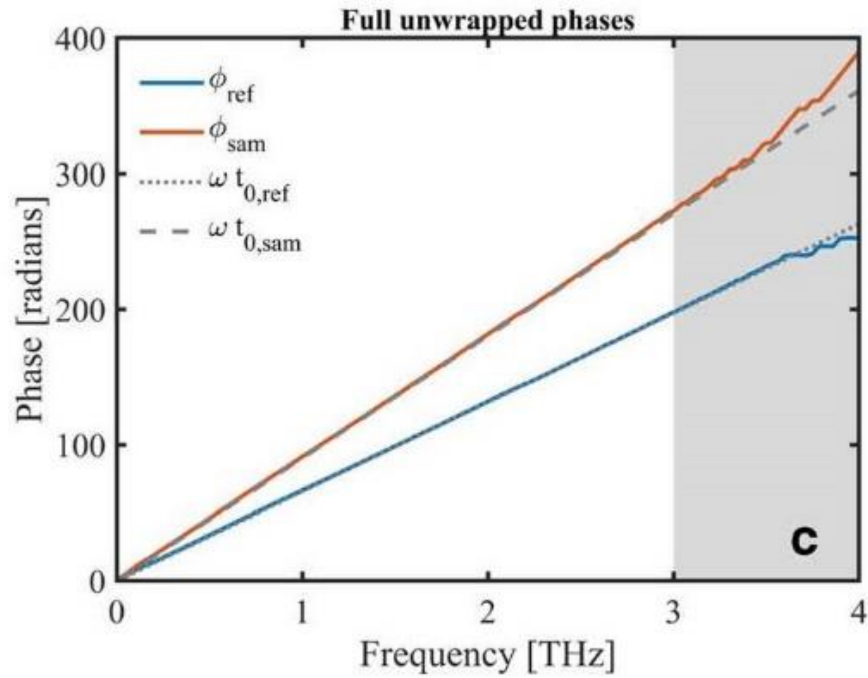

Figure 69. Unwrapped phase: From the experiment on literature (Jepsen, 2019)

From the above phase information in frequency domain, we can then derive the phase difference between the two signals by subtracting the two column on the spreadsheet and make the graph. Results for each samples are shown in Figures 70 and 71. Figure 72 shows the result reported from the experiment on literature for comparison.

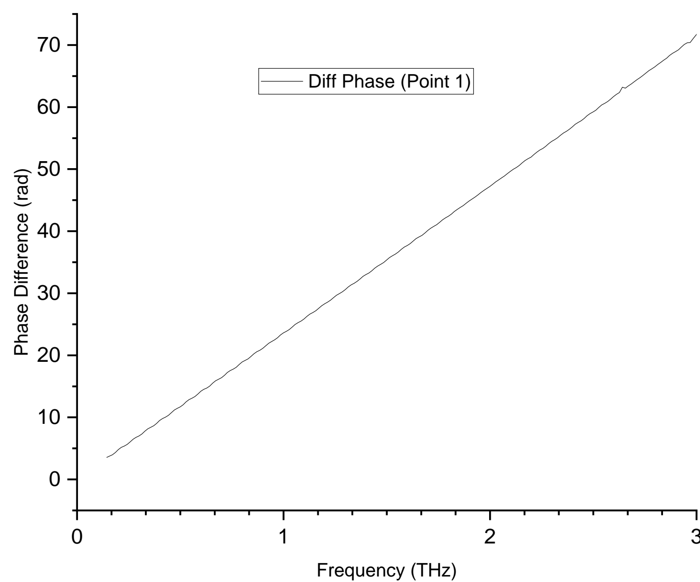

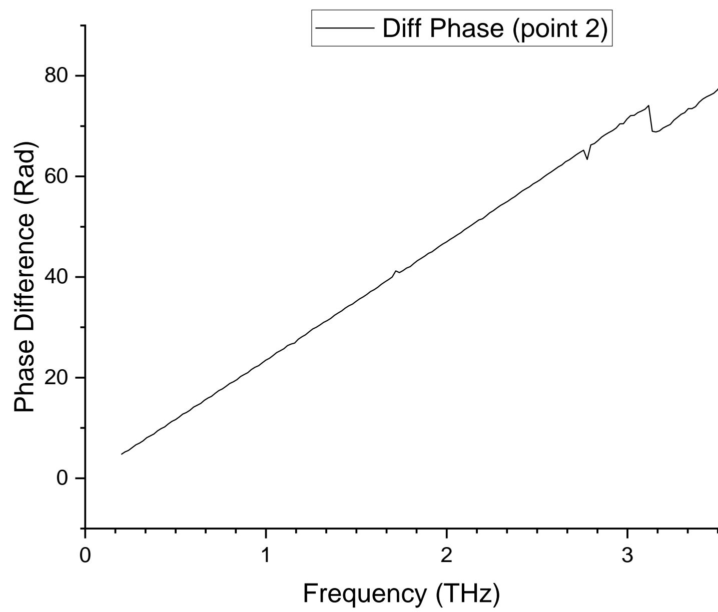

Figure 70. Phase Difference on points 1, and 2.

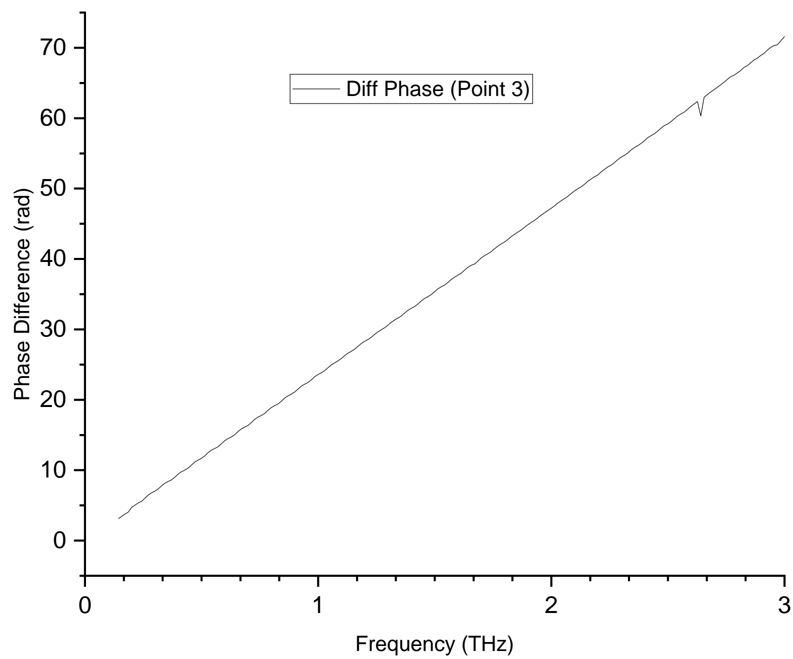

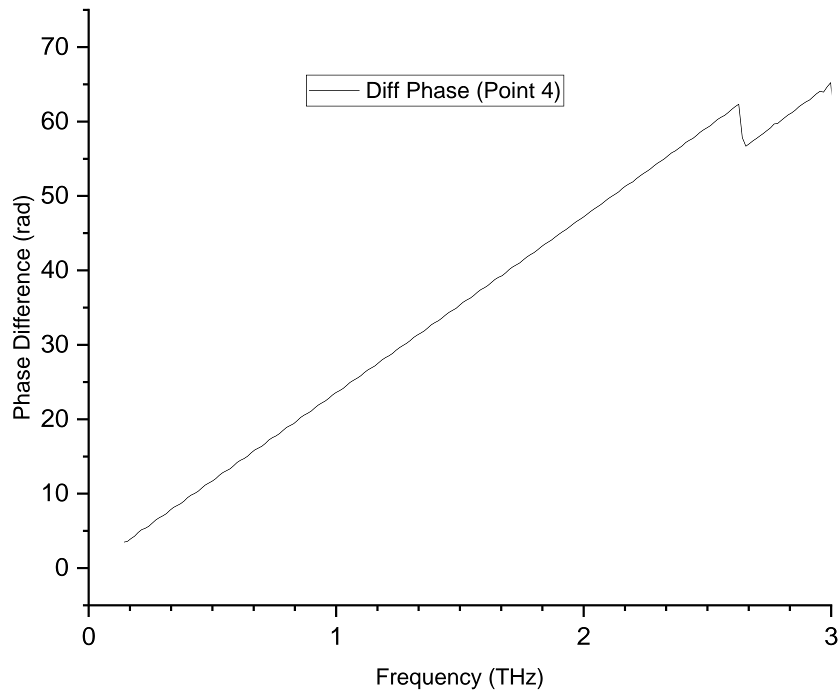

Figure 71. Phase Difference on points 3 and 4.

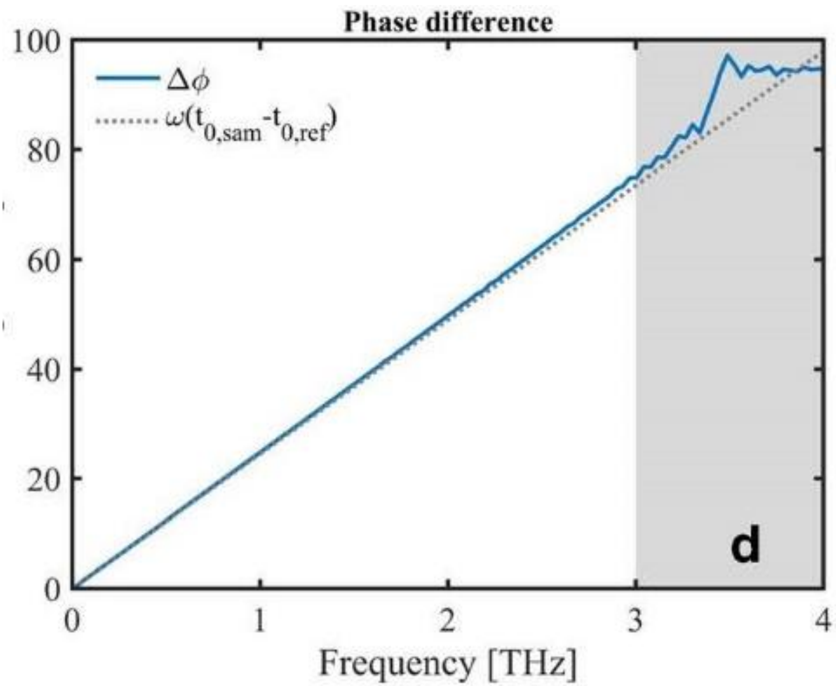

Figure 72. Phase different from literature (Jepsen, 2019)

After having the phase difference, we can directly apply formula (2) for calculating the corresponding refractive index. The following graphs show the reflective index of quartz glass sample at point 1, 2, 3 and 4, respectively, in frequency domain.

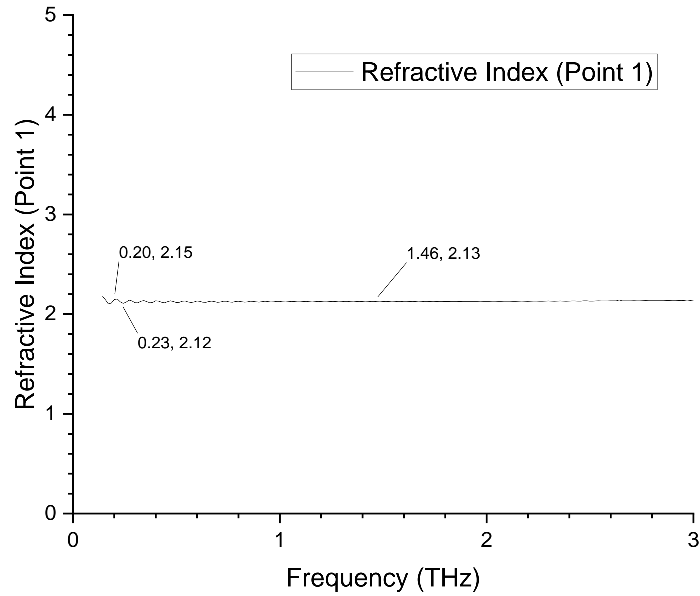

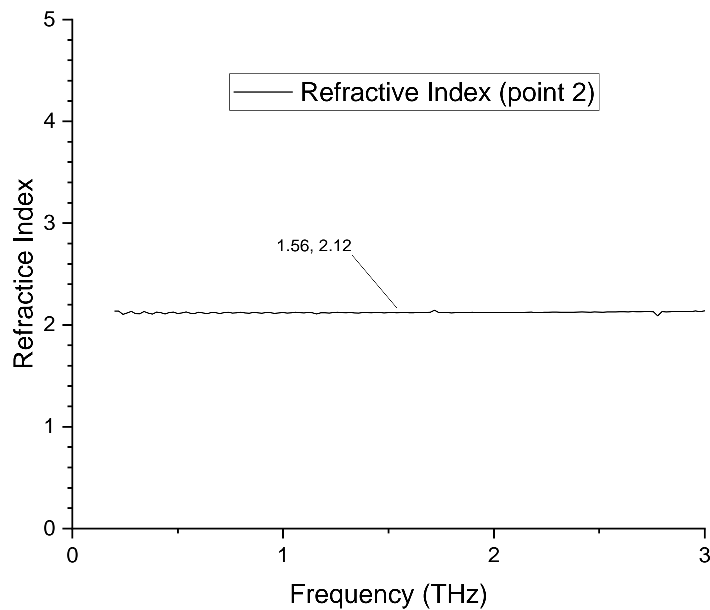

Figure 73. Refractive index of sample on point 1 and point 2

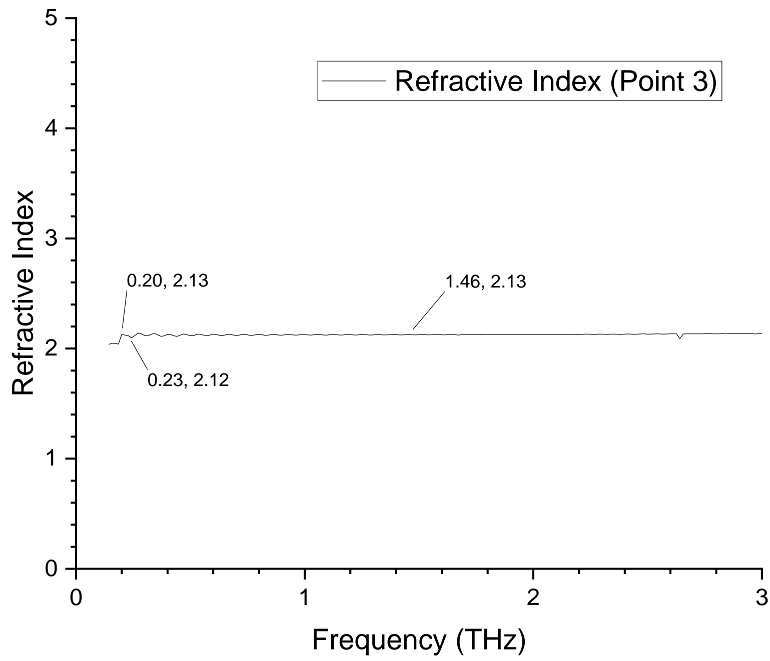

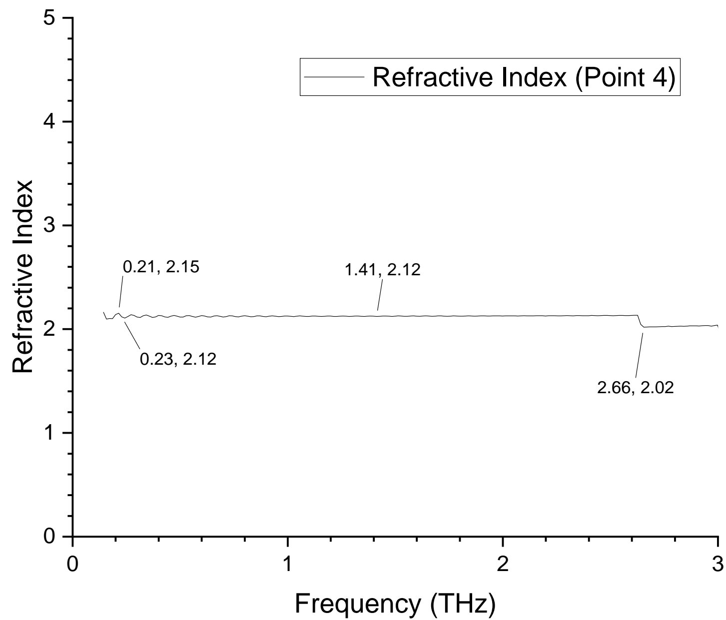

Figure 74. Refractive index of sample on point 3 and point 4

Finally, we use the results of the refractive index of the four samples calculated above to get the average value. Figure 75 shows the average refractive index of the quartz glass. Please note

that when comparing with Figure 76, we see that it agrees with the reported data got from the literature. Moreover, it match well with the estimated result calculate from the data got in the time domain (n = 2.125 from section 4.2.1 – b).

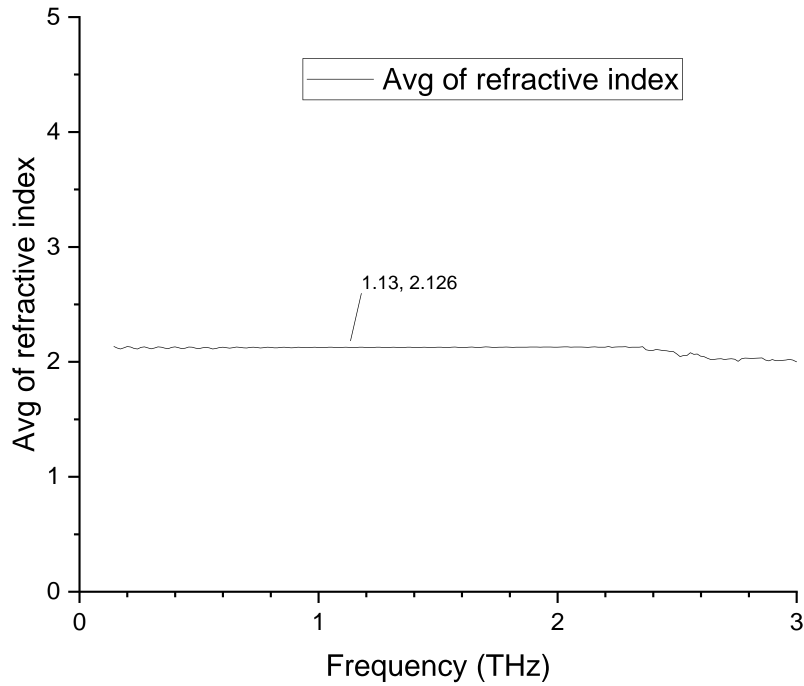

Figure 75. The average of refractive index of the quartz glass.

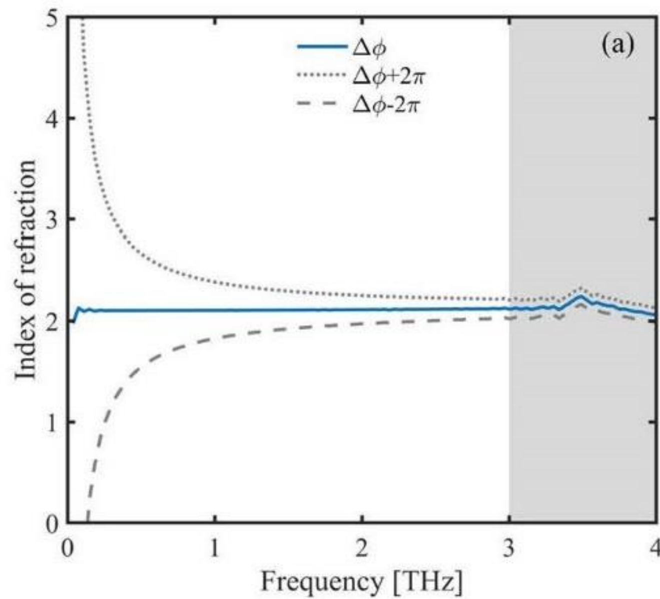

Figure 76. Refractive index of Quartz glass as in literature (Jepsen, 2007).

4.2.2 Absorption Coefficient

Similarly, we can apply the formula (3) for calculating the corresponding absorption coefficient. Because we have all the data from the last step, the extracted value is straightforward. The following graphs show the absorption coefficient graphs of quartz glass at points 1, 2, 3, and 4, respectively, in the frequency domain.

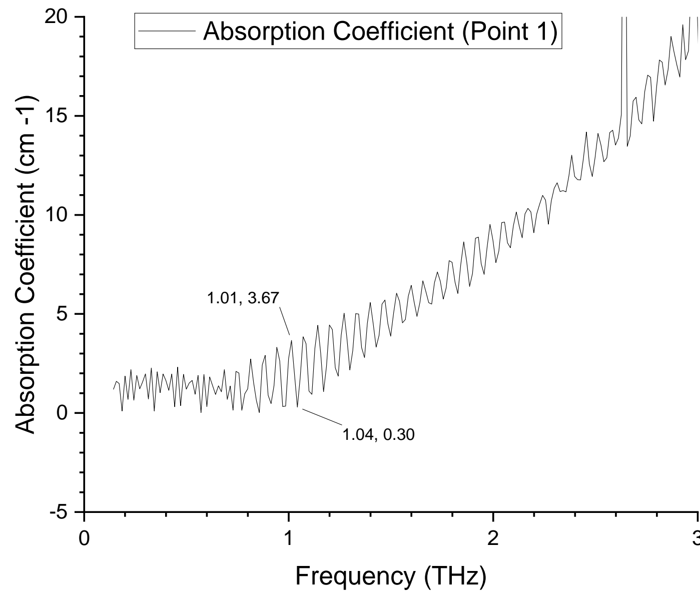

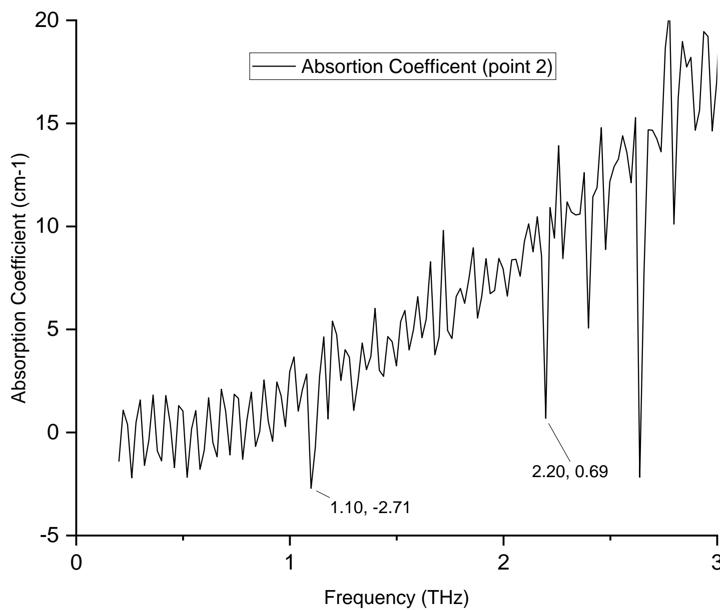

Figure 77. Absorption Coefficient of quartz sample on point 1 and point 2

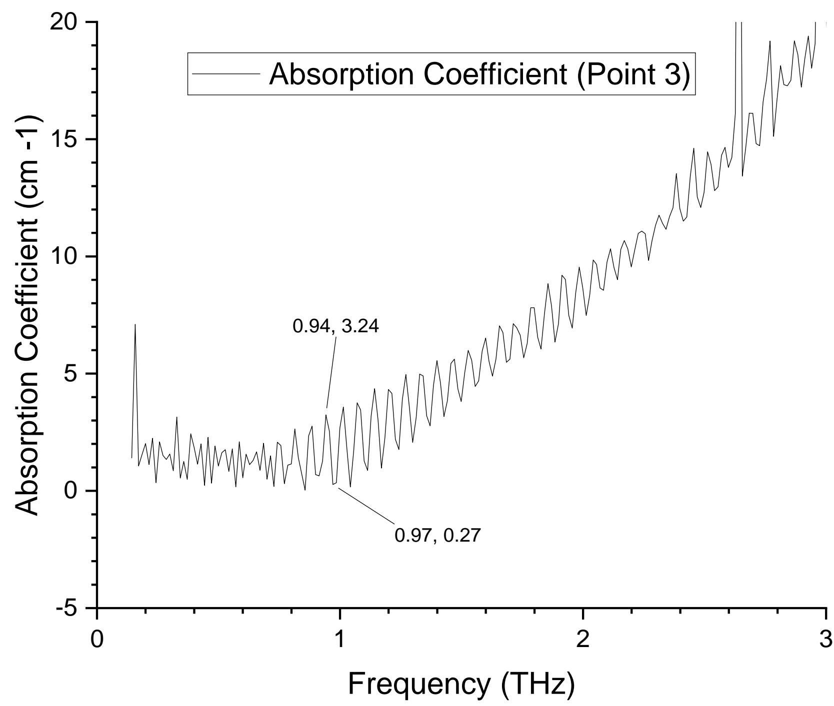

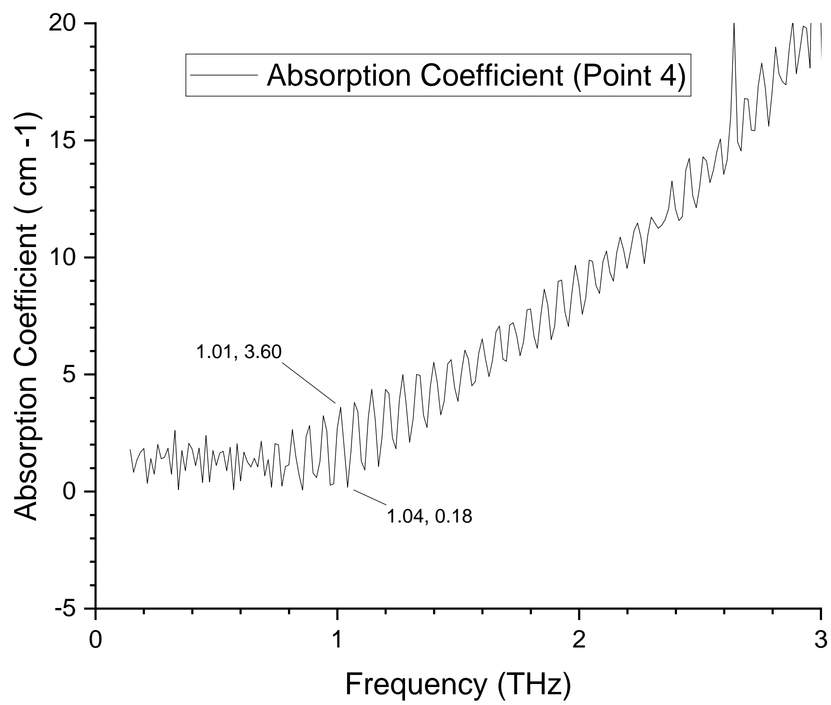

Figure 78. Absorption Coefficient of quartz sample on point 3 and point 4

The graph of the average of absorption coefficient is shown in Figure 79. We note that from the frequency 0.63 THz, the extracted absorption coefficient zigzag increases rapidly.

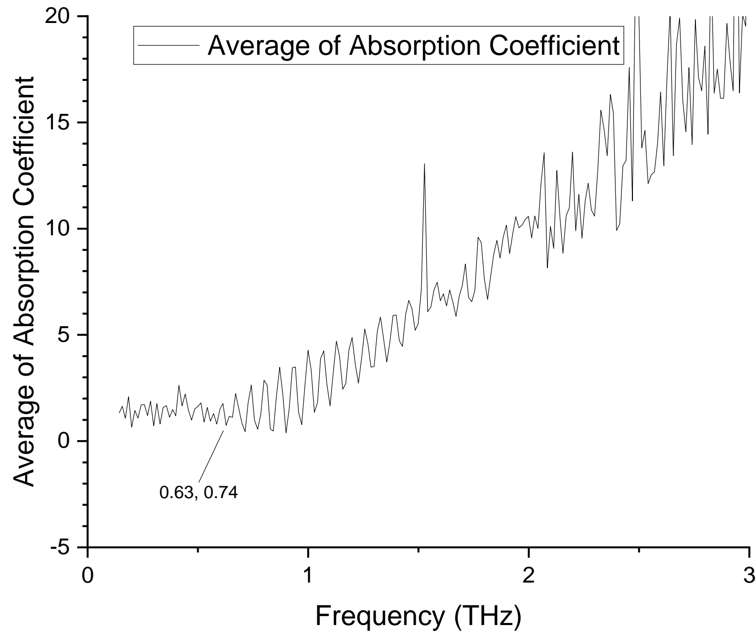

Figure 79. Average of Absorption Coefficient of the quartz glass slide.

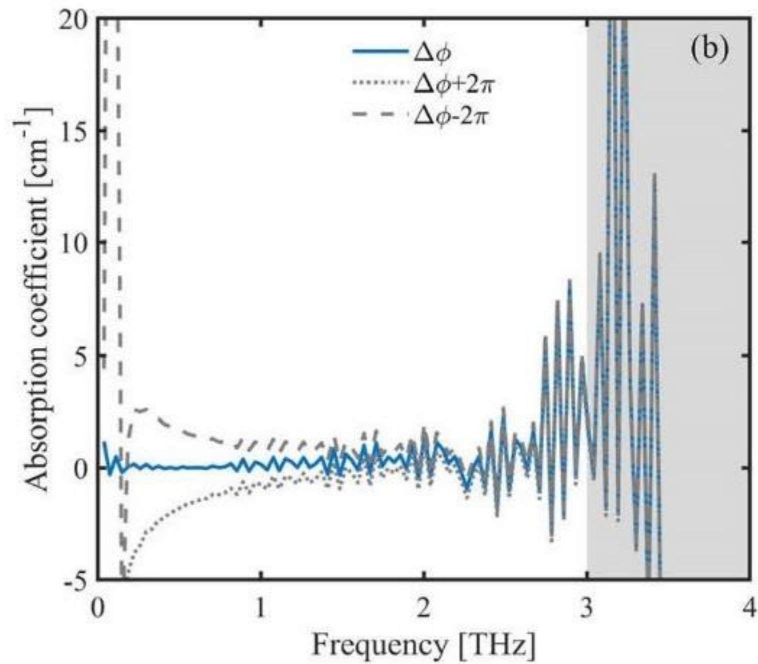

Figure 80. Absorption Coefficient of Quartz glass from Jepsen (2007) [12].

4.3 Conclusion:

Comparing the Figure 75 with figure 76 and Figure 79 with Figure 80, we can draw some conclusions:

- In general, the refractive index value of quartz glass agree with the reported data in the literature (Jepsen, 2019) and it also matches well with the calculation from the data directly measured in the time domain (section 4.2.1 – b).
- The absorption coefficient curves are not smooth. It varied zigzag between -1.2 and 2.1 cm^{-1} when the frequency 0 – 0.8 THz and then increased rapidly when the f > 0.8 THz. It may be because of the humidity (water vapor) affected when taking the experiment.
- The absorption coefficient curve of the experiment did not agree to the results from the experiment on literature (Jepsen, 2019). From formula 3 (section 4.1), we know that the absorption coefficient relies on the refractive index, which indicates that the resulting discrepancy may be caused by the algorithm we used. This problem can be improved by using another algorithm for extracting absorption coefficients from raw data, such as MATLAB or LabVIEW.

Chapter 5: Broader Impacts

5.1 Engineering Ethics

Engineering is limited to those who possess the required qualifications and have the responsibility to apply engineering skills, scientific knowledge, and ingenuity to advance human welfare and quality of life. One of the fundamental principles of engineer behavior is to serve society with honesty, truthfulness, and trustworthiness and to always use honorable and ethical practices that demonstrate fairness, courtesy, and good faith toward clients, colleagues, and others [13].

While implementing this project, we always adhere to the above ethical principles, particularly in being honest in the data collected as well as manipulated during the experiment. Besides, we pay much attention to accurate and complete references. In this way, we hope that this project's results will be used effectively by many others.

5.2 Codes and Standards

In this project, we have used the TeraFlash TeraHertz spectroscopy. Based on the manufacturer manual, the TERAFLASH system is manufactured according to the Laser Safety Standard EN 60825-1:2014 and complies with US laws 21 CFR §1040.10 and §1040.11 [9, p.10]. The IEC 60825-1 standard applies to the safety of laser products emitting laser radiation in the wavelength range 180 nm to 1 mm.

The TERAFLASH system used in LEAP emits invisible pulsed laser radiation of up to 2 x 25 mW average power, and it is classified as a Class 1 laser product by the above Safety Standard, and therefore, we need to avoid exposing eyes and skin to the laser beam, including any laser stray light.

To be more specific, we also take a look at the Code of Federal Regulations Title 21 – FDA: section 1040.10 for laser products (21 CFR §1040.10) [14] and section 1040.11 for specific purpose laser products (21 CFR §1040.11) [15].

Chapter 6: Conclusion and Outlook

6.1 Conclusion:

Although this project has acquired some results, there were areas in which we encountered a variety of challenges. Because we often realize the problem when there is not much time left for the project, therefore, we did not have enough time to adequately address all aspects of the assignments. However, there still have been some suggestions for improving the specific tasks that we realized might become helpful in the future.

Here, we would like to reiterate some of the conclusions we have in the previous chapters for easy reference.

6.1.1 Spin Coater and Profilometer:

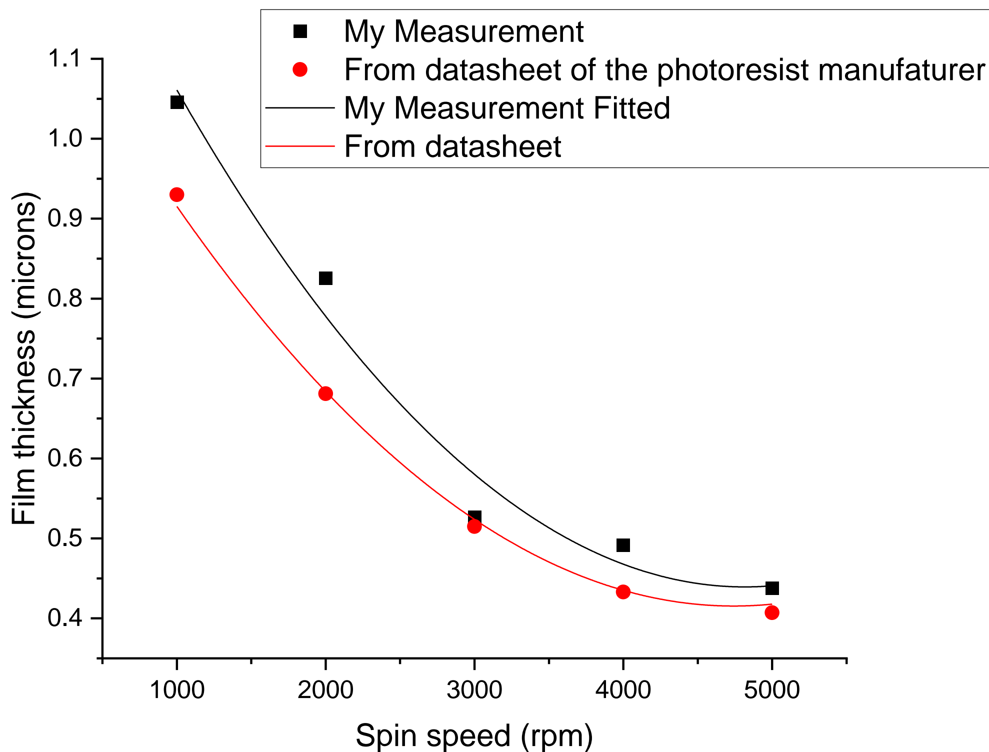

Figure 59. The spin curve of KL 5305 from the experiment and from the datasheet

The photoresist thickness can be tested more accurately by following the procedure as in the datasheet [10], such as using HMDS (hexamethyldisilazane) primer to increase the adhesion of photoresist to most substrates as well as find the optimum exposed dose for the photoresist is used. In this project, we started with the value of 60 mJ@365 nm and found that it seems to be high for KL5305 positive photoresist.

Furthermore, because we only use a small piece of a wafer to test, the task to center correctly the wafer over the spindle chuck has a decisive role in making the photoresist spread evenly.

6.1.2TeraFlash TeraHertz Spectroscopy:

As discussed at the beginning of chapter 4, in this project, we are just able to explore some basic features of TeraFlash Time-Domain Terahertz Spectroscopy. We used terahertz time-domain spectroscopy (THz-TDS) to extract the refractive index of a quartz glass slide with known thickness. Based on what we have investigated in that chapter, we can draw some conclusions:

- In general, the refractive index value of quartz glass agree with the reported data in the literature (Jepsen, 2019) and it also matches well with the calculation from the data directly measured in the time domain.
- The absorption coefficient curves are not smooth. It varied zigzag between -1.2 and 2.1 cm^{-1} when the frequency 0 – 1 THz and then increased rapidly when the f > 1 THz. It may be because of the humidity (water vapor) affected when taking the experiment.
- Furthermore, the result of the absorption coefficient of our experiment did not agree with the reported data obtained from the literature (Jepsen, 2019). But because the absorption coefficient relies on the refractive index, which shows that it meets with literature, thus the resulting discrepancy may be caused by the algorithm we used (calculated directly from spreadsheet in OriginPro software). This problem can be improved by using another algorithm for extracting absorption coefficient from raw data, such as using MATLAB or LabVIEW.

6.4 Outlook

6.4.1 Spin Coater and Profilometer

Recall that in chapter 3, we have combined testing the spin coater and the Profilometer with the samples that was just processed through the soft bake step of the lithography process. While simplifying project implementation, this method has some disadvantages, such as made some artifacts on the edge where we used the Kapton tape to make the step for measurement the photoresist thickness. Besides, due to the photoresist in use did not go through all the steps of the lithography process, we are unable to find the correct thickness of the photoresist for each recipe as in the manufacturer datasheet. But this thickness is very critical in many practical applications. This problem can be solved if we can use the ABM Mask Aligners & Exposure Systems in combination with the spin coater and the profilometer in future project.

6.4.2 TeraHertz Spectroscopy

In this project, we are just only able to use some basic features of the TeraFlash TeraHertz spectroscopy at the LEAP. Among other features of this equipment that we would use in future work is its direct thickness measurement capabilities. The TERAFLASH Control Software

instrument permits basic thickness measurements with a known refractive index material in both transmission or reflection mode [9, p. 37]. The measurement mode is actuated via a switch (Transit/Reflex). Moreover, in terms of using this device for measuring thickness, we can improve the quality of using the Terahertz equipment by setting up a housing mechanism. This can be done in one other future project that can help control the environment's humidity. Because the terahertz pulse is very sensitive to moisture (water vapor in the air).

Acknowledgments

Our sincerest gratitude goes out to Professor Yuxiang Liu, Professor Douglas Petkie, and Dr. James Eakin, who has been our fantastic MQP advisors throughout our project. Without their support, we are unable to complete this work. Their enthusiasm, expertise, research advice, and guidance have proved invaluable. We would like to particularly appreciate Prof. Liu, an excellent mentor to us throughout this process, discussing our progress and was always ready to encourage us as well as find solutions to our problems.

References

[1] Lab for Education & Application Prototypes. Retrieved October 18, 2020 from https://www.wpi.edu/research/core-research-facilities/leap.

[2] LEAP@WPI/QCC: Improving a Service Model Through Customer Discovery and Web-Scraping. https://digitalcommons.wpi.edu/iqp-all/5824/.

[3] https://eprojects.wpi.edu/group/3681

[4] R. Paschotta, article on 'photonics' in the Encyclopedia of Laser Physics and Technology, 1. edition October 2008, Wiley-VCH, ISBN 978-3-527-40828-3. Retrieved October 14,2020 from https://www.rp-photonics.com/encyclopedia_cite.html?article=photonics.

[5] Gines, Lifante. Integrated Photonics: Fundamentals - PDF Free Download. https://epdf.pub/integrated-photonics-fundumentals.html.

[6] Apogee Spin Coater Manual. https://www.costeffectiveequipment.com/wp-content/uploads/2019/02/Apogee-Spin-Coater-Manual.pdf.

[7] DataStream Manual. https://www.costeffectiveequipment.com/wp-content/uploads/2019/01/DataStream-Manual.pdf.

[8] Alpha-Step® D-500 and D-600 User Manual . https://www.kla-tencor.com/products/instruments/stylus-profilers/alphastep-d-600.

[9] TERAFLASH. Time-Domain Terahertz Spectroscopy Platform Manual. 2018.

[10] KemLab KL 5300 Positive Photoresist Datasheet. http://micromaterialstech.com/wp-content/uploads/2019/01/KL5300-positive-photoresist-datasheet.pdf.

[11] Xander Phillips. TeraHertz Technology. The English Press, Delhi 2011.

[12] Jepsen, P.U. Phase Retrieval in Terahertz Time-Domain Measurements: a "how to" Tutorial. *Journal of Infrared, Millimeter, and Terahertz Waves* 40**,** 395–411 (2019). https://doi.org/10.1007/s10762-019-00578-0

[13] National Society of Professional Engineers, "Code of Ethics." https://www.nspe.org/resources/ethics/code-ethics. Accessed 3 Apr. 2021

[14] 21 CFR §1040.10. https://www.govinfo.gov/content/pkg/CFR-2000-title21-vol8/pdf/CFR-2000-title21-vol8-sec1040-10.pdf. Retrieved 3 Apr. 2021

[15] 21 CFR §1040.11. https://www.govinfo.gov/content/pkg/CFR-2000-title21-vol8/pdf/CFR-2000-title21-vol8-sec1040-11.pdf. Retrieved 3 Apr. 2021